Evaluation of LNA Gapmer efficacy in FSHD patients' muscle cells

By

Ashley Guncay

A thesis submitted to the Faculty of Graduate Studies and Research in partial fulfillment of the requirements for the degree of

Master of Science

Medical Sciences - Medical Genetics
University of Alberta

ABSTRACT

Facioscapulohumeral muscular dystrophy (FSHD) is a neuromuscular disorder characterized by early involvement of muscle weakness. FSHD is most commonly caused by a deletion of a subset of D4Z4 macrosatellite repeats at the locus located on chromosome 4q35. Within each D4Z4 repeat unit is a double homeobox sequence encoding the DUX4 protein. In FSHD patients, mis-expression of DUX4 results in the production of a pathogenic protein and causes a transcriptional deregulation cascade which triggers muscle atrophy, apoptosis, and oxidative stress. Currently, no curative treatment options for FSHD patients have been established, further illustrating the importance of determining the biological impact of DUX4 suppression via antisense oligonucleotides. Implication for antisense oligonucleotides in FSHD could help towards progressing the development of therapeutic approaches.

Using *in vitro* methods, in immortalized control myoblasts and immortalized FSHD patient muscle cells, three culture media additives were investigated, fetal bovine serum (FBS), knockout serum replacement (KOSR) and dexamethasone, to determine their effects on DUX4 expression in culture. Various RT-conditions were also examined for sensitive detection of DUX4. In addition, suppression of DUX4 was examined via RNase H-mediated degradation using locked nucleic acids (LNA)-DNA chimeras, called gapmers, targeting DUX4. In this work, I have shown that SuperScript III reverse transcriptase (RT) and GoTaq® G2 green master mix is the most sensitive cDNA synthesis strategy to use for detection of DUX4. Supplementing culture medium with dexamethasone enabled better detection of DUX4 expression in immortalized healthy and FSHD myoblasts. Transfection with LNA gapmers 1, 1*, 3*, 4, 6, and 7, all which target exon 3 of the DUX4 mRNA, suppress the expression of DUX4 in immortalized FSHD patient muscle cells. Transfection with LNA gapmers 1 and 3 was also found to change the localization of MuRF1 in the nucleus of FSHD myotubes. In addition, I found that *PITX1* expression in immortalized FSHD

patient muscle cells is not suppressed by LNA gapmers targeting DUX4. These results establish a sensitive detection strategy and culture method for detection of DUX4, identify potential LNA gapmers sequences which prevent *DUX4* expression and change the localization of MuRF1 in nucleus and indicate that PITX1 *per se* is not a direct target of DUX4. This thesis also outlines the therapeutic potential of antisense chemistries, specifically LNA gapmers, in FSHD targeting DUX4.

PREFACE

This thesis is an original work by Ashley Guncay. No part of this thesis has been previously published.

For my Gramma, Joyce Cook, who was a little bit parent, a little bit teacher, and a little bit best friend. You were easily the strongest woman I knew.

ACKNOWLEDGEMENTS

I would like thank my supervisor, Dr. Toshifumi Yokota, for his continuous guidance and expertise throughout the duration of my graduate studies. I would like to thank the members of my committee, Dr. Michael Walter, and Dr. David Eisenstat for their overwhelming support, guidance and knowledge, which immensely made me grow as a scientist and made me explore areas of science outside of my project. I would also like to thank my external examiner, Dr. Heather McDermid.

To Dr. Yusuke Echigoya, my gratitude for your patience day in and day out and your guidance and support with experimental designs and troubleshooting. To Dr. Rika Maruyama, thank you for always being someone I could talk to, whether it was science related or life related, and for your guidance and knowledge which helped me move forward with my project. In addition, thank you to Hosna Jabbari for your expertise and knowledge of the computer science world and your helpful contributions to my project.

A special thank you to my lab mates Aleksander Touznik and Joshua Lee for welcoming me into the Yokota family with open arms, for their comic relief and their constant help in the lab. As well, thank you to all my colleagues in Medical Genetics, you all have made my experience in Edmonton amazing. I also owe my gratitude to Shari Barham for her expertise in administration and her helpfulness with any questions I ever had for her.

I would also like to recognize my funding sources, as this research would not have been attainable without the assistance of the Department of Medical Genetics, the Faculty of Medicine and Dentistry, MatCH and CIHR. Lastly I would also like to thank my family, my fiancé and my friends outside of Medical Genetics who provided me with encouragement throughout the process of my Master's degree training.

Ashley Guncay

TABLE OF CONTENTS

LIST OF TABLES

LIST OF FIGURES

LIST OF ABBREVIATIONS

2’MOE – 2’-methoxyethoxy

2’O-MePS-2’O-methyphorothioate

5’UTR: Five prime untranslated region

ANOVA: Analysis of variance

AON: Antisense oligonucleotide

Bic: Biceps Muscle

BiPAP: Nocturnal bilevel positive airway pressure

BMD: Becker Muscular Dystrophy

bp: Base pair

BSA: Bovine serum albumin

CDK4: Cyclin-dependent kinase 4

cDNA: Complementary DNA

CDS: Coding sequence

CER: Cytoplasmic Extraction Reagent

CMD: Congenital Muscular Dystrophy

DAPI: 4’,6-Diamidino-2-Phenylindole, Dihydrochloride

DM: Differentiation medium

DMEM: Dulbecco’s Modified Eagle Medium

DMD: Duchenne Muscular Dystrophy

DMD: Dystrophin

DNA: Deoxyribonucleic acid

DUX4: Double homeobox 4

EDMD: Emery-Dreifuss Muscular Dystrophy

FBS: Fetal bovine serum

fl-DUX4: Full-length double homeobox 4

FOP: Fibrodysplasia ossificans progressiva

FSHD: Facioscapulohumeral Muscular Dystrophy

GAPDH: Glyceraldehyde 3-phosphate dehydrogenase

GM: Growth medium

HEPES: 4-(2-hydroxyethyl)-1-piperazineethanesulfonic acid

hESC: Human embryonic stem cells

hFGF: Human Fibroblastic Growth Factor

hHGF: Human Hepatocyte Growth Factor

hTERT: Human telomerase reverse transcriptase

iPSC: Induced pluripotent stem cells

KOSR: KnockOut Serum Replacement

LGMD: Limb-Girdle Muscular Dystrophy

LNA: Lock nucleic acid

MD: Muscular Dystrophy

MMD: Myotonic Muscular Dystrophy

mRNA: Messenger ribonucleic acid

MuRF1: Muscle RING-finger protein 1

NER: Nuclear Extraction Reagent

NT: Non-treated

nt: nucleotide

ORF: Open reading frame

OPMD: Oculopharyngeal Muscular Dystrophy

PBS: Phosphate buffered saline

PBSTr: Phosphate buffered saline (Triton-X)

PBSTw: Phosphate buffered saline (Tween 20)

PCNA: Proliferating cell nuclear antigen

PFA: Paraformaldehyde

PITX1: Paired-like homeodomain 1

PMO: Phosphorodiamidate morpholino oligomer

PSA: Poly(A)-signal

PVDF: Polyvinylidene difluoride

qRT-PCR: Quantitative reverse transcriptase polymerase chain reaction

RNA: Ribonucleic acid

RT: Reverse transcriptase

RT-PCR: Reverse transcriptase polymerase chain reaction

s-DUX4: Short double homeobox 4

SDS: Sodium dodecyl sulfate

TAGC: The Applied Genomic Center

TBP: Anti-TATA binding protein

VB_{12}: Vitamin B_{12}

$ZnSO_4$: Zinc Sulfate

Chapter 1

Introduction

1 Introduction

1.1 Muscular Dystrophies

Muscular Dystrophy (MD) comprises a group of 30 or more inherited disorders which are characterized by muscle weakness and replacement of muscle cells with connective tissue and fat (Emery, 1991). Although all MDs share common characteristics such as muscle weakness and muscle cell death, the disorders differ from one another in terms of their severities (i.e. progression variability), age of onset as well as muscles and other organ systems affected (Barakat-Haddad *et al.,* 2016).

The most common type of MD is Duchenne Muscular Dystrophy (DMD), a recessive X-linked genetic disorder, occurring in approximately 1 in 3500 males worldwide (Emery, 1991 & Koenig *et al.*, 1987). DMD is predominately caused by frame-shift mutations in the dystrophin (*DMD*) gene, causing lethal muscle wasting in DMD patients (Hoffman *et al.*, 1987). Mutations in the *DMD* gene can, however, result in two distinct forms, DMD and Becker Muscular Dystrophy (BMD). DMD begins in early childhood, with symptoms arising at age 3, and progresses rapidly causing wheelchair-dependency by age 12, as well as the need for ventilation (Sbiti *et al.*, 2002). BMD, the less commonly occurring form of the disease, is a milder form, which arises mostly from in-frame deletions, resulting in patients having the ability to produce semi-functional dystrophin protein products. Patients with BMD have slower disease progression, with symptoms typically arising at age 12 (Ramellia *et al.*, 2006).

Limb-Girdle Muscular Dystrophy (LGMD) comprises a group of muscular dystrophies with predominant muscle weakness and muscle wasting occurring in the arms and legs. Most often it is proximal muscles such as the muscles of the shoulders, upper arms, pelvic area and thighs that are commonly affected. LGMD has numerous subtypes which are categorized into two broader types: LGMD1 and LGMD2. Those with LGMD1 typically have dominant inheritance, whereas those

with LGMD2 experience autosomal recessive inheritance. Clinical course and age of onset varies greatly between subtypes and even amongst single families, with both childhood and adult onset being reported (Urtasun *et al.*, 1998 & van der Kooi *et al*., 1996). Diagnosis of LGMD is also quite challenging due to high number of loci (more than 50) being reported for mutations (Pegoraro & Hoffman, 2000).

Emery-Dreifuss Muscular Dystrophy (EDMD) has three common types, distinguished by their inheritance patterns: X-linked, autosomal dominant and autosomal recessive. Although the three types differ by their mode of inheritance, all three are characterized by deformities known as contractures beginning in early childhood, which restrict the movement of specific joints (Emery, 2000). Affected individuals also experience slow progressive muscle weakness and atrophy in muscles of the upper arms and lower legs with progression into the shoulders and hips, as well as cardiac problems into adulthood (Emery, 2000). X-linked EDMD is known to be caused by mutations in the *EMD* and *FHL1* genes, whereas autosomal dominant and recessive EDMD are caused by mutations involving the *LMNA* gene (Bonne *et al.,* 2004).

Congenital Musuclar Dystrophy (CMD) is a group of muscular dystrophies apparent at or near birth and are the most common autosomal recessive neuromuscular disorders (Voit, 2001). Over the last two decades more than 13 pathogenic variants have been identified in varying genes to cause CMD (Wang *et al.*, 2010). Common signs of the disease consist of muscle weakness, early onset of "floppiness" or hypotonia, contractures and delay of gross motor development (Voit, 2001).

Myotonic Muscular Dystrophy (MMD) is a multisystemic disease affecting skeletal muscles, heart and central nervous system and is inherited in an autosomal dominant pattern (Harper, 2001). This disorder is characterized by progressive weakness and muscle atrophy as well as prolonged muscle contractions and the inability to relax certain muscles after use (Harper, 2001). MMD is divided

into two types: Type 1 (DM1) and Type 2 (DM2). DM1 is caused by mutations in the *DMPK* gene whereas DM2 is caused by mutations in the *CNBP* gene, also known as *ZNF9* gene. MMD1 is classified by three different phenotypes: mild (age of onset between 20-70 years), classic (age of onset between 10-30 years), and congenital (age of onset between birth to 10 years) whereas MMD2 commonly presents itself in adulthood typically between age 30-60 (Bird, 1999 & Dalton, Ranum, & Day, 2006).

Oculopharyngeal Muscular Dystrophy (OPMD) is characterized by muscle weakness that typically begins in adulthood around the age 40 (Brais *et al.*, 1999). Initial symptoms of the disease consist of droopy eyelids, difficulty swallowing, weakness and wasting of the tongue, and weakness of muscles in the upper legs and hips (Brais *et al.*, 1999). There are two forms of OPMD, distinguished by their inheritance pattern, autosomal dominant or autosomal recessive. For both forms of the disease, OPMD is caused by mutations in the *PABPN1* gene (Marusin *et al.*, 2016).

1.2 Facioscapulohumeral Muscular Dystrophy

Facioscapulohumeral muscular dystrophy (FSHD) is an autosomal dominant disorder characterized by early involvement of muscle weakness and atrophy in facial muscles and shoulder girdle muscles (Padberg, 1982). With disease progression, muscle weakness and atrophy often spreads to the upper arms, pelvic girdle and lower limb muscles (Padberg, 1982). FSHD is the third most common muscular dystrophy, with a birth incidence of approximately 1 in 14,000 (Mostacciuolo *et al.*, 2009). The frequency of occurrence for FSHD is often underestimated due to the high degree of clinical variability in addition to the large proportion of individuals who remain asymptomatic or experience mild symptoms (Deenen *et al.*, 2014). In 1884, Landouzy and Dejerine were first to describe the classical FSHD phenotype with the disease being formerly known as Landouzy-Dejerine's disease (Landouzy & Dejerine, 1884 and Landouzy & Dejerine, 1886). However, it wasn't until 1980 when a rise in interest led to a greater understanding of FSHD,

its clinical variability and its genetic complexities (Wijmenga, Padberg & Moerer *et al.*, 1991). When the disorder was first described, FSHD and its association to chromosome 4 was unknown. However, since then, the fundamental cause of FSHD and the finding of D4Z4 reduced alleles at 4q35 has become clearer (Upadhyaya *et al., 1997)*.

1.3 Clinical characteristics

Patients with FSHD most commonly present with symptoms of weakness starting in the scapula-fixators, with a few patients reporting facial weakness before shoulder weakness (Padberg, 1982). Unique to FSHD patients is the clinical feature which involves distinct asymmetric muscle weakness in the face, shoulder girdle and extremities (Padberg, 1982). In some FSHD patients, progression beyond the shoulder muscle does not occur; however, other patients suffer from weakness of the upper-arm muscles, abdomen, foot-extensor, and pelvic girdle. In patients who suffer from upper-arm muscle weakness, it is often seen that the biceps and triceps have atrophic involvement, whereas the deltoid muscles remain mildly affected late into the disease (Padberg, 1982). When weakness has progressed to the abdominal muscles, it is often noticed that an inward lordotic curvature of the lumbar spine occurs. Muscle weakness progression to the legs is quite variable, with weakness sometimes affecting the pelvic girdle muscles or causing foot drop (Landouzy & Dejerine, 1884). Other characteristics that present within a small subset of FSHD patients, include cardiac conduction defects and compromised respiratory function (van der Maarel, Frants & Padberg, 2007 and Wohlgemuth *et al.*, 2004).

The age of onset for individuals with FSHD is quite variable, due to the irregular nature of disease progression. In more than 90% of affected individuals, patients are symptomatic before the age of 20; however, rare cases have suggested that onset can occur as early as infancy (Padberg, 2004). Although many FSHD patients show symptoms by age 20, other individuals experience mild symptoms or remain asymptomatic for their lifetime (van der Maarel, 2000).

1.4 Genetic defect

FSHD is associated with the deletion of a subset of D4Z4 macrosatellite repeat arrays in the subtelomeric region of chromosome 4, 4q35 (Figure 1.1). The genetic defect in FSHD was first identified by a reduction seen in an *Eco*RI fragment of genomic DNA using the p13E-11 probe compared to healthy individuals (Wijmenga *et al.*, 1992). Non-affected control individuals typically contain between 11 and 100 D4Z4 repeats, with *Eco*RI fragments being 40-300 kb in size, while FSHD patients carry between 1 and 10 repeats on one allele, with *Eco*RI fragments being 10-38 kb in size (Figure 1.1) (Lunt, 1998). The deletion of a subset of D4Z4 macrosatellite repeat arrays occurs in early embryonic development through mitotic rearrangement (van der Maarel *et al.,* 2000).

There are two forms of FSHD, FSHD1, which occurs in over 95% of cases, and the less common form, FSHD2, which occurs in the other 5% of individuals (Jones *et al.*, 2012). FSHD1 is genetically linked to contractions of the macrosatellite D4Z4 repeat array (Wijmenga *et al.*, 1990), whereas FSHD2 shows chromatin relaxation at D4Z4, but does not have a contraction of the D4Z4 locus (de Greef *et al.*, 2010). In majority of patients with FSHD2, the disease is caused by digenic inheritance of a heterozygous mutation in the chromatin modifier gene on chromosome 18, Structural Maintenance of Chromosomes Flexible Hinge Domain Containing 1 (*SMCHD1*), as well as a distally located PAS-containing chromosome 4 (Lemmers *et al.*, 2012). *SMCHD1* is an important gene known for its role in regulating the repression of the D4Z4 array via DNA CpG methylation (Lemmers *et al.*, 2012). Recent evidence however suggests that there is evidence for locus heterogeneity with FSHD2, due to the lack of *SMCHD1* mutations seen in approximately 20% of FSHD2 affected patients. This evidence suggesting the presence of other modifier loci that too are potentially affecting the structure of D4Z4 (Lemmers *et al.*, 2012).

The open reading frame (ORF) for *double homeobox 4* (*DUX4*) gene was mapped in each unit of the D4Z4 repeat arrays remaining after partial deletion associated with FSHD (Gabriels *et al.*, 1999). Initially, *DUX4* was not considered a suitable candidate gene for FSHD because of its lack of introns and polyadenylation signal. However, recent studies have shown that *DUX4* could produce a polyadenylated mRNA from the ORF in the most distal D4Z4 unit that extends into the flanking *pLAM* sequence (Dixit *et al*., 2007). 4q variants were discovered distal to D4Z4, 4qA and 4qB, both of which occur commonly in the Caucasian population (van Geel *et al.*, 2002). Interestingly, for FSHD, the polyadenylation site is required for a pathogenic contraction of the D4Z4 array and is only intact on the permissive 4qA allele, whereas this signal is missing on the non-permissive 4qB allele (refer to Figure 1.1) (Lemmers *et al.*, 2010).

Two full-length isoforms of DUX4 exist with alternative splicing in the 3' untranslated region (Snider *et al.*, 2010). One full-length isoform of DUX4 is detected in FSHD skeletal muscle cells which contains the entire DUX4 ORF and in the 3'UTR has one or two spliced introns, ending in exon 3 (Snider *et al.*, 2009). A second full-length *DUX4* mRNA (*fl-DUX4)* isoform was characterized in induced pluripotent stem cells and in human testis cells by the addition of four exons and a more downstream polyadenylation signal in exon 7 (Figure 1.2) (Snider *et al.,* 2010). In control muscles and in other somatic tissues, a shorter *DUX4* mRNA variant (*s-DUX4*) was discovered because of its ability to remove the carboxy-terminal end of DUX4 while maintaining the amino-terminal double-homeobox domains, ending in exon 3. *s-DUX4* is unique from *fl-DUX4* in that it encodes a non-pathogenic protein (Snider *et al.*, 2010).

1.5 Genetics in FSHD

A high correlation between FSHD disease severity and fragment size has been identified with individuals with a large deletion of the D4Z4 array having earlier-onset disease in addition to rapid progression, compared to those patients with smaller contractions of the D4Z4 locus (Zatz *et al.,*

1995, Tawil *et al.,* 1996 & Bindoff *et al.*, 2006). Currently the existence and precise mechanism for anticipation in FSHD remains uncertain. The anticipation in FSHD was originally described by Zatz *et al.*, 1995 in which observations in multigenerational families showed offspring being more severely affected than parents (Zatz *et al.,* 1995 & Tawil *et al.*, 1996). Although there remains evidence for support of the hypothesis of anticipation for FSHD, FSHD differs from other autosomal dominant disorders by three distinct aspects: 1) the gender of the transmitting parent has not been found to affect the severity of phenotype; 2) there is a high proportion of cases arising de novo; and 3) affected male offspring overall have a reduction in reproductive fitness (Zatz *et al.,* 1995 & Tawil *et al.*, 1996).

1.6 *de novo* FSHD

It is currently estimated that 10%-30% of FSHD patients carry a new mutation (Padberg *et al.,* 1995 & Zatz *et al.,* 1995), and show an array of D4Z4 array lengths varying from 1 to >50 units (van der Maarel *et al.*, 2000). Several studies have shown that approximately half of these reported D4Z4 rearrangements are mitotic in origin, and are likely occurring from postzygotic array contraction during early cell divisions in embryogenesis, resulting in somatic mosaicism. The other half of *de novo* cases likely occur before fertilization (Upadhyaya *et al.,* 1995, Lemmers *et al.,* 2004 & van der Maarel *et al.*, 2000).

1.7 DUX4 function

DUX4 is a double-homeodomain transcription factor encoded within the D4Z4 tandem repeat. DUX4 is a nuclear protein that is normally transcriptionally silenced in healthy individuals after early development; however, in FSHD, truncations of the D4Z4 array leading to fewer than 11 units cause a failure to maintain complete suppression of full-length DUX4. Chromatin relaxation of the D4Z4 array (inability to suppress DUX4 fully), causes occasional bursts of DUX4 expression in a small number of skeletal muscle nuclei (Snider *et al.*, 2010). In healthy individuals, DUX4 is

normally expressed in early development and silenced during cellular differentiation but maintains expression levels within the seminiferous tubules in male testis (Snider *et al.,* 2010). The primary role of DUX4 remains unclear; however, some previously identified targets include cancer-testis antigens, as well as a broad set of genes involved in germ cell maintenance and development and stem cell biology (Geng *et al.,* 2012).

1.8 Epigenetic disease mechanism

Several molecular models have been proposed to elucidate how the deletion of a subset of D4Z4 macrosatellite repeat arrays resulted in the FSHD pathology. Many studies have focused on understanding the chromatin structure of D4Z4 in hopes of detecting possible changes in the chromatin structure in FSHD compared to healthy individuals. In a DNA methylation study, the deletion of D4Z4 arrays at disease alleles caused D4Z4 arrays to be hypomethylated (Figure 1.1) (van Overveld *et al.,* 2003). Interestingly, in a small population of phenotypic FSHD patients without the D4Z4 deletion, hypomethylation of the D4Z4 array was still very pronounced. This evidence suggested that even though hypomethylation of the D4Z4 array occurred in FSHD patients, it did not sufficiently cause FSHD (van Overveld *et al.,* 2003). Further research also showed that an inverse relationship between the level of DNA methylation at the D4Z4 array correlates with FSHD disease progression and penetrance (van Overveld *et al.*, 2005).

1.9 Transcriptional Cascade caused by mis-expression of DUX4

Unlike other disorders which are caused by structural mutations within the disease gene, FSHD involves an intricate cascade of epigenetic events after the deletion of a subset of D4Z4 macrosatellite repeat arrays (van der Maarel, Frants & Padberg, 2007). Several studies have shown that *DUX4* expression induces the expression of genes involved in muscle atrophy, such as muscle *RING finger 1 (MuRF1) and atrogin-1/MAFbx*, sensitizes cells to oxidative stress, thereby inducing the expression of *mu-crystallin (CRYM),* inhibits the *MYOD1* gene resulting in differentiation

abnormalities, and causes a *p53*-dependent myopathy in mouse muscles *in vivo* (de Palma *et al.*, 2008, Vie *et al.*, 1997 and Wallace *et al.,* 2011). Recent evidence has also shown that *paired-like homeodomain 1* (*PITX1*), *tripartite motif containing 43* (*TRIM43*), *and methyl-CpG binding domain protein 3-like 2* (*MBD3L2*) are also upregulated in FSHD (Dixit *et al.*, 2007 and Ferreboeuf *et al.*, 2014) (Figure 1.3). Although *DUX4* is emerging as an intriguing FSHD candidate because of its position within the D4Z4 repeats, the downstream transcriptional abnormalities, in addition to the other up-regulated genes seen in FSHD patients, should not be ignored.

1.10 PITX1 function

When an analysis was performed comparing genome-wide expression profiles of patients with FSHD in relation to 11 neuromuscular disorders, *PITX1* was the most dramatically up-regulated gene seen in both affected and unaffected muscle biopsies from FSHD patients (Dixit *et al.*, 2007). PITX1 is a homeobox transcription factor which was first known for its role in pituitary formation (Lamonerie *et al.*, 1996). Further research using CBA x C57B16 mice has shown that in hindlimbs, *Pitx1* expression is present in the lateral plate mesoderm, specifically within the posterior portion of the embryo; interestingly however, its expression is only detectable in the hindlimbs and not in the forelimbs (Lanctôt *et al.*, 1997). In mice, *Pitx1* is also suggested to have roles in proliferation and differentiation of select mesenchymes and is essential for proper bone development of the hindlimbs and mandible (Lanctôt *et al.*, 1999). Hindlimb structural abnormalities are a hallmark of *Pitx1* knockout mice, demonstrating left-right asymmetry in the abnormally formed hindlimbs (Marcil *et al.,* 2003). Although *Pitx1* seems to play vital roles in the pituitary gland and hindlimbs, to date no known human disease has reported up-regulated expression levels of PITX1 (Pandey *et al.*, 2012).

PITX1 is a unique up-regulated gene in FSHD because it is the only known direct transcriptional target of DUX4 (Dixit *et al.*, 2007). Although the role of PITX1 in postnatal muscles is currently

unclear, the apparent FSHD-specific up-regulation suggests it may provide a molecular basis for the clinical symptoms present in FSHD patients. Further support for PITX1 and its potential role in FSHD was shown *in vivo* using tet-repressible muscle-specific *Pitx1* transgenic mice (Pandey *et al.*, 2012). In a study by Pandey *et al.,* 2012, *Pitx1* transgenic mice suffered from muscle wasting within several muscles, developed mild necrosis and cellular infiltration, all of which are similarly experienced in patients with FSHD (Pandey *et al.*, 2012).

1.11 MuRF1 function

MuRF1 belongs to a subgroup of the TRIM family and is a muscle specific E3 ubiquitin ligase (Centner *et al.,* 2001). It is found to be transcriptionally up-regulated before the onset of atrophy in skeletal muscles (Bodine *et al.*, 2001). Skeletal muscle atrophy is often caused by a variety of stressors including glucocorticoids, oxidative stress, malnutrition, and inflammation. These stressors can influence an array of transcriptional mediators by ultimately causing changes in their expression levels. Downstream of these transcriptional mediators, the MuRF1 promoter region is then bound by the up-regulated transcriptional mediators resulting in increased MuRF1 expression levels within skeletal muscles (Bodine & Baehr, 2014). Localization of MuRF1 has been detected in three important regions of the muscle fiber, at the M-line of the sarcomere, at the Z-lines and in the nucleus (Centner *et al.*, 2001, McElhinny *et al.*, 2002). Although it still remains unclear how all the molecular mechanisms work to control structural and regulatory proteins in striated muscles, and in this case how E3 ubiquitin ligase MuRF1 is regulated, one candidate gene in particular, *SUMO-3*, has been shown to bind to MuRF1's RING domain and regulate its localization pattern and nuclear import (Dai and Liew, 2001 and Bodine and Baehr, 2014).

In a study by Vanderplanck *et al.* 2011, MuRF1 protein levels were increased in FSHD myotubes compared to healthy control myotubes. Interestingly, immunofluorescence also detected co-localization of MuRF1 and DUX4 within the nuclei of DUX4-expressing myotubes. Evidence of

MuRF1 up-regulation before the onset of atrophy in skeletal muscles and its up-regulation in FSHD myotubes suggests its potential as an FSHD marker.

1.12 Treatment Options

Despite the progress made in understanding the underlying genetic and pathophysiological complexities of FSHD, no curative treatment options have been established. Currently, standard disease management options include physical therapy, exercise, management of respiratory dysfunction and orthopedic intervention (Tawil *et al.*, 2014). After diagnosis, patients are often referred to physical therapists to establish an appropriate exercise plan that may enhance mobility and reduce episodes of falling. For patients who wish to remain active, physical therapists will design specialized exercise programs that utilize appropriate weights and resistances to cater to each patient's physical limitations and cardiovascular status. Exercise with moderate weight and/or resistance is not damaging to patients suffering from muscle weakness or atrophy with FSHD (Milner-Brown & Mill 1988). Although respiratory problems occur only in patients most severely affected, ventilator support (e.g., nocturnal bilevel positive airway pressure or BiPAP) should be used in addition to routine pulmonary function assessments. Lastly, orthopedic intervention is another management option for some FSHD patients. Upon surgery, an evaluation of each patient is done to determine the potential benefits and functionality the surgery would have for that individual. Ankle or foot orthopedic surgeries have been implemented to help improve the mobility of patients with foot drop. Surgical fixation of the scapula to the chest is another surgery performed in patients with FSHD with limited shoulder range of motion. Range of motion using the shoulder is often limited in patients with periscapular muscle weakness. After surgical fixation patients often have improvement in their range of motion; however, the duration of this improvement is variable, depending on the progressive nature of weakness within each individual.

1.13 Antisense Therapy

Antisense therapy is a strategy that uses short single-stranded DNA/RNA-like molecules called antisense oligonucleotides (AONs), to selectively hybridize to nascent pre-mRNA via Watson-Crick base pairing (as reviewed in Touznik *et al.*, 2014). AONs are usually between 8 and 30 base pairs in length and once bound to their target pre-mRNA sequence, AONs can act via exon skipping, splice modulation or through inhibition of gene expression via RNA degradation (as reviewed in Touznik *et al.*, 2014).

Currently, antisense therapy shows considerable promise for treating an array of disorders; however, the prominence of this theoretical approach did not occur overnight. Since the late 1970s, great improvements have been made in antisense-mediated RNA regulation after Zamecnik *et al.* demonstrated that transfection of a short antisense (complementary) DNA sequence could sufficiently inhibit expression of genes (Zamecnik *et al.*, 1978). Several changes made to first generation AONs (i.e. phosphorothioate deoxynucleotides (PS-ODN)), improved the feasibility of these drugs (Agrawal *et al.*, 1995 and Campbell *et al.*, 1990). Although beneficial improvements were made, first generation AONs still have room for optimization. A variety of problems and/or challenges were associated with first generation AONs. First, systemic drug delivery was hardly, if at all, attainable because these AONs could not easily cross the lipid bilayer of cells (Torchilin, 2006). Secondly, induction of harmful off-target effects was often reported, mainly resulting in immune responses through toll-like receptors (Muntoni *et al.,* 2011). Another associated problem was the highly degradable nature of AONs by intracellular and extracellular nucleases (Lee & Yokota, 2013).

Several new chemistries have since been developed to resolve some of the challenges faced with first generation AONs, with many of the new chemistries showing great success in clinical trials. New chemistries such as 2'O-methylphosphorothioate-modified (2'OMePS) antisense oligo, phosphorodiamidate morpholino oligomer (PMO), 2'methoxyethoxy (2'-MOE-modified)

oligonucleotides, vivo-morpholinos (vPMOs), PMOs with peptide conjugates (PPMOs), peptide nucleic acids (PNAs) and locked nucleic acid (LNA) have been developed to increase stability, reduce off-target effects and decrease nuclease susceptibility (Lee & Yokota, 2013). They have also been designed to replace the deoxyribose/ribose back-bone using a similar chemistry that is less readily targeted by nucleases or DNA/RNA-binding proteins (Lee & Yokota, 2013).

In vivo studies exploring gene therapy using AONs suggests great promise for potential treatment of FSHD (Pandey *et al.*, 2014). Two chemistries, in particular, phosphorodiamidate morpholino oligomers (PMOs) and locked nucleic acids (LNA), are strong candidates for exploration of therapeutic potential.

PMOs are unlike first generation ASOs, as they are unrecognizable by nucleases, they have increased binding efficiency to RNA targets, they are not readily targeted by metabolic degradation, and they do no activate toll-like receptors (Lee & Yokota, 2014). In comparison to other chemistries, such as 2'-OMePS or PPMOs, PMOs have relatively low levels of toxicity (Summer & Weller, 1997). PMO chemistry has replaced the phosphodiester backbone with a phosphorodiamidate linkage, resulting in little charge of the molecule (Wang *et al.*, 2014). The chemistry has also incorporated morpholino rings opposed to the deoxyribose/ribose rings used in conventional nucleic acid chemistries (Lee & Yokota, 2014). One ongoing challenge associated with PMO chemistry is the relative low delivery efficiency *in vivo*. Current work by Marsollier *et al.* 2016 shows great potential for the use of PMO chemistry in FSHD. Using immortalized FSHD cells, this group showed that transfection with PMOs targeting either the DUX4 mRNA polyadenylation signal or the cleavage site efficiently suppressed the expression of *DUX4* as well as other abnormally expressed downstream target genes of DUX4 (Marsollier *et al.*, 2016). In an *in vivo* study using muscle-specific *Pitx1* transgenic mice, Pandey *et al.*, 2014, also showed support

for the use of PMOs in FSHD. In this study they found that mice who received intravenous injections of octaguanidinium dendrimer-conjugated morpholino (vivo morpholino) to *Pitx1*, had significantly reduced expression of PITX1 in both the triceps and quadriceps.

Comparatively, the other strong antisense chemistry candidate, LNAs, are composed of a class of RNA analogues, where the furanose ring, making up the ribose sugar, is locked in a confirmation which mimics the RNA structure (Kauppinen *et al.,* 2005). Introduction of a 2'O-4'C-methylene linkage effectively locks the furanose ring in a C3'-end conformation (Figure 1.4) (Nielsen *et al.*, 2004). LNA-modified oligonucleotides show exceptional thermal stability when heteroduplexes are formed with the target RNA molecules, increased melting temperature, impose significant protection against nucleolytic degradation and have high binding affinity (Koshkin *et al.,* 1998, Nielsen *et al.*, 2004 and Braasch *et al.,* 2001). Oligonucleotides composed of modified LNA segments flanking a central DNA gap that can be phosphorothioated are known as gapmers (Figure 1.5). Modifications to the LNA gapmer chemistry have also shown great success and are compatible with RNase H-mediated RNA cleavage. LNA/DNA/LNA gapmers consisting of 6 or more nucleotides within the DNA gap are essential for eliciting RNase H activity. Fully modified 11 mer LNA or 11 mer LNA/DNA mixmer oligonucleotides, however, are unable to elicit RNase H-mediated cleavage (Kurreck *et al.,* 2002 and Elmen *et al.*, 2004). Further understanding has confirmed that RNase H activity can be partially recruited under the presence of six DNA nucleotides. However, a DNA gap size consisting of between 7 and 10 nucleotides is optimal for complete RNase H activity (Kurreck *et al.,* 2002 and Frieden *et al.*, 2003). Once an LNA gapmer is bound to its target RNA strand, a heteroduplex is formed which initiation RNase H-mediated cleavage of the RNA target strand, causing efficient gene silencing. In a study by Lee *et al.* 2012*,* ASOs containing 3-4 modified nucleic acid residues (LNAs) to induce RNase H-mediated degradation were used in a myotonic dystrophy type 1 (DM1) mouse model to target the pathogenic

RNA causing abnormal transcripts (Lee *et al.,* 2012). The authors reported that the LNA gapmer was successful at knocking down the abnormal transcript in cell culture and in the DM1 mouse model (Lee *et al.,* 2012). This study provides evidence that modifications to the LNA chemistry can have beneficial effects and could be a good antisense chemistry for targeting DUX4 in FSHD.

1.14 Current FSHD animal models

Due to the unique nature of FSHD and its complex genetic components, the disease is not yet entirely understood. Progress with therapeutic discovery and specific treatments options for patients has been slow because of the lack of suitable animal models. Recent understanding of the disease has led to advances in the genetic premise causing FSHD and have enabled researchers to move forward with recapitulating the disease in preclinical animal models.

With the unusual nature of the disease mechanism associated with FSHD, it is unlikely that any one model will entirely replicate the disease (Lek *et al.*, 2015). One of the most significant hurdles with FSHD is that the D4Z4 macrosatellite encoding DUX4 is unique to higher primates (Leidenroth & Hewitt, 2010), which denies researchers the opportunity to work with the natural model of the disease within a laboratory setting (Lek *et al.*, 2015). In addition to the challenges associated with introducing DUX4 expression into non-primate species (Lek *et al.*, 2015), there lacks definitive proof that the genetic defect in FSHD is caused by DUX4 alone. Emerging evidence shows the potential role of other candidate genes in FSHD, which should be considered when attempting to model FSHD preclinically. Consequently, there lie a number of associated weaknesses with the current FSHD animal models based solely on the DUX4 expression (refer to Table 1.1). Until the specific roles of other candidate genes become known, a suitable disease model which encompasses all genetic and pathophysiological attributes of the human disease cannot be derived. Lastly, although currently one model may not be entirely suitable for modeling

FSHD, the available models (refer to Table 1.1), based on DUX4 solely or based on other candidate genes, can still be beneficial and may further advance our understanding of FSHD.

1.15 Culture conditions

Several groups have confirmed that *DUX4* is up-regulated in patient myoblasts, with many groups showing detectable levels of DUX4 at both the mRNA and protein level (Dixit *et al.*, 2007, Tassin *et al.*, 2013). Although many groups have had success at detecting DUX4, its detection remains challenging. Snider *et al.* determined that 1 in 1000 nuclei were positive for DUX4 in proliferating primary FSHD myoblasts. In a similar study conducted by Tassin *et al.,* 2013, low expression of DUX4 protein was confirmed via Western blot analysis in proliferating FSHD myoblasts. However, FSHD primary myoblasts differentiated for 4 days showed increased DUX4 expression by Western blot analysis. The increased DUX4 protein levels resulted in approximately 1 in 200 nuclei being DUX4 positive (Tassin *et al.,* 2013). The observed increase in DUX4 protein levels after differentiation suggested that *DUX4* transcription could be influenced by the physiological state of the cells and perhaps the surrounding culture environment (Pandey *et al.*, 2015).

In a study done by Tehrani *et al.*, 2014, using cells cultured from human endometrium, dexamethasone, a glucocorticoid, was shown to accelerate and increase muscle differentiation in myocytes (Tehrani *et al*., 2014). In another study, when dexamethasone was supplemented into culture media, the polygonal epithelial morphology of hepatocytes was maintained and an increase in hepatocyte survival *in vitro* was also noticed (Laishes *et al.*, 1976). Another media additive, also shown to influence cells in culture is KnockOut Serum Replacement (KOSR, Thermo Fisher Scientific), which was reported to increase the growth rate of human embryonic stem cells (hESCs) (Koivisto *et al.*, 2004). In a study by Skottman *et al.*, 2006, hESC cells cultured in culture media supplemented with KOSR, caused a variety of genes involved in the regulation of transcription, RNA processing, and cell proliferation to be differentially expressed (Skottman *et al.,* 2006).

Due to the great success of others who added dexamethasone or KOSR to the growth medium to influence cells in culture, Pandey *et al.* 2015 explored the effects of medium supplemented with or without dexamethasone and KOSR, in cultured immortalized FSHD myoblasts (Pandey *et al.*, 2015). Interestingly, supplementation of dexamethasone into the culture medium containing KOSR showed lower expression of DUX4 in immortalized FSHD cells compared to expression levels of DUX4 detected with the implementation of just KOSR into the culture medium (Pandey *et al.*, 2015). In addition to various applications of culture conditions for increased DUX4 expression, several different detection strategies using different reverse transcriptases (RTs) and primers for cDNA synthesis and DUX4 detection have also been explored (Lemmers *et al.,* 2010, Stadler *et al.,* 2013, and Jones *et al.,* 2012). However, due to the fact that there are currently multiple FSHD cell lines available, many of which differ in their characteristics (i.e. contraction number, severity, age or muscle type), determining the best culture conditions and the most effective detection strategy for DUX4 transcripts in FSHD cells is proving to be cell line dependent (Pandey *et al.*, 2015, Tsumagari *et al.*, 2011 and Block *et al.*, 2015).

1.16 Skeletal Muscle Growth and Differentiation

Skeletal muscles are derived from somites during embryogenesis. Within the body, most skeletal muscles come from dorsally located cells of the somite (Bharathy *et al.*, 2013). In response to signals from the notochord, a structure known to serve as a source of centrally located signals that pattern surrounding tissues and specify cell types in forming somites (Yamada *et al.*, 1993), expression of the paired homeobox transcription factors paired box 3 (Pax3) and paired box 7 (Pax7) is induced, specifically in muscle progenitor cells, and results in muscle cell specification (Bharathy *et al.*, 2013). Pax3 induces the expression of the myogenic regulatory factors (MER), Myogenic factor 5 (Myf5) and Myogenic Differentiation (MyoD), which results in cell commitment to the myogenic lineage. Differentiation of skeletal myoblasts occurs via two classes

of transcription factors - Myogenic regulatory factors (MRF), such as MyoD, Myf5, MRF4 and Myogenin, and Myocyte Enhance Factor (MEF2), such as MEF2-A, -B, -C and –D. MyoD expression is selectively restricted to skeletal muscle cells, but is epigenetically regulated in non-muscle cells by DNA methylation. Once MyoD is induced in committed myoblasts, expression of MyoD enables cell cycle exit by regulating the expression of p21 and myogenin. Terminally differentiation multinucleated myotubes then express late differentiation markers known as myosin heavy chain (MHC) and Troponin T (Refer to Figure 1.6) (Bharathy *et al.*, 2013).

1.17 Rationale for Project

As discussed above, antisense therapy is an attractive approach for knockdown of target mRNA to restore the function of deficient genes or silence mis-expressed genes, within a broad range of progressive cancers, infectious diseases and genetic diseases (Du, 2009). Ongoing challenges with the treatment of diseases by antisense technology have paved the way for new and improved chemistries such as LNA gapmers. Overall, FSHD is thought to be an autosomal dominant gain-of-function disease caused by the mis-expression of DUX4 in patient skeletal muscles (Tassin *et al.*, 2013). This suggests that DUX4 is a promising therapeutic target for antisense therapy. The purpose of this study was to investigate the efficacy of LNA gapmers for the treatment of FSHD by targeting *DUX4* in immortalized FSHD cells. My hypothesis for this project is that implementation of antisense oligonucleotides, using LNA gapmer chemistry, could suppress the expression of DUX4, as well as other downstream targets mis-expressed in FSHD patients. To test this hypothesis, I had three main aims. I first sought to determine the most sensitive detection strategy for DUX4 mRNA transcripts in FSHD cells. I next sought to determine whether culture conditions could affect the expression of DUX4 in FSHD cells. Lastly, I sought to investigate the efficacy of LNA gapmers targeting different locations on *DUX4* mRNA, in FSHD patient cell lines, to determine the most effective LNA gapmers at suppressing DUX4 expression.

Table 1.1: Current FSHD animal models and their features

Model (animal)	Genetic/biological modifications	Expression pattern	Cellular phenotype	Refs
AAV6-DUX4 (mouse)	TA injection of AAV6-DUX4 into C57BL/6 mice aged 6-8 weeks	DUX4 protein expression in TA muscle; cytoplasmic and myonuclei staining	DUX4-induced cell death via a p53 dependent pathway	Wallace *et al.* , 2011
D4Z4-2.5 (mouse)	Transgenic insertion of 2.5 copies of D4Z4 from permissive haplotype of pathogenic allele	DUX4 transcripts detected in ES cells, tongue, testes, heart, dia, pec, mas, orb, qua, TA, gas. DUX4 transcripts also detected in myoblast, and mytoubes	Satellite cell derived myoblasts with DUX4-positive nuclei fail to fuse into myotubes	Krom *et al.* , 2013
D4Z4-12.5 (mouse)	Transgenic insertion of 12.5 copies of D4Z4 from permissive haplotype of pathogenic allele	DUX4 transcript detected in ES cells and testes Muscle expression in pec, qua, TA	Unspecified	Krom *et al.* , 2013
iDUX-2.7 (mouse)	Doxycycline-inducible *DUX4* transgene on the X chromosome	Transcript level highest in retina, testis, brain; lower levels in skin, thymus, kidney, lung DUX4-positive nuclei in myotubes (5%) and myoblasts (1.5%)	Growth inhibition of DUX4-positive myoblasts and differentiation of myotubes DUX4-positive cells show imparied contribution to myogeneic regeneration	Dandapat *et al.* , 2014
DUX4 transgenic (zebrafish)	Transgenic zebrafish expressing MHCK7 (muscle-specific)-driven DUX4	MHCK7 activity in skeletal muscle Detected in myocardium	Unspecified	Wallace *et al.* , 2011
DUX4 RNA injection (zebrafish)	Microinjection of human DUX4-fl mRNA into one cell stage	Approximately 1 RNA molecule per 1000 cells before somitogenesis	Aberrant localization of myogenic cells in the head region	Mitsuhashi *et al.* , 2013
Xenograft (mouse)	Human muscle engraftment into immunodeficient mice	DUX4 expression was detected in xenografth extracted from mouse TA muscle	FSHD biomarker profile maintained in xenograft	Zhang *et al.* , 2014
FRG1 (mouse)	Transgenic insertion of FRG1 driven by a human skeletal α - actin promoter	Skeletal muscle	Evidence of aberrant alternative splicing of specific pre-mRNAs	Gabellini *et al.* , 2006
FAT1 (mouse)	Kockout of *Fat1*	Loss of Fat1 in Pax3-derived cells	Altered myoblast migration polarity	Caruso *et al.* , 2013
Pitx1 (mouse)	Transgenic overexpression of *Pitx1* induced in the absence of doxycycline	PITX1 protein was ~threefold higher in skeletal muscle	Upregulation of p53 in PITX1-expressing muscle groups	Pandey *et al.* , 2012

Abbreviations: AAV6, adeno-associated virus 6; dia, diaphragm; ES, embryonic stem; gas, gastrocnemius; mas, masseter; orb, orbicularis; pec, pectoralis; qua, quadriceps; TA, tibialis anterior. Modified from Lek *et al.*, 2015.

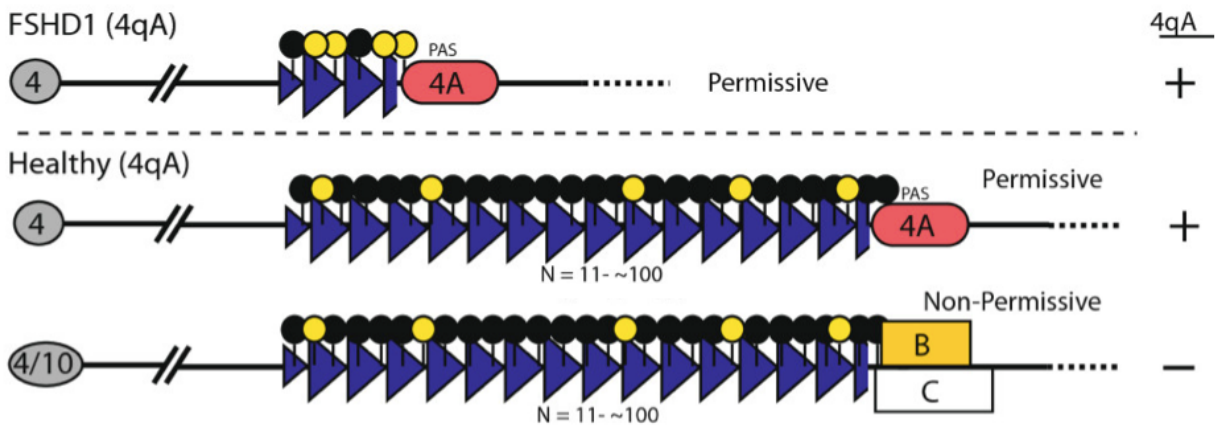

Figure 1.1: Schematic overview of epigenetic and genetic changes in FSHD compared to Healthy individuals

In healthy individuals, their polymorphic macrosatellite repeat consists of more than 10 D4Z4 repeat units. In FSHD1, there is a contraction of the D4Z4 allele, resulting in between 1 and 10 D4Z4 repeat units, whereas in FSHD2 the D4Z4 allele is contraction-independent. There are two main allelic variants in the subtelomere distal to the repeat arrays, known as 4qA and 4qB. Both FSHD1 and FSHD2 are exclusively linked to the 4qA subtelomere allelic variants. Both FSHD1 and FSHD2 are associated with epigenetic hypomethylation of the D4Z4 array. Yellow circles represent hypomethylated CpGs. Black circles represent hypermethylated CpGs. Abbreviation PAS, DUX4 polyadenylation signal. Modified from Jones *et al.*, 2014.

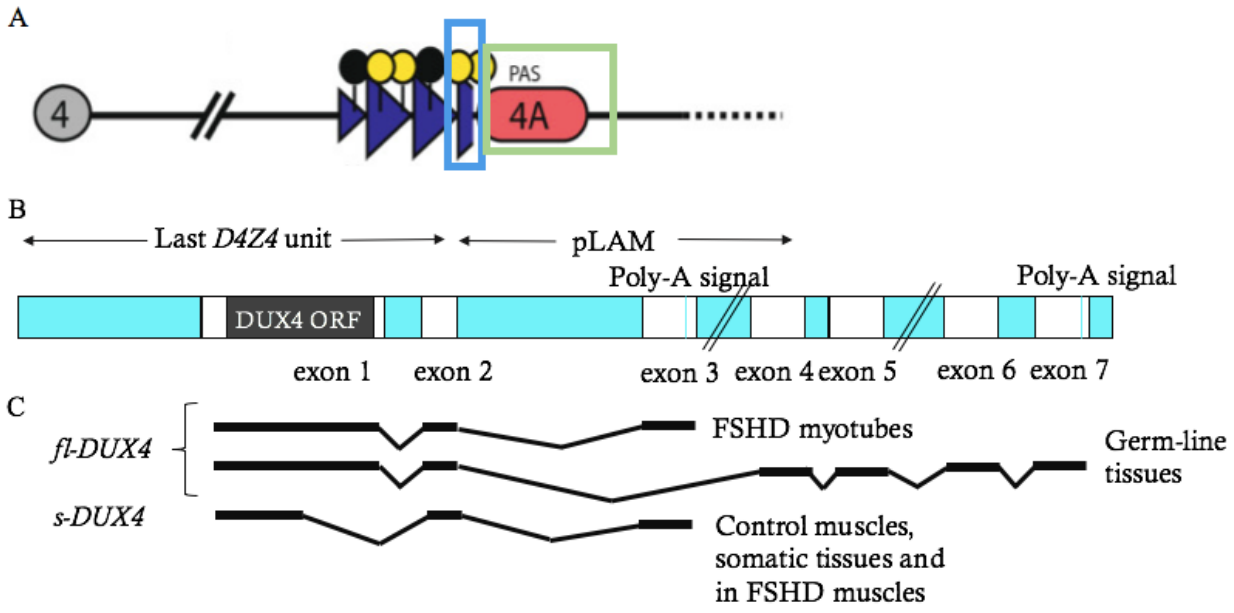

Figure 1.2: *DUX4* mRNA variants

A. Contraction of D4Z4 macrosatellite repeats in FSHD1 relaxes the chromatin structure, causing an induction of DUX4 expression from the distal-most repeat unit (indicated by blue box). Polyadenylated DUX4 transcripts expressed from the 4qA allele (indicated by green box) are stable and translate into a toxic transcription factor, DUX4. Modified from Jones *et al.*, 2014. B. Schematic representation of the distal-most D4Z4 repeat, the pLAM region or 4qA allele or permissive allele, and the distally located exons. The DUX4 ORF is within the first exon. Two poly-A signals were reported in exons 3 and 7. The pLAM region is associated with the 4qA allele. C. Two *fl-DUX4* mRNA isoforms. *fl-DUX4* mRNA detected in FSHD myoblasts contain the full ORF in exon 1 and end in exon 3. These mRNAs were derived from chromosome 4. fl-DUX4 was also detected in germline tissue and contain the full ORF in exon 1, but have 4 addition exons, 4, 5, 6 and 7. *s*-DUX4 was detected in healthy unaffected muscles (patients without the FSHD phenotype), in somatic tissues and in FSHD affected muscles. Modified from Vanderplanck *et al.*, 2011.

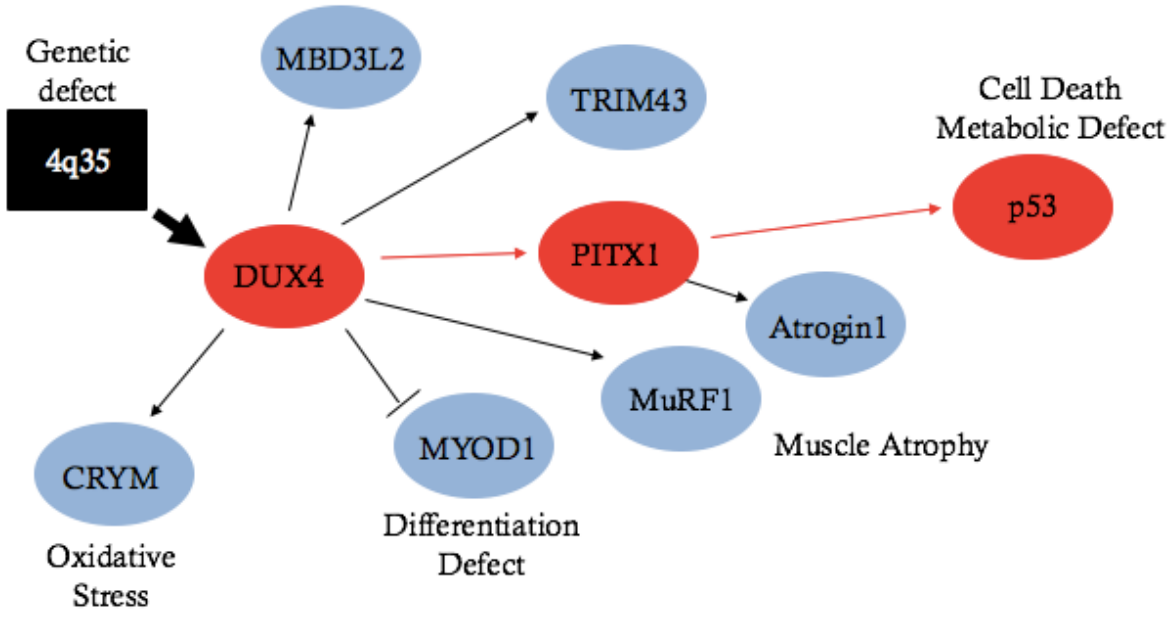

Figure 1.3: Transcriptional cascades downstream of DUX4 in FSHD

Mapped within the D4Z4 element at 4q35 is a transcription factor DUX4. DUX4 directly targets PITX1, a gene up-regulated in FSHD compared to 11 neuromuscular disorders. PITX1 up-regulation induces E3 ubiquitin ligases (Atrogin1 and MuRF1), which are associated with atrophy in adult skeletal muscles. Among the PITX1 target genes is p53 which has shown to have a role in apoptosis in FSHD. DUX4 inhibits *MYOD1* causing inhibition of the MYOD1 target genes in FSHD. DUX4 also induces the expression of the *mu-crystallin* (*CRYM*) gene. Other robust markers for DUX4 expression are MBD3L2 and TRIM43 which are up-regulated in FSHD fetal and adult biopsies. Legend: Activate: → Inhibit: ---|. Figure adapted from Vanderplanck *et al*., 2011.

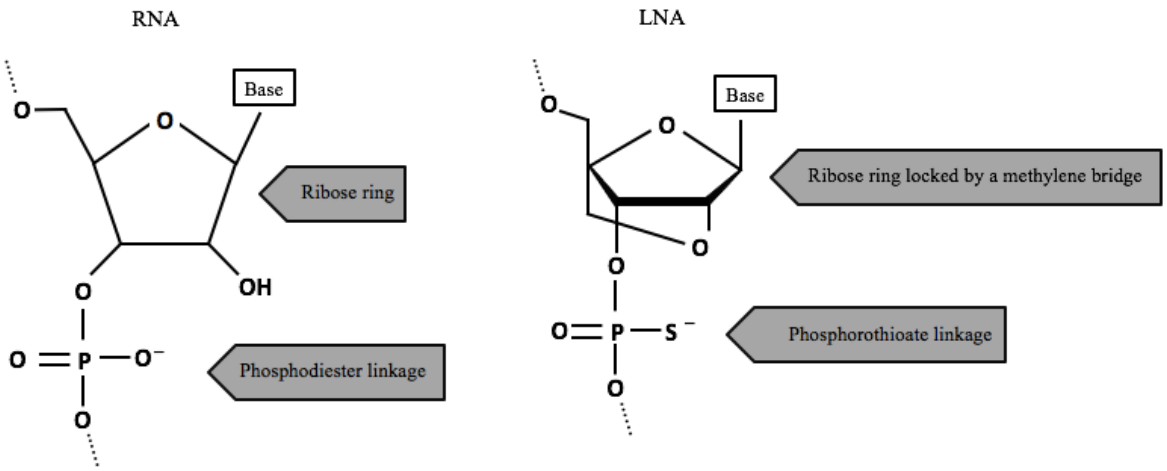

Figure 1.4: Molecular structure of LNA antisense oligonucleotide chemistry compared to RNA

Locked nucleic acid (LNA) structure contains a furanose ring of the ribose sugar. The key difference between DNA and LNA is the introduction of a 2'O-4'C-methylene linkage, which imposes a locked RNA-mimicking conformation.

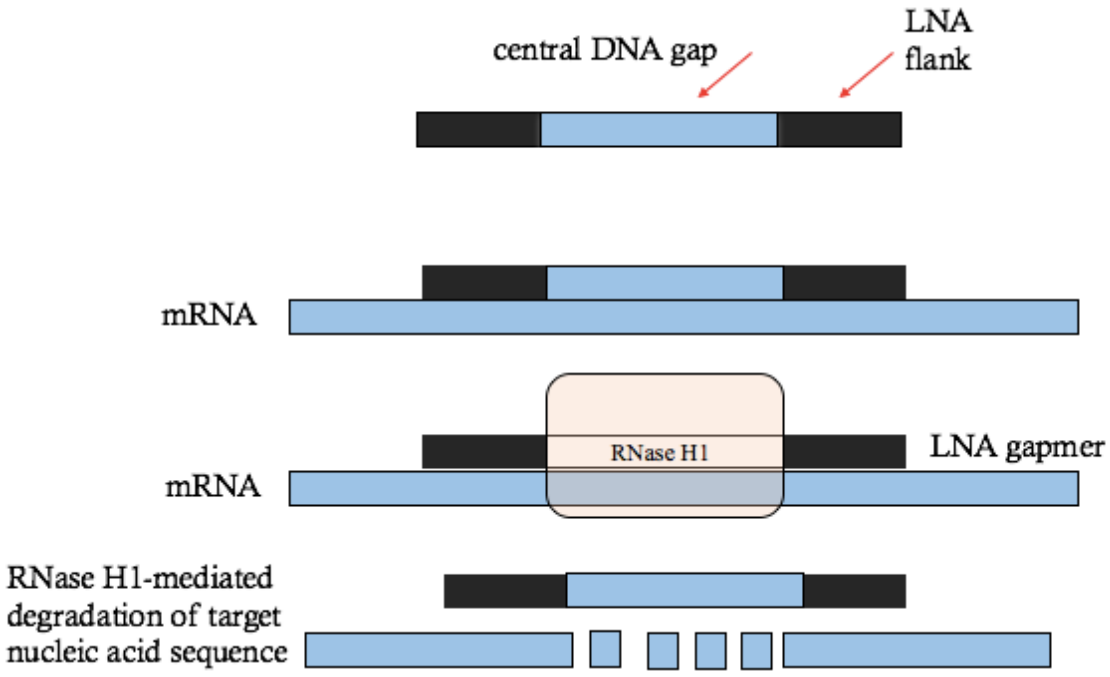

Figure 1.5: Mechanism of antisense silencing via RNase H1-mediated degradation

RNase H1-mediated degradation of target mRNA can occur via LNA gapmers. LNA gapmers are composed of a central DNA gap and flanked by LNA monomers at the 5' and 3'-ends. The central DNA gap works through RNase H1 activity, whereas the LNA flanks are used to target binding affinity to the mRNA sequence. Figure adapted from Lee and Yokota, 2014.

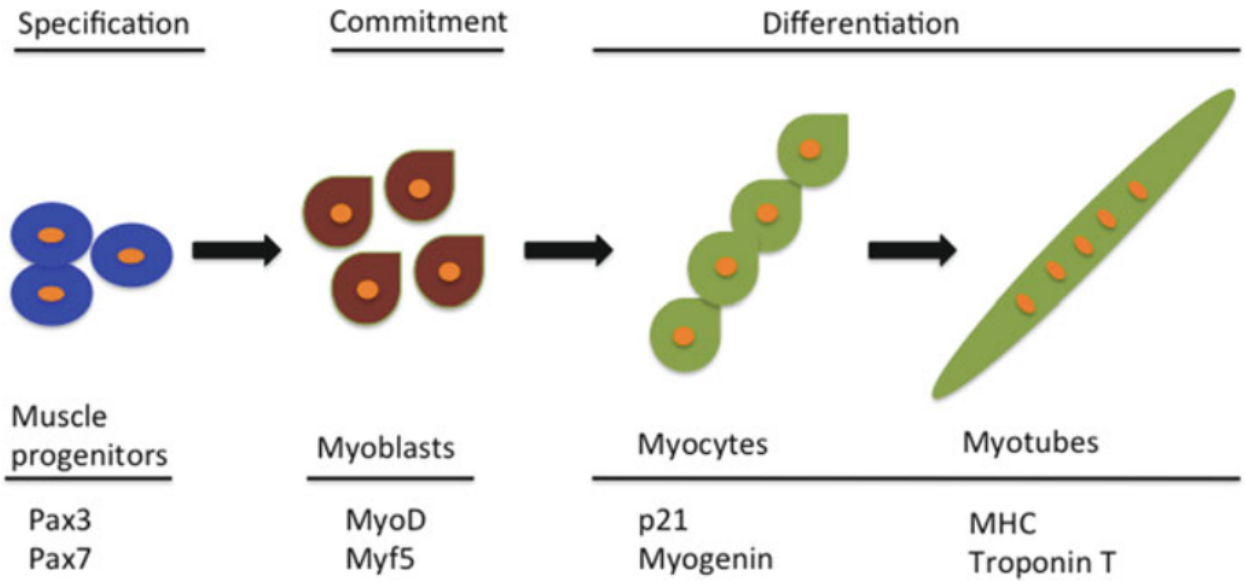

Figure 1.6: Schematic representation of skeletal muscle differentiation

Muscle progenitors cells positive for Pax3/Pax7 initiate myogenic lineage commitment. Cells expressing both MyoD and Myf5 undergo expansion and proliferation to become myoblasts. Upon the initiation of differentiation, myoblasts exit the cell cycle and myocytes begin to express two differentiation markers; p21 and Myogenin. Terminally differentiated multinucleated myotubes positively express myosin heavy chain (MHC) and Troponin T. Taken from Bharathy *et al*., 2013.

Chapter 2

Materials and Methods

2 Materials and Methods

2.1 Human Myoblasts Cell lines and stock management

Anne Bigot and Vincent Mouly at the Institute of Myology, Paris, kindly provided immortalized human myoblasts (refer to Table 2.1). In brief, the patient myoblast cell line was derived from a patient with FSHD with 2 *D4Z4* units from a 27-year-old male, termed KM186. The control myoblasts were derived from the semitendinosus muscle of a 41-year-old male, termed KM155. More specifically, KM155 control myoblasts were derived from a healthy unaffected individual confirmed without the FSHD genotype (referred to in Figures 3.3 A & 3.4 A as "Healthy KM155"). The second set of immortalized myoblasts was kindly provided by Jennifer Chen at the University of Massachusetts Medical School (refer to Table 2.1). In brief, this patient myoblast cell line was derived from a biceps biopsy of a 66-year-old man with FSHD, termed 15ABic. The control myoblasts were derived from a biceps biopsy of the 60-year-old sister of the patient, termed 15VBic. More specifically, 15VBic control myoblasts were derived from a healthy unaffected individual confirmed without the FSHD genotype (referred as Healthy 15VBic). All immortalized human myoblast cell lines used for the purpose of this project were immortalized as previously reported (Mamchaoui *et al*, 2011). In brief, cyclin-dependent kinase 4 (CDK4) and human telomerase reverse transcriptase (hTERT) cDNA were inserted into pBabe vectors containing neomycin- and hygromycin-resistance genes.

Once cell lines KM186, KM155, 15Abic and 15Vbic had reached 80% confluency, cells were frozen at a concentration of approximately 3.5 x 10^6 cells/mL in 1 mL of Recovery™ Cell Culture Freezing Media (Gibco). Stock vials were frozen in a Nalgene™ Cryo Freezing Container (Thermo Fisher Scientific), overnight at -80°C. 24 hours after freezing at -80°C, all stock vials were moved into liquid nitrogen (-196°C), for long-term storage.

2.2 Cell Culture Methods

Three cell culture methods were used for detection of *DUX4* in non-treated immortalized KM186, KM155, 15ABic, and 15VBic cell lines. Refer to Table 2.2 for the list of culture reagents used in each corresponding condition. Myoblasts were grown in their corresponding growth medium (see Table 2.2), at 37 °C under 5% CO_2. Once myoblasts reached 80% confluency, myoblast cultures were differentiated by replacing the growth medium with differentiation medium (refer to Figure 2.1). Undifferentiated myoblasts were collected at day 0, and differentiated myotubes were collected at days 3, 6 and 9 (refer to Figure 2.1, for culture schedule) and samples were analyzed by reverse transcription polymerase chain reaction (RT-PCR).

2.3 The cDNA Synthesis and RT-PCR

Total RNA from non-treated (NT) KM186 myotubes, NT KM155 myotubes, NT 15Abic myotubes, NT 15Bbic myotubes, treated 15Abic myotubes and treated 15Vbic myotubes, were extracted using TRIzol Reagent (Life Technologies) according to the manufacturer's protocol. In brief, spent media was aspirated, and 1 mL of TRIzol reagent was added to each well in a 12-well plate. Each well was rinsed 10 times with TRIzol to ensure detachment of all cells, followed by collection of the 1 mL of TRIzol containing cells. All collected samples were stored on ice, vortexed for 15 seconds at maximum speed and then stored at -80°C until further use. When ready for use, all samples were thawed on ice for 15 minutes; once thawed 200, µL of chloroform was added to each sample. Samples were mixed by shaking vigorously for 15 seconds, followed by incubation at room temperature for 2 minutes. All samples were then spun down at 12,000 g for 15 minutes at 4°C. After centrifugation, three layers including the RNA layer (top), DNA layer (middle), and protein layer (bottom) were visible. The bottom protein layer was removed and all samples were spun down at 12,000 g for 15 minutes at 4°C. The top RNA layer (clear aqueous

phase) was then transferred into a new tube and 500 µL of molecular grade isopropanol and 1 µL of RNA grade glycogen (Thermo Scientific) was added to the aqueous solution. Each sample was then vortexed for 15 seconds and incubated for 10 minutes at room temperature. Following incubation, the samples were centrifuged at 12,000 g for 10 minutes at 4°C. The supernatant within each sample was removed, and 1 mL of 75% ethanol was used to wash the RNA pellet. The samples were then spun down at 7500 g for 5 minutes at 4°C. All ethanol was decanted carefully and the RNA pellet was left to dry for 5 minutes. Once the RNA pellet was dry and any remaining ethanol had evaporated, the pellet was resuspended in 35 µL of UltraPure™ RNase/DNase-free distilled water (Invitrogen) and heated at 65°C for 10 minutes. RNA concentrations were measured using a NanoDrop LITE spectrometer (Thermo Fisher Scientific) and samples were stored at -80°C.

Reverse transcription was performed using two different methods. First, the SuperScript III One-Step RT-PCR System with Platinum *Taq* DNA Polymerase (Thermo Fisher Scientific) was used. In a 0.2-mL tube, 12.5 µL of 2X Reaction Mix, 0.5 µL of forward *DUX4* primer 5'-CCCAGGTACCAGCAGACC–3', 0.5 µL of reverse *DUX4* primer 5'-TCCAGGAGATGTAACTCTAATCCA– 3' (see Table 2.4), 1.0 µL of SuperScript® III Taq polymerase, 4.5 µL of UltraPure RNase/DNase-free distilled water, and 5 µL of RNA sample at a concentration of 50 ng/µL were combined, gently mixed by centrifuging and incubated using the thermocycler conditions listed in Table 2.3. The *DUX4* primer sequences were kindly provided by Dr. Yi-Wen from George Washington University.

The second type of reverse transcription was performed using SuperScript III RT (Life Technologies) and GoTaq® G2 green master mix (Promega). Briefly, first strand cDNA synthesis was carried out by incubating RNA samples at 65 °C for 5 min with 1 µL oligo(dT) (Life Technologies), 1 µL dNTPs (10 mM each) (New England Biolabs, Ipswich, MA, USA) and

RNase/DNase-free distilled water (filled up to 13 µL/sample) and 1 µg of total RNA. After incubation, a master mix of 4 µL 5X first strand buffer (Life Technologies), 1 µL DTT (Life Technologies), 1 µL RNaseOUT (Life Technologies) and SuperScript III® RT (Life Technologies), were added to each existing sample and incubated for 1 hour at 50 °C and 70 °C for 15 min. Following incubations, 1 µL of RNase H inhibitor (Life Technologies) was added to each sample of cDNA synthesis and incubated for 37 °C for 20 min. Following first strand cDNA synthesis, the PCR reaction was carried, the cDNA was amplified using GoTaq green master Mix (Promega) using 0.3 µM of forward and reverse primers specific to each gene and 4 µL of cDNA template when amplifying for *DUX4,* and 3 µL of cDNA template when amplifying for *PITX1*, and *Glyceraldehyde-3-phosphate dehydrogenase* (*GAPDH*), in a total volume of 25 µL. The thermal cycling conditions were optimized for each gene (refer to Table 2.3). Primer sequences used for human *DUX4,* human *PITX1* and internal control (*GAPDH*) are described in Table 2.4. 5 µL of PCR products were loaded into their corresponding wells and were visualized in 1.5% agarose gels by electrophoresis. Electrophoresis was performed for 5 minutes at 135 V followed by 25 minutes at 100 V. Following electrophoresis, the agarose gel was stained for 30 minutes under light agitation, using SYBR® safe DNA gel stain (Life Technologies). Band intensity quantification of SYBR safe-stained gels for DUX4, PITX1 and GAPDH bands was performed using Image J software (NIH, Bethesda, MD, USA).

2.4 cDNA sequencing

For purification of PCR products, the Wizard®SV Gel and PCR Clean-Up System (Promega) was used. Bands of interest were excised from 1.5% agarose gels and were placed into their corresponding tubes, containing the membrane-binding solution. Tubes were vortexed and incubated at 65°C until the agarose was completely dissolved. Using an SV minicolumn attached

to a collection tube, all dissolved agarose mixtures were placed separately into minicolumns and incubated at room temperature for 1 minute. Following incubation, each minicolumn was centrifuged at 16,000 g for 1 minute, and any flow through was discarded. 700 µL of Membrane Wash Solution was added to the minicolumn and centrifuged for a second time for 1 minute at 16,000 g. After the second centrifugation, a second wash using 500 µL of Membrane Wash Solution was spun down for 5 minutes at 16,000 g. The minicolumn was transferred into a new tube and 35 µL of UltraPure™ RNase/DNase-free distilled water was added to the minicolumn. This tube was incubated at room temperature for 1 minute. The minicolumn was then centrifuged at 16,000 g for 1 minute and the cDNA sample was diluted to 0.3 ng/µL and samples were sent away for sequencing to The Applied Genomic Center (TAGC) at the University of Alberta. Sequenced results were analyzed using RefSeq: NCBI Reference Sequence Database (http://blast.ncbi.nlm.nih.gov/Blast.cgi).

2.5 AOs design

LNA gapmer oligonucleotides (positions given in Fig 2.2 and Table 2.5), were purchased through Exiqon (Vedbaek, Denmark). LNAs 1, 2, 3, MOCK A and MOCK B were designed by Exiqon to target human *DUX4* mRNA and were produced by submitting the nucleotide sequence of the DUX4 gene. The LNA gapmers designed by Exiqon are typically between 14-16 nucleotides in length consisting of a DNA central gap, flanked by LNA regions on either side and contain a fully phosphorothioated backbone. Although Exiqon has not released their precise design tools or all of their design parameters for their LNA gapmers, it is known that Exiqon follows three primary design parameters. First, their LNA gapmers are synthesized based on predictive software, which selects a target sequence based on local secondary structure. Second, LNA gapmer sequences are aligned against ENSEMBL to ensure the most specific LNA gapmer is selected, with minimal off-

target hits. Lastly, oligonucleotide design parameters such as length, melting temperature, GC content, gap size and self-complementarity are optimized for each individual sequence. In addition to these three important design parameters, Exiqon incorporates more than 30 other parameters for each individual RNA target in order to synthesize the most efficient LNA gapmers for specific target suppression. Although Exiqon provided the sequences for LNAs 1, 2, 3, MOCK A and MOCK B, the company did not disclose which nucleotides within the sequence were LNA or DNA. Therefore, new LNA gapmers were designed by Dr. Maruyama in order to decipher between LNA and DNA regions. Dr. Maruyama designed eight LNA gapmers, LNAs 1*, 2*, 3*, 4, 5, 6, 7 and MOCK C. LNAs 1*, 2* and 3* were designed using the same sequences as LNAs 1, 2 and 3; however, the first three nucleotides and the last three nucleotides were confirmed to be LNA flanks surrounding a DNA gap (Refer to Table 2.5). LNAs 4, 5, 6, 7 and MOCK C also were designed to have a central gap of DNA, flanked by 3 nucleotides of LNA on either side (refer to Table 2.5). Dr. Maruyama based the sequences of LNAs 4, 5, 6, and 7 from the LNA 1 sequence, altering the sequences by one or two base pairs upstream or downstream, or by increasing the sequence length by one base pair. Once a variety of sequences were derived from LNA 1, Dr. Maruyama aligned all possible sequences against ENSEMBL to ensure there was minimal off-target binding, as well she ensured the GC content of each possible sequence was below 55%.

2.6 LNA gapmer preparation

All LNA gapmers synthesized by Exiqon were received in a lyophilized form, with every LNA gapmer amount received, varying in weight. In order to equilibrate the concentrations of the individual LNA gapmers received, stocks were made for each LNA gapmer. Each LNA gapmer was spun down for 30 seconds using a tabletop microcentrifuge, followed by re-suspension in UltraPure™ RNase/DNase-free distilled water. All stocks were prepared at a 100 μM concentration. Working stocks were then further prepared by diluting each 100 μM LNA gapmer

to 10 μM, which is the optimal concentration for storage. Working stocks of 10 μM were aliquoted at 10 μL and were stored at -20°C. Small aliquot amounts are required for storage at -20°C for LNA gapmers, because no more than 5 freeze/thaw cycles should be performed.

2.7 LNA gapmer transfection

Both 15ABic and 15VBic cell lines were used for LNA gapmer transfection experiments. Briefly, both cell lines were seeded at $1.2x10^5$ cells/mL into either a single well of a gelatin-coated 12 well plate for RNA analysis, into a single well of a gelatin-coated chamber slide for immunofluorescence, or into a 60 cm^2 gelatin-coated petri dish for protein analysis. Four LNA gapmer transfection protocols were tested (refer to Figure 2.3). For all four LNA gapmer transfections, 15ABic and 15VBic myoblasts were seeded and were left to proliferate for 2-3 days in DMEM/Medium 199 with 0.5% Pen-Strep antibiotics which contains Penicillin (10,000 Units/mL) and Streptomycin (10,000 μg/mL) (Gibco), 0.02M 4-(2-*H*ydroxy*e*thyl)-1-*p*iperazine *e*thane*s*ulfonic acid (HEPES, Gibco), Zinc sulfate ($ZnSO_4$, Fisher Scientific), Vitamin B_{12} (Sigma-Aldrich), human recombinant hepatocyte growth factor (hrHGF, Chemicon International), human recombinant fibroblastic growth factor (hrFGF, Bioionner), 15% Fetal bovine serum (FBS, Gibco) and 0.055 ug/mL Dexamethasone (Sigma-Aldrich) at 37 °C under 5% CO_2 (refer to Figure 2.3). For LNA gapmer transfection **method one**, two days after seeding the 10 μM stocks of the different LNA gapmers were thawed and diluted into a tube containing OPTI-MEM® Reduced Serum Media (containing HEPES, 2.4 g/L sodium bicarbonate and L-glutamine) (Gibco®). This step was performed in order to dilute the 10 μM LNA gapmer stock down to 1 uM (3 μL LNA gapmer per 147 μL of Opti-MEM). In a second tube, Lipofectamine RNAiMAX (Invitrogen) was diluted in OptiMEM (4.5 uL RNAiMAX per 145.5 μL of OPTI-MEM). Both tubes, the first containing the 1 μM LNA gapmer and Opti-MEM and the second tube containing RNAiMAX and Opti-MEM were then combined and the contents were incubated at room temperature for five minutes. After

the five-minute incubation, the LNA gapmer/Opti-MEM/RNAiMAX mixture was further diluted into differentiation medium, DMEM/Medium 199 with 1 mM Sodium pyruvate (Invitrogen), 2% Horse serum (Invitrogen) and 0.02 M HEPES (Gibco) (300 µL LNA gapmer/Opti-MEM/RNAiMAX mix was added to 1200 µL of differentiation medium). Undifferentiated myoblasts were transfected with LNA gapmers at a final concentration 100 nM (refer to Figure 2.3), and were incubated with LNA gapmers at 37 °C under 5% CO_2, for 24 hours.

For LNA gapmer transfection **method two**, confluent myoblast cultures were differentiated two days after seeding by replacing the growth medium with DMEM/Medium 199 with 1 mM Sodium pyruvate, 2% Horse serum and 0.02 M HEPES (Gibco) (refer to Table 2.2). Two days after changing to differentiation medium, the spent media was replaced and all myotube cultures were incubated for another two days at 37°C under 5% CO_2 (refer to Figure 2.3). On the fourth day after differentiation, LNA gapmer transfection was performed at a concentration of 100 nM and myotubes were incubated with LNA gapmers at 37 °C under 5% CO_2, for 24 hours (refer to Figure 2.3).

For LNA gapmer transfection **method three**, two days after seeding confluent myoblast cultures were differentiated by replacing the growth medium with DMEM/Medium 199 with 1 mM Sodium pyruvate, 2% Horse serum and 0.02 M HEPES (refer to Table 2.2). Two days after changing to differentiation medium, the spent media was replaced and all myotube cultures were incubated for another two days at 37 °C under 5% CO_2 (refer to Figure 2.3). On the fourth day after differentiation, LNA gapmer transfection was performed at a concentration of 100 nM. Transfected cells were incubated at 37 °C under 5% CO_2, for 48 hours (refer to Figure 2.3).

For LNA gapmer transfection **method four**, two days after seeding confluent myoblast cultures were differentiated by replacing the growth medium with DMEM/Medium 199 with 1 mM Sodium pyruvate, 2% Horse serum and 0.02 M HEPES (refer to Table 2.2). At days 3 and 6 days after

differentiation to myotubes, the spent media was replaced with fresh differentiation medium, and incubated at 37°C under 5% CO_2 (refer to Figure 2.3). On the ninth day after differentiation, LNA gapmer transfection was performed at a concentration of 100 nM. Transfected cells were incubated at 37°C under 5% CO_2, for 24 hours (refer to Figure 2.3).

2.8 Immunocytochemistry

15Abic and 15Vbic myotubes were seeded at $1.2x10^5$ cells/mL into a well within the Nunc™ Lab-Tek™ II Chamber Slide™ System. After the 24 hour-incubation period with LNA gapmers (see Figure 2.3 for the LNA gapmer transfection protocol), spent medium was aspirated from all wells and 15Abic and 15Vbic myotubes were fixed with 200 µL/well of 4% paraformaldehyde (PFA) (Sigma-Aldrich) for 5 minutes at room temperature. Following fixation, each chamber well was washed with 400 µL/well of 1x PBS containing 0.1% Triton X-100 detergent (PBSTr) for 5 minutes under light agitation (this step was repeated 3 times). Cells were blocked with 200 µL/well of PBS containing 0.5% Triton X-100 detergent and 20% FBS, for 20 minutes under light agitation. After blocking, cells were incubated with primary antibody overnight at 4°C. The rabbit polyclonal antibody anti-MuRF1 at a dilution of 1/300 (ECM Biosciences, KY, USA) was used. After washing with 400 µL/well with 0.1% PBSTr for 5 minutes at room temperature, under light agitation (this step was repeated three times), cells were incubated for 1 hour at room temperature with Alexa Fluor secondary antibodies 1/500 (goat anti-rabbit 594, Life Technologies) when visualizing cells at Day 4 in differentiation medium after 24-hour incubation with LNA gapmers. After incubation, the secondary antibody was washed off using PBSTr for 5 minutes under light agitation (this step was repeated 3 times). Slides were then treated with ProLong® Gold Antifade Mountant containing DAPI (Life Technologies) and stored at 4°C. A Zeiss LSM 710 confocal microscope was used for imaging and Zen Blue imaging software 2012 was used for image processing.

2.9 Protein Collection

Two protein collection methods were used for this project. For nuclear extracts, the NE-PER Nuclear and Cytoplasmic Extraction Reagent kit (Thermo Scientific) was used. Spent media was aspirated and 600 µL of Cytoplasmic Extraction Reagent I (CERI) was added to a 60 cm^2 petri dish. Cells were detached using a sterile cell scraper, and were collected in a 15 mL tube. The tube was vortexed for 15 seconds to ensure cell pellet suspension and was incubated on ice for 10 minutes. After incubation, 33 µL of ice-cold Cytoplasmic Extraction Reagent II (CERII) was added to the tube and vortexed for 5 seconds and incubated on ice for 1 minute. The tube was vortexed again for 5 seconds and was centrifuged at 16, 000 rcf at 4°C for 5 minutes. After centrifugation, supernatant, also referred to as "Cytoplasmic extract", was transferred into another tube and stored at -80°C. The left over pellet containing the nuclei was resuspended in 300 µL using ice-cold Nuclear Extraction Reagent (NER). The tube was vortexed for 15 seconds and incubated on ice for 10 minutes (this step was repeated 4 times). A final vortex for 15 seconds was carried out followed by centrifugation at 16,000 rcf for 10 minutes at 4°C. The supernatant, which contains the nuclear extract, was transferred into a pre-chilled tube and was stored at -80°C.

For whole cell extracts, RIPA lysis buffer with 1x Roche cOmplete™ protease inhibitor was used, after spent medium was removed by aspiration. Cells were washed with 5 mL of PBS. 700 µL of the lysis buffer was used per petri dish. Cells were detached well using a sterile cell scraper and the lysis buffer and cells were collected. Collected cells were incubated for 30 minutes on ice. After the incubation the cell lysate was passed through a 21-G needle and cells were spun down at 14,000 g for 15 minutes at 4°C. The supernatant (protein containing) was transferred to a new tube and were stored at -80°C. Protein concentrations were measured using the Pierce BCA Protein Assay Kit, according to the manufacturer's instructions. Standards were prepared as listed in Table 2.6.

For each corresponding round, protein samples were diluted to match the concentration of the healthy 15VBic control sample and samples were stored at -80°C.

2.10 Immunodetection on Western blot

All protein samples, whether whole cell or nuclear extracts, were diluted in 4x sodium dodecyl sulfate (SDS) sample buffer. Once samples were diluted in 4x SDS, samples were incubated for 10 minutes at 70°C using a heating block. Each whole cell extract or nuclear extract was separated by electrophoresis using NuPAGE™ Novex™ 4- 12% Bis-Tris Midi Protein Gels (Life Technologies) (Refer to Table 2.7 for micrograms of protein loaded for each sample type). Protein size was marked using the Spectra™ Multicolor Broad Range protein ladder (Thermo Scientific). Testis tissue lysate (Abcam, CA) was used as a positive control for DUX4 Western blots. The electrophoresis ran for 1 hour at 150V. The electrophoresis system XCell4 SureLock™ Midi-Cell (Invitrogen) was used.

The Novex® Semi-Dry Blotter and extra thick blotting sheets were submerged in transfer buffers and used to transfer protein onto polyvinylidene difluoride (PVDF) membrane (pore size 0.45 μm). The semi-dry transfer equipment was set up by placing the blotting papers, PVDF membrane and gel as follows: Bottom Cathode plate → extra thick blotting sheet in concentrated anode buffer (0.3 M Tris, 20% methanol) →anode buffer (0.03 M Tris, 20% methanol) → PVDF membrane → midi gel → cathode buffer (25 mM Tris, 20% methanol, 40 mM 6-amino-n-hexanoic acid, 0.01 % SDS) → Top Anode plate. Transfers were run for 30 minutes at 20V. For nuclear-extracted samples, the PVDF membrane was blocked overnight at 4°C with 5% skim milk in 0.05% Tween 20 detergent in PBS (PBSTw). For whole cell extracted samples, the PVDF membrane was blocked at 4°C with 5% skim milk in 0.05% Tween 20 detergent in PBS (PBSTw) for 1 hour at room temperature. For

a list of primary antibodies used see Table 2.7; all primary antibodies were diluted in 5% skim milk blocking solution. For loading control Cofilin primary antibodies (New England Biolabs Cofilin (D3F9) XP® Rabbit mAb) dilutions see Table 2.7. The anti-cofilin antibody was diluted in 5% skim milk blocking solution. Primary antibody incubation was under light agitation for 1 hour at room temperature. Primary antibody solutions were decanted, and the PVDF membranes for the corresponding proteins were washed using PBS with 0.05% Tween 20 detergent (PBSTw) for 10 minutes under light agitation (this washing step was repeated three times). For secondary antibody dilutions (HRP conjugated goat anti-mouse IgG (H+L) (Bio-Rad) and HRP conjugated goat anti-rabbit IgG (H+L) (Bio-Rad) in PBSTw, see Table 2.7. Secondary antibody incubation was performed under light agitation for 1 hour at room temperature. Secondary antibody solutions were decanted, and the PVDF membranes for the corresponding proteins were washed using PBSTw for 10 minutes under light agitation (this washing step was repeated three times). The Amersham ECL Select Western blotting detection kit (GE Healthcare) was used for band detection, according to the manufacturer's instructions. Western blot images for nuclear extract samples were taken using the Kodak scientific imager and western blot images for whole cell extracted samples were taken using the ChemiDoc Touch (Bio-RAD). Band intensity quantification was performed using Image J software (NIH, Bethesda, MD, USA).

2.11 *Secondary Structure Prediction*

To assess the accessibility of the targeted exons, secondary structures of exons were predicted using the iterative HFold method of Jabbari and Condon, 2014. Iterative HFold follows the relaxed hierarchical folding hypothesis which after formation of initial base pairs in the secondary structure allows minor modifications (unpairings) of the structure to form the possibly pseudoknotted minimum free energy structure.

2.12 Statistical Analysis

Analyses were conducted using Graph Prism version 7.0a. I assessed the significance of LNA gapmer treatment on FSHD patients' muscle cells using a one way-ANOVA. Post-hoc comparisons between LNA gapmers were performed using Tukey HSD tests and Dunnett's multiple comparisons test.

Table 2.1: Human immortalized cell lines and their characteristics

Code	References	Age	Sex	D4Z4 units
KM186	Immortal myoblasts (FSHDcl17)	27	M	2
	Institute of Myology, Paris			
KM155	Immortal myoblasts (LHCN-M2)	41	M	>10
	Institute of Myology, Paris			
15ABic	Immortal myoblasts (WS229)	66	M	8
	University of Massachusetts Medical School			
15VBic	Immortal myoblasts (WS234)	60	F	>10
	University of Massachusetts Medical School			

Table 2.2: Culture methods used for proliferation and differentiation of immortalized FSHD cell lines and Healthy control cell lines

	Culture Method 1	Culture Method 2	Culture Method 3
Growth Medium	DMEM/F12 Medium	DMEM/Medium 199	DMEM/Medium 199
	Supplement Mix	0.5% antibiotics	0.5% antibiotics
	0.5% antibiotics	0.02M HEPES	0.02M HEPES
	20% FBS	$ZnSO_4$	$ZnSO_4$
		Vitamin B_{12}	Vitamin B_{12}
		hrHGF	hrHGF
		hrFGF	hrFGF
		15% KOSR	15% FBS
			0.05 ug/mL Dexamethasone
Differentiation Medium	DMEM/F12 Medium	DMEM/Medium 199	DMEM/Medium 199
	2% Horse serum	1 mM Sodium pyruvate	1 mM Sodium pyruvate
	100x ITS supplement	15% KOSR	2% Horse serum
	0.5% antibiotics		0.02M HEPES

Table 2.3: Thermocycler conditions used for RT-PCR

Gene	Cycle No.	Temperature (°C)	Duration
One-Step RT-PCR			
DUX4	1	50	5 minutes
	1	94	2 minutes
	35	94	15 seconds
		60	30 seconds
		68	15 seconds
	1	68	5 minutes
	1	4	5 minutes
	1	15	Hold
Two-Step RT-PCR			
DUX4	1	95	2 minutes
	40	95	30 seconds
		60	30 seconds
		72	15 seconds
	1	72	5 minutes
	1	4	5 minutes
	1	15	Hold
PITX1	1	95	2 minutes
	30	95	30 seconds
		60	30 seconds
		72	26 seconds
	1	72	5 minutes
	1	4	5 minutes
	1	15	Hold
GAPDH	1	95	2 minutes
	25	95	30 seconds
		60	30 seconds
		72	20 seconds
	1	72	5 minutes
	1	4	5 minutes
	1	15	Hold

Table 2.4: Primers used for RT-PCR

Gene	Type	Sequence[5'→3']	Length (bp)	Annealing temp.	GC content (%)	Amplicon size (bp)
DUX4	Forward	CCCAGGTACCAGCAGACC	18	62.0	66.7	164
	Reverse	TCCAGGAGATGTAACTCTAATCCA	24	62.0	41.7	
PITX1	Forward	GACCCAGCCAAGAAGAAGAA	20	54.7	50.0	431
	Reverse	ATGGTCATGGAGGAGATGGA	20	55.2	50.0	
GAPDH	Forward	TCCCTGAGCTGAACGGGAAG	20	65.0	60.0	218
	Reverse	GGAGGAGTGGGTGTCGCTGT	20	65.0	65.0	

Table 2.5: LNA gapmer sequences and their characteristics

LNA Gapmer Name	Position	Target exon	Sequence (5'-3')	Length (bp)
LNA 1	98-112	Exon 3 (3'UTR)	5’-AGCGTCGGAAGGTGG-3’	15
LNA 2	675-688	Exon 1 (CDS)	5’-AGATCCCCTCTGCC-3’	14
LNA 3	182-197	Exon 3 (3'UTR)	5’-ATAGGATCCACAGGGA-3’	16
LNA 1*	98-112	Exon 3 (3'UTR)	5’-AGC-GTCGGAAGG-TGG-3’	15
LNA 2*	675-688	Exon 1 (CDS)	5’-AGA-TCCCCTCT-GCC-3’	14
LNA 3*	182-197	Exon 3 (3'UTR)	5’-ATA-GGATCCACAG-GGA-3’	16
LNA 4	99-113	Exon 3 (3'UTR)	5'-CAG-CGTCGGAAG-GTG-3'	15
LNA 5	99-114	Exon 3 (3'UTR)	5'-ACA-GCGTCGGAAG-GTG-3'	16
LNA 6	100-115	Exon 3 (3'UTR)	5'- GAC-AGCGTCGGAA-GGT-3	16
LNA 7	101-116	Exon 3 (3'UTR)	5'- AGA-CAGCGTCGGA-AGG-3'	16
LNA MOCK A	N/A	Negative Control A	5’-AACACGTCTATACGC-3’	15
LNA MOCK B	N/A	Negative Control B	5'-GCTCCCTTCAATCCAA-3'	16
LNA MOCK C	N/A	Negative Control C	5'-ACT-CTCGTCAATC-CAT-3'	16

Table 2.6: BSA Standards

Standards (60 µL Total)	**Water** (µL)	**BSA** (2mg/mL)	**Final Conc.** (µg/mL)
A	0.00	60.00	2000
B	15.00	45.00	1500
C	30.00	30.00	1000
D	37.50	22.50	750
E	45.00	15.00	500
F	52.50	7.50	250
G	56.25	3.75	125
H	59.25	0.75	25
I	60.00	0.00	0
J	60.00	0.00	0

Table 2.7: Western blot and antibodv details

Protein	Extraction Method	Loading amount (µg)	Blocking Duration	Primary Ab	Primary Ab Concentration	Loading Control (Concentration)	Secondary Ab	Secondary Ab Concentration	Secondary Ab Loading Control (Concentration)
DUX4	Nuclear	9	24 hours	9A12 anti-Dux4	1/1,000		HRP conjugated goat anti-mouse IgG (H+L)	1/10,000	
MuRF1	Nuclear	9	24 hours	anti-MuRF1	1/1,500		HRP conjugated goat anti-rabbit IgG (H+L)	1/10,000	
p53	Nuclear	9	24 hours	7F5 anti-p53	1/1,500	Cofilin	HRP conjugated goat anti-rabbit IgG (H+L)	1/10,000	HRP conjugated
DUX4	Whole cell	18	1 hour	9A12 anti-Dux4	1/1,000	1/8,000	HRP conjugated goat anti-mouse IgG (H+L)	1/10,000	goat anti-mouse IgG (H+L)
MuRF1	Whole cell	9	1 hour	anti-MuRF1	1/1,500		HRP conjugated goat anti-rabbit IgG (H+L)	1/10,000	1/10,000
p53	Whole cell	9	1hour	7F5 anti-p53	1/2,500		HRP conjugated goat anti-rabbit IgG (H+L)	1/10,000	

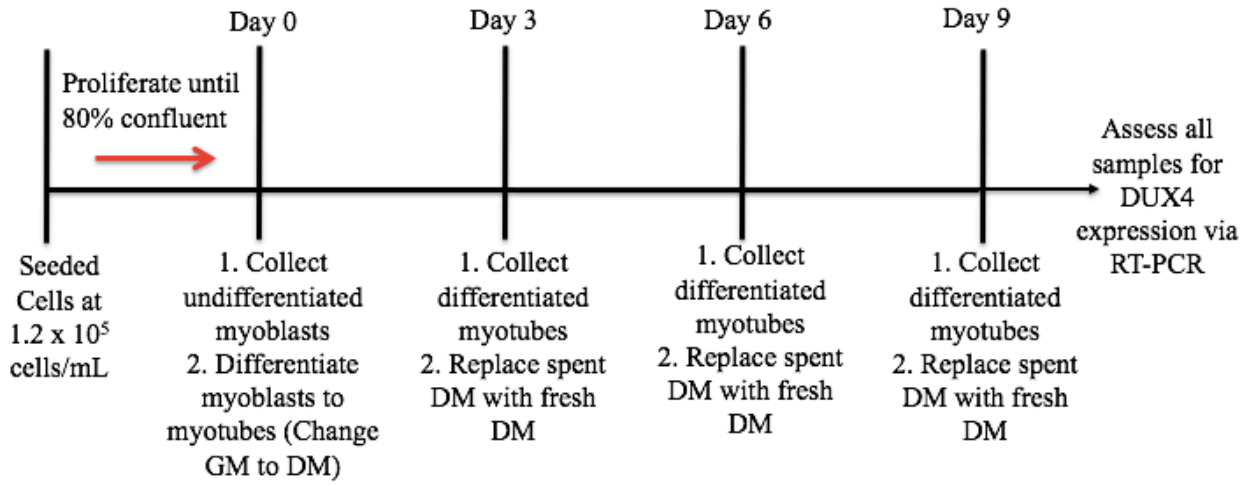

Figure 2.1: Culture schedule for optimization of culture conditions, best suited for detection of DUX4 expression *in vitro* using immortalized human patient cells

Immortalized KM186, KM155, 15ABic and 15VBic cell lines were all seeded at 1.2 x 10^5 cell/mL, into 4 separate 12-well plates (plate 1: Day 0, plate 2: Day 3, plate 3: Day 6, plate 4: Day 9). All seeded cells were grown for 2 days until reaching 80% confluency. At Day 0, all cells seeded into plate 1 were collected for RT-PCR analysis, and all cells seeded into plates 2, 3 and 4 were differentiated from myoblasts to myotubes. All differentiated myotubes in plate 2 were collected on Day 3 for RT-PCR analysis, and the medium in plates 3 and 4 was replaced. All differentiated myotubes in plate 3 were collected on Day 6 for RT-PCR analysis, and the medium in plate 4 was replaced. At Day 9 all differentiated myotubes in plate 4 were collected for RT-PCR analysis. Abbreviations: GM, growth medium; DM, differentiation medium.

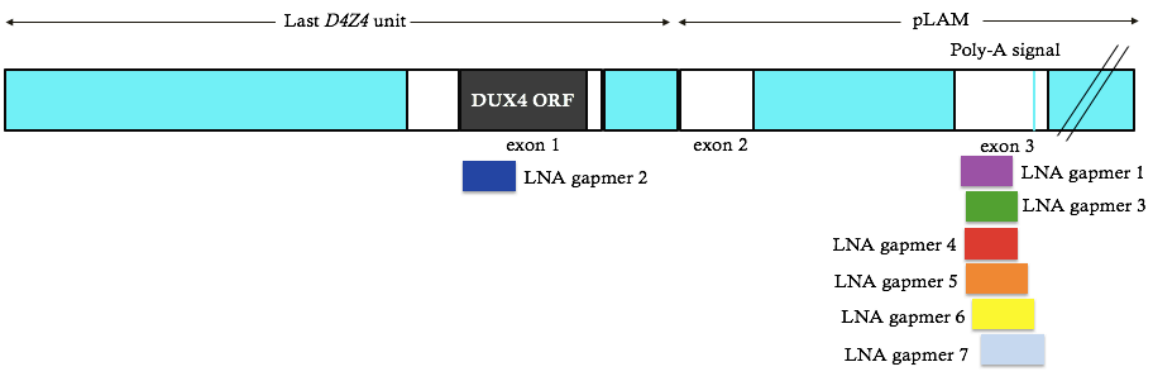

Figure 2.2: LNA gapmer location on *DUX4* mRNA

Schematic representation of the location of LNA gapmers 1, 2, 3, 4, 5, 6, 7 on DUX4 mRNA.

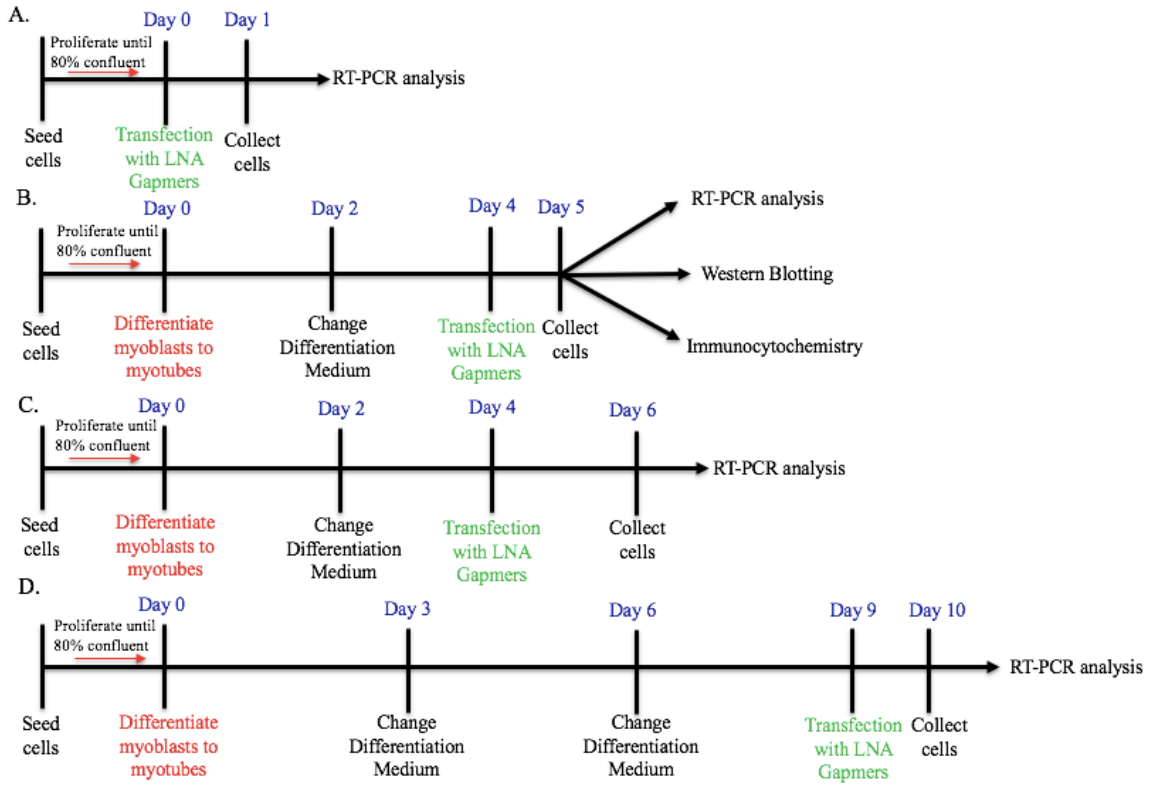

Figure 2.3: LNA gapmer transfection schedule

15ABic and 15VBic cells were seeded, and grown until reaching 80% confluency. 15ABic cells were transfected with an LNA gapmer or a mock LNA gapmer at 100 nM concentration. (A) LNA gapmer transfection method one: 15ABic undifferentiated myoblasts were transfected with an LNA gapmer or mock LNA gapmer at Day 0, and treated cells were collected on Day 1 for RT-PCR analysis. (B) LNA gapmer transfection method two: 15ABic myoblasts were differentiated to myotubes after becoming 80% confluent (termed Day 0). Differentiation medium was replaced on Day 2, and differentiated myotubes were transfected with an LNA gapmer or mock LNA gapmer at Day 4. Treated myotubes were collected on Day 5 for RT-PCR analysis, western blotting and immunocytochemistry. (C) LNA gapmer transfection method three: 15ABic myoblasts were differentiated to myotubes at Day 0. Differentiation medium was replaced on Day 2, and

differentiated myotubes were transfected with an LNA gapmer or mock LNA gapmer at Day 4. Treated myotubes were collected on Day 6 for RT-PCR analysis. (D) LNA gapmer transfection method four: 15ABic myoblasts were differentiated to myotubes after becoming 80% confluent (Day 0). Differentiation medium was replaced on Days 3, and 6, and differentiated myotubes were transfected with an LNA gapmer or mock LNA gapmer at Day 9. Treated myotubes were collected on Day 10 for RT-PCR analysis.

Chapter 3

Results

3 Results

3.1 Identification of a sensitive detection strategy for *DUX4* transcripts in immortalized FSHD patients' muscle cells

Detection of DUX4 in FSHD myoblasts has proven quite challenging, due to the extremely low expression levels detectable in affected FSHD skeletal muscles. Mis-expression of DUX4 in FSHD patient muscles causes cytotoxicity to its surrounding environment while in cell culture results in very few cells expressing DUX4. A variety of cDNA synthesis strategies have previously been reported to amplify DUX4 amongst different FSHD cell lines. To identify the most effective detection strategy for DUX4 in immortalized FSHD cell line KM186 and immortalized healthy control cell line KM155, two commonly used methods were tested (Pandey, 2015 and Yusuke, 2015). First, I tested the SuperScript III One-Step RT-PCR System with Platinum *Taq* DNA Polymerase and second, I tested the SuperScript III RT with oligo(dT) primers and GoTaq® G2 Master Mix. To test SuperScript III RT, oligo(dT) primers, dNTP mix, first-strand buffer, DTT and RNaseOUT were used to carry out the first-strand synthesis, followed by use of GoTaq Green Master Mix for the amplification reaction.

3.1.1 SuperScript III One-Step RT-PCR System with Platinum Taq DNA polymerase

To examine whether the SuperScript III One-Step RT-PCR System with Platinum Taq DNA polymerase could be used as a sensitive detection strategy for *DUX4* transcripts, an initial test using positive control sample human testes total RNA was tested. The testes total RNA sample was run using the one-step RT-PCR thermocycler conditions listed in Table 2.3 and the *DUX4* PCR primers (Table 2.4). Semi-quantitative RT-PCR results indicated that expression of *DUX4* at 164 bp in the human testis positive control sample was highly detectable (data not shown). This result indicates that SuperScript III One-Step RT-PCR System with Platinum Taq DNA polymerase can be used to detect *DUX4* when it is highly expressed in healthy male testes.

Next, to confirm that the band visualized via semi-quantitative RT-PCR in the human testes total RNA sample was *DUX4*, the band was isolated and Sanger sequenced. Sanger sequencing results indicated that the *DUX4* PCR primers were successful at amplifying *DUX4* mRNA in human testes, as both the target sequence and sequence of interest aligned and showed identity (Figure 3.1 (A)). These results confirmed that the band visualized by RT-PCR represents the *DUX4* transcript indicated by the presence of the exon 2/exon 3 junction which are the two exons the reverse and forward primer span (Figure 3.1 (B)).

To examine whether the RT-condition SuperScript III One-Step RT-PCR System could be used to detect *DUX4* in FSHD cells, which express endogenous DUX4 at a considerably lower level compared to human testes, the immortalized FSHD patient cell line KM186 and the immortalized healthy control cell line KM155 were tested. Both cell lines were cultured using cell culture method 1 (refer to Table 2.2) and were cultured using the culture schedule listed in Figure 2.1. Using semi-quantitative RT-PCR analysis, and *DUX4* PCR primers (Table 2.4), *DUX4* expression at days 0, 3, 6 and 9 was undetectable in the immortalized FSHD cell line KM186 or immortalized healthy control cell line KM155 (Figure 3.2). These results indicate that the SuperScript III One-Step RT-PCR System is not sufficiently sensitive for amplifying endogenous DUX4 in KM186 or KM155 (see SuperScript III RT with GoTaq® G2 green master mix results below).

3.1.2 SuperScript III RT with GoTaq® G2 green master mix

Next, the SuperScript III RT with GoTaq® G2 green master mix was tested to determine if this method could be used as a sensitive strategy for detection of *DUX4* transcripts in the immortalized FSHD patient cell line KM186 and the immortalized healthy control cell line KM155. Again, both immortalized cell lines were cultured using cell culture method 1 (refer to Table 2.2) and were cultured using the culture schedule listed in Figure 2.1. Semi-quantitative RT-PCR analysis showed that *DUX4* expression at days 0, 3, 6 and 9 was undetectable in the immortalized healthy control

cell line KM155 (Figure 3.3 (A)) using *DUX4* PCR primers (Table 2.4). At day 3 in KM186 cells, *DUX4* expression was detectable (Figure 3.3 (B)), indicating that the SuperScript III RT with GoTaq® G2 green master mix is a better strategy to use, when compared to the SuperScript III One-Step RT-PCR System for detection of *DUX4* mRNA transcripts in immortalized KM186 cells.

3.2 Determination of an effective culture condition that can potentially induce *DUX4* and *PITX1* expression in FSHD patients' muscle cells

In addition to various cDNA synthesis strategies for amplification of *DUX4*, culture conditions have also been reported to affect DUX4 expression in cultured FSHD myoblasts.

3.2.1 DUX4 expression in immortalized cell lines KM186 and KM155

When immortalized cell lines KM186, and KM155 were cultured using cell culture method 1 (refer to Table 2.2), semi-quantitative RT-PCR results indicated that expression of *DUX4* at day 3 in KM186 myotubes was considerably low and that *DUX4* expression did not increase with more days in differentiation medium after day 3 (Figure 3.3 B). A second culture method (refer to Table 2.2) was tested with 15% KOSR in the growth medium, to determine the effects KOSR had on *DUX4* expression in the immortalized cell lines KM186 and KM155. Using SuperScript III RT, GoTaq® G2 green master mix and *DUX4* PCR primers (Table 2.4), preliminary semi-quantitative RT-PCR results showed high expression of *DUX4* at days 0, 3, 6 and 9 in both KM155 cells (Figure 3.3 (A)) and in KM186 cells (Figure 3.3 (B)). These results indicate that culturing cell lines KM186 and KM155 in growth medium with 15% KOSR induces the expression of *DUX4* at all days of differentiation. Preliminary results after quantifying band intensities indicated that KOSR increased the expression of *DUX4* in KM155 myotubes at days 6 and 9 at a higher level than it did for KM186 myotubes at corresponding days relative to the testis positive control (Figure 3.3 (A & B)). From these results, two conclusions can be made. First, supplementation of KOSR into the

growth medium may not be the best culture method to use for detection of *DUX4* in these cell lines, as KOSR may influence the expression pattern of *DUX4* to deviate from its expected phenotype. Second, the healthy control KM155 cell line may be easily influenced by manipulations to the culture media, and therefore, this may not be the best control cell line to use.

3.2.2 DUX4 expression in immortalized cell lines 15ABic and 15VBic

To determine whether the healthy control KM155 cell line was easily influenced by manipulations to the culture medium, this cell line was cultured using a third culture method and *DUX4* expression levels were assessed (Fig 3.4 (A)). KM155 cells were cultured using culture method 3 (see Table 2.2) with 0.055 µg/mL Dexamethasone in the growth medium and were cultured according to the culture schedule listed in Figure 2.1. Next, I tested a different immortalized patient cell line 15ABic and healthy control cell line 15VBic using culture method 3 (see Table 2.2) with 0.055 µg/mL Dexamethasone in the growth medium and the culture schedule listed in Figure 2.1. A different FSHD cell line was tested to determine whether higher expression levels of *DUX4* could be detectable in another cell line. The *DUX4* expression levels in healthy control KM155 cells and patient 15ABic cells cultured using Dexamethasone were then compared using semi-quantitative RT-PCR analysis, relative to the positive control, human testis total RNA (Fig 3.4 (A)). Preliminary semi-quantitative results showed that use of Dexamethasone in culture media (culture method 3) induced the expression of *DUX4* in KM155 healthy cells at days 0, 3, and 9 compared to *DUX4* expression levels detected using culture method one (Fig 3.3 (A & B). Interestingly, use of Dexmethasone also showed similar induction of *DUX4* expression compared to expression levels detected using culture method two (Fig 3.3 (A & B). When comparing immortalized patient 15ABic cells and healthy control 15VBic cells cultured using culture method three, via semi-quantitative analysis, *DUX4* expression was quantifiable at days 0, 3, 6 and 9 in both cell lines (Figure 3.4 (B)). Although not statistically different, these preliminary results show

that there is a trend towards a higher average expression of *DUX4* at days 3, 6 and 9 in 15ABic patient cells compared to *DUX4* expression at days 3, 6 and 9 in 15VBic control cells (Figure 3.4 (C)). Band intensities for *DUX4* expression were corrected against GAPDH. These results suggest that the healthy control KM155 cell line is undoubtedly affected by manipulations of the culture media, seen by drastic differences in *DUX4* expression amongst the three culture methods (FBS, KOSR, Dexamethasone). These results show that Dexamethasone (culture method three, Table 2.2) in growth medium, allows for detectable *DUX4* expression more similar to the expected phenotype of FSHD patients, compared to culture method one and two. Lastly, immortalized 15ABic and 15VBic cell lines are good alternative cell lines to use instead of KM186 and KM155, as *DUX4* expression levels are more easily detectable and the use of Dexamethasone in culture medium does not drastically influence the expression of *DUX4* after 15ABic cells have been differentiated into myotubes.

3.2.3 PITX1 expression in immortalized cell lines 15ABic and 15VBic

In addition to detecting expression levels of *DUX4* in immortalized 15ABic and 15VBic cell lines, I was also interested in assessing the expression levels of *PITX1,* a downstream target of DUX4 that is induced in FSHD patients. Using *PITX1* PCR primers (listed in Table 2.4) and the *PITX1* thermocycler conditions listed in Table 2.3, I assessed the expression of *PITX1* via semi-quantitative RT-PCR in the same samples used to test expression of *DUX4* at days 0, 3, 6, and 9 (using culture method three, Figure 3.5). These preliminary results show that *PITX1* expression is highest at day 6 after differentiation. *PITX1* expression is significantly higher at day 6 in FSHD cells (15ABic) compared to *PITX1* expression at day 6 in healthy cells (15VBic) ($p<0.05$). Although a significant difference between *PITX1* expression levels is noticed when comparing healthy cells and FSHD cells, *PITX1* in FSHD is not as drastically up-regulated in immortalized cells compared to healthy cells as previously described in patient muscle biopsies compared to

control muscle biopsies (Dixit *et al.*, 2007). Therefore, when using this particular FSHD cell line (15ABic), other downstream genes of *DUX4*, such as *MuRF1*, *TRIM43*, *MBD3L2*, *CRYM* or *p53*, should also be explored in addition to *PITX1*.

3.3 Evaluation of LNA gapmers efficacy *in vitro*

Previously, others have shown that transfection at day 0 and day 4 with phosphorodiamidate morpholino oligomer (PMOs) has the highest success (Aoki *et al.*, 2013). To examine the efficacy of LNA gapmers at suppressing the expression of *DUX4*, four separate transfection protocols were tested *in vitro* at day 0, day 4 and day 9 in differentiation medium (see Figure 2.2).

3.3.1 DUX4 expression after LNA gapmer transfection at Day 0 in differentiation medium after 24-hour incubation with LNA gapmers

LNA gapmers 1, 2 and 3 designed by Exiqon were tested at a concentration of 100 nM, using transfection method one (Day 0 in differentiation medium, 24-hour incubation with LNA gapmers), to determine the efficacy of these LNA gapmers at suppressing the expression of *DUX4* in FSHD patient myotubes (15ABic). Treated FSHD patient cells (15ABic) and non-treated healthy controls cells (15VBic) were collected after 24-hour incubation with LNA gapmers. Semi-quantitative results indicated that LNA gapmer 3 induced the expression of *DUX4* in treated FSHD samples, compared to the non-treated FSHD (NT) sample at Day 0 ($p<0.005$) (Fig 3.6 (A & B)). This data suggests that LNA gapmer 3 may have adverse effects and may be targeting another gene apart from *DUX4* when transfected at Day 0 potentially causing increased expression of *DUX4*. However further tests, including for toxicity, should be performed to determine whether LNA gapmer 3 has a cytotoxic nature.

3.3.2 DUX4 expression after LNA gapmer transfection at Day 4 in differentiation medium after 24-hour incubation with LNA gapmers

At a second experimental time point, LNA gapmers 1, 2 and 3 were tested at a concentration of 100 nM. LNA gapmers were transfected using transfection method two (Day 4 in differentiation medium, 24-hour incubation with LNA gapmers, Figure 2.3), to determine the efficacy of these LNA gapmers at suppressing the expression of *DUX4* in FSHD patient cells (15ABic). Semi-quantitative RT-PCR results indicated that LNA gapmer 1, targeting exon three of the *DUX4* mRNA transcript, sufficiently decreased *DUX4* expression levels in 15ABic FSHD myotubes, compared to the non-treated FSHD myotubes ($p < 0.005$) (Figure 3.7 A & B). 15ABic myotubes treated with LNA gapmers 2 or 3 were unable to significantly decrease *DUX4* expression levels in non-treated FSHD myotubes (Figure 3.7 A & B). These results indicate that LNA gapmers targeting exon 3 may be the most effective at suppressing *DUX4* at the mRNA level. However, results for LNA gapmer transfection at Day 0 (Figure 3.6 A & B) emphasize that LNA gapmer sequence location is crucial. Lastly, these results also suggest that when *DUX4* expression in differentiated 15ABic myotubes is relatively high (i.e. after day 3 in differentiation medium, Figure 3.4), LNA gapmer 1 is more effective at decreasing *DUX4* expression, contrary to transfection at day 0 in undifferentiated cells when *DUX4* expression is relatively low (Figure 3.4 B).

3.3.3 DUX4 protein levels after LNA gapmer transfection at Day 4 in differentiation medium after 24-hour incubation with LNA gapmers

After determining the efficacy of LNA gapmers 1, 2 and 3 at the mRNA transcript level, the efficacy of these LNA gapmers was further assessed at the protein level to see if there could also be a reduction in mis-expressed DUX4 protein. Two methods of protein extraction were used for detection of DUX4 protein, nuclear extraction, and whole cell extraction. Due to the low expression levels of DUX4 in cultured cells, utilizing an extraction protocol which could detect the highest quantity of DUX4 protein was vital. Using the nuclear extraction method, the highest quantity of protein yielded was 9 µg (see Table 2.7), whereas the whole cell extraction method yielded 18 µg

of protein (see Table 2.7). For both extraction methods, FSHD patient cells (15ABic) were transfected using LNA gapmer transfection method two (refer to Figure 2.3). Preliminary results from the nuclear-extracted samples indicated that treatment with LNA gapmers 1 (85% and 68%), LNA gapmer 2 (66% and 67%) and LNA gapmer 3 (57% and 74%) changed the levels of DUX4 protein compared to the NT sample (100%) and Mock C sample (95%) (Figure 3.8 (A). Interestingly, Western blotting results showed that both LNA gapmers 2 and 3 changed DUX4 protein levels similarly to LNA gapmer 1 (Figure 3.8 (A)), contrary to the semi-quantitative results with LNA gapmers at day 4 after differentiation, 24-hour incubation (Figure 3.7). This data suggests that perhaps there is no significant difference in efficacy of LNA gapmers which target exons one or three at the protein level. Lastly, it should be noted that this data is preliminary and further replicates would have to be performed to determine the statistical significance of use of these LNA gapmers.

Similar to the western blotting results from nuclear extracts, preliminary results from the whole cell extract samples indicated that LNA gapmers 1 (86%), LNA gapmer 2 (83%) and LNA gapmer 3 (56%) all changed the levels of DUX4 protein in 15ABic myotubes compared to the both the non-treated sample (100%) and the Mock C sample (92%) (Figure 3.8 B). DUX4 protein levels were changed the most by LNA gapmer 3 (56%) compared to LNA gapmers 1 (86%) and LNA gapmer 2 (83%); however, further tests would have to be performed in order to determine if the change in DUX4 protein levels is being caused by degradation of the protein or if this cause is due to other off-target toxic effects. For whole cell extracts, the Mock B gapmer was not tested because previous results showed that the Mock C gapmer was a better control gapmer to use, showing more similar DUX4 protein levels compared to the NT sample (Figure 3.8 A). Lastly, it should be noted that this data is preliminary and further replicates would have to be performed to determine the statistical significance of these results.

3.3.4 MuRF1 protein levels after LNA gapmer transfection at Day 4 in differentiation medium after 24-hour incubation with LNA gapmers

Since western blotting data indicated that LNA gapmers 1, 2 and 3 could change DUX4 protein levels in 15ABic FSHD myotubes, compared to the NT sample, I sought to look at the atrophic marker MuRF1 to further determine whether LNA gapmers targeting DUX4 were causing any changes to other FSHD markers. Both the nuclear extraction method and the whole cell extraction method were used for detection of MuRF1 protein. Preliminary results showed that relative to the NT sample (100%), MuRF1 protein levels after treatment with LNA gapmer 1 were 89%. MuRF1 protein levels in 15ABic FSHD myotubes treated with LNA gapmers 2 were 214% and after treatment with LNA gapmer 3 were 193% relative to NT FSHD myotubes (100%) indicated by Western blot results from nuclear extracted samples (Figure 3.9 A). Preliminary results from the whole cell extracted samples showed that relative to the NT FSHD sample, after treatment with LNA gapmers 1, MuRF1 protein levels were 104%, for LNA gapmer 2 105% and for LNA gapmer 3 98% (Figure 3.9 B). These results suggest that in addition to DUX4, other genes influence the expression of atrophic marker MuRF1 in FSHD patients.

3.3.5 Localization of MuRF1 after LNA gapmer transfection at Day 4 in differentiation medium after 24-hour incubation

Although preliminary results from Western blotting indicated that LNA gapmers 1, 2 or 3 did not significantly reduce protein levels of MuRF1 in 15ABic FSHD myotubes (Figure 3.9 A &B), I sought to determine whether localization of MuRF1 in the nucleus was influenced by decreasing DUX4 protein levels. To do this, I performed immunocytochemistry on 15ABic cells treated with LNA gapmers 1, 2 or 3, following LNA gapmer transfection method two (Figure 2.3). 15VBic cells were differentiated at day 0 when cells reached 80% confluence. Two and four days after differentiation, the spent differentiation medium was replaced with new differentiation medium.

At day 4 in differentiation medium, FSHD myotubes were transfected with LNA gapmers at 100 nM concentration and incubated for 24-hours with LNA gapmers, non-treated FSHD myotubes were incubated with differentiation medium containing Opti-MEM and RNAiMAX, and healthy control cells were incubated for 24-hours with regular differentiation medium. Following the 24-hour incubation period, all cells were fixed with 4% paraformaldehyde and stained with the anti-MuRF1 antibody. In the healthy non-treated myotubes (15VBic), immunofluorescence images showed that there was no localization of MuRF1 within the nucleus of differentiated myotubes (Figure 3.10 A). However, in the FSHD non-treated myotubes (Figure 3.10 B) and the Mock C treated myotubes (Figure 3.10 C), the atrophic marker MuRF1 within the nucleus of differentiated myotubes is visible. Interestingly, in the FSHD myotubes treated with LNA gapmers 1 (Figure 3.10 D) and 3 (Figure 3.10 F), immunofluorescence indicated that there was no longer localization of MuRF1 in the nucleus after LNA gapmer treatment. Similar to semi-quantitative RT-PCR results in Figure 3.7, treatment with LNA gapmer 2 (Figure 3.10 E) does not influence the localization of MuRF1 in the nucleus in 15ABic myotubes. These results suggest LNA gapmers targeting exon 3 of the mRNA transcript change the localization of MuRF1 in the nucleus.

3.3.6 PITX1 expression after LNA gapmer transfection at Day 4 in differentiation medium after 24-hour incubation with LNA gapmers

Since LNA gapmer 1 decreased levels of mis-expressed *DUX4* mRNA transcripts (Figure 3.7) and decreased DUX4 protein levels (Figure 3.8) in 15ABic FSHD myotubes, I next sought to determine if either of the three LNA gapmers targeting *DUX4* could also suppress the expression of *PITX1* in 15ABic myotubes (Figure 3.5). Testing LNA gapmers at a concentration of 100 nM, using LNA gapmer transfection method two (see Figure 2.3), semi-quantitative results indicated that neither LNA gapmers 1, 2 or 3 could suppress the expression of *PITX1* in 15ABic myotubes compared to the non-treated FSHD sample (Figure 3.11 A & B). Although contradictory to previous findings

(Dixit *et al.*, 2007), these results support the hypothesis that DUX4 does not directly target PITX1, as suggested by new evidence from Zhang *et al.*, 2016.

3.3.7 DUX4 expression after LNA gapmer transfection at Day 4 in differentiation medium after 48-hour incubation with LNA gapmers

At a third experimental time point, using LNA gapmers 1, 2 and 3, at a concentration of 100 nM, LNA gapmer transfection method three was tested (Day 4 in differentiation medium, 48-hour incubation with LNA gapmers, see Figure 2.3). This test was done to determine whether a longer incubation period could produce a greater efficacy in LNA gapmers 1, 2 or 3 to suppress *DUX4* in FSHD patient myotubes (15ABic). Preliminary semi-quantitative RT-PCR analysis results showed that incubation with LNA gapmers 1, 2 or 3 for 48-hours did not significantly change the expression of *DUX4* mRNA transcripts in 15ABic myotubes, compared to the non-treated FSHD sample (Figure 3.12 A & B). Although 48-hour incubation with Opti-MEM and RNAiMAX does not significantly change the efficacy of LNA gapmers 1, 2 or 3 compared to incubation for 24-hours (Figure 3.7), the trend towards higher *DUX4* expression seen with transfection of LNA gapmer 3 after 48-hours, suggests that co-transfection with Opti-MEM and RNAiMAX for 48 hours may be too long, causing these reagents to be potentially harmful.

3.3.8 DUX4 expression after LNA gapmer transfection at Day 9 in differentiation medium after 24-hour incubation with LNA gapmers

At a fourth experimental time point, LNA gapmers 1, 2 and 3, were tested at a concentration of 100 nM, using LNA gapmer transfection method four (Day 9 in differentiation medium, 24-hour incubation with LNA gapmers, see Figure 2.3). A fourth experimental time point at day 9 was carried out because other groups have previously reported that *DUX4* expression increases with days in differentiation (Tassin *et al.,* 2013). Therefore I sought to determine whether LNA gapmer 1, 2 and 3 would have a better efficacy at suppressing *DUX4* expression with a longer

differentiation period and potentially higher *DUX4* levels. Preliminary screening for *DUX4* expression in FSHD patient cells (15ABic) indicated that the relative expression of *DUX4* at day 9 after differentiation was high compared to relative *DUX4* expression at day 6 after differentiation (Figure 3.4 C), and therefore transfection at day 9 in differentiation medium was tested. Semi-quantitative RT-PCR results indicated that neither LNA gapmer 1, 2 or 3 could significantly decrease *DUX4* expression levels in 15ABic FSHD myotubes, compared to the non-treated FSHD myotubes (Figure 3.13 A & B). Although not statistically significant, these preliminary results show a trend towards lower *DUX4* expression after treatment with LNA gapmer 1 in 15ABic cells; however, further replicates would have to be done in order to determine if this possible change is significant.

3.3.9 PITX1 expression after LNA gapmer transfection at Day 9 in differentiation medium after 24-hour incubation with LNA gapmers

PITX1 expression levels were also assessed via semi-quantitative analysis after treatment with LNA gapmers 1, 2 and 3 at 100 nM following LNA gapmer transfection method four (Figure 2.3). Similar, to the results shown after transfection at Day 4 after differentiation with 24-hour incubation (Figure 3.11), LNA gapmer transfection at day 9 after differentiation showed no reduction in *PITX1* mRNA transcripts in 15ABic myotubes compared to the non-treated 15ABic myotubes (Figure 3.14 A & B). These results indicate that suppression of *PITX1* cannot be achieved by targeting the DUX4 gene via LNA gapmer chemistry. Secondly, these results suggest that the induction of *PITX1* in FSHD patients is caused by many genes, not just *DUX4*.

3.3.10 DUX4 expression after LNA gapmer transfection at Day 4 in differentiation medium after 24-hour incubation with LNA gapmers 1,2*, 3*, 4, 5, 6 and 7*

Since transfection with LNA gapmer 1 in 15ABic patient cells showed a consistent trend towards suppression of *DUX4* at all days of transfection (i.e. trend towards suppression at Day 0 (Figure

3.6), significant reduction of *DUX4* at Day 4, 24-hour incubation ($p < 0.005$) (Figure 3.7) and a trend towards suppression at Day 9, 24-hour incubation (Figure 3.13)), new LNA gapmers were designed with similar sequences to LNA gapmer 1. Newly designed LNA gapmers only deviated by one, two or three base pairs (see Table 2.5). These newly designed LNA gapmers were transfected using LNA gapmer transfection protocol two (Figure 2.3) and were transfected at a concentration of 100 nM. Semi-quantitative RT-PCR analysis indicated that LNA gapmers 1, 3, 7 ($p<0.05$), 4 and 6 ($p<0.005$), all of which targets exon 3 of *DUX4* mRNA transcript, sufficiently decrease *DUX4* expression levels in 15ABic FSHD myotubes, compared to the NT FSHD myotubes (Figure 3.15 A & B). Together, these results suggest that at the mRNA level, LNA gapmers targeting exon 3 are more efficient at decreasing *DUX4* expression levels in 15ABic myotubes, compared to LNA gapmers targeting exon 2. These semi-quantitative results also demonstrate that LNA gapmer 3* was able to significantly suppress *DUX4* expression levels (Figure 3.15 B), whereas LNA gapmer 3 wasn't (Figure 3.7 B). These results emphasize that specific LNA gapmer sequence design (i.e. LNA flank length and/or DNA gap length) is essential for suppression of *DUX4* in FSHD myotubes.

3.3.11 PITX1 expression after LNA gapmer transfection at Day 4 in differentiation medium after 24-hour incubation with LNA gapmer 1, 2*, 3*, 4, 5, 6, and 7*

Previous results with newly designed LNA gapmers showed that sequence length, LNA flank length and/or DNA gap length, are all parameters which cause LNA gapmers to change *DUX4* expression levels in 15ABic myotubes (Table 2.5 and Figure 3.15). Since noticeable differences in expression levels were detectable using the newly designed LNA gapmers, one final test was done to determine whether any of the newly designed LNA gapmers targeting the *DUX4* mRNA could also suppress expression levels of *PITX1* in FSHD myotubes. Using LNA gapmer transfection protocol two (Figure 2.3), LNA gapmers 1*, 2*, 3*, 4, 5, 6, and 7 were transfected at a

concentration of 100 nM. Similar to results shown after transfection at day 4 (Figure 3.11) and day 9 (Figure 3.14), semi-quantitative RT-PCR analysis indicated that there was no significant reduction in *PITX1* mRNA transcripts in 15ABic myotubes, compared to the non-treated 15ABic myotubes (Figure 3.16 A & B). It can, therefore, be suggested that suppression of *PITX1* cannot be achieved by targeting the DUX4 gene via LNA gapmer chemistry, no matter the sequence length, LNA flank length and/or DNA gap length. Furthermore, these results suggest that the suppression of *PITX1* in FSHD patients may be attainable by targeting other genes which directly interact or influence PITX1 expression.

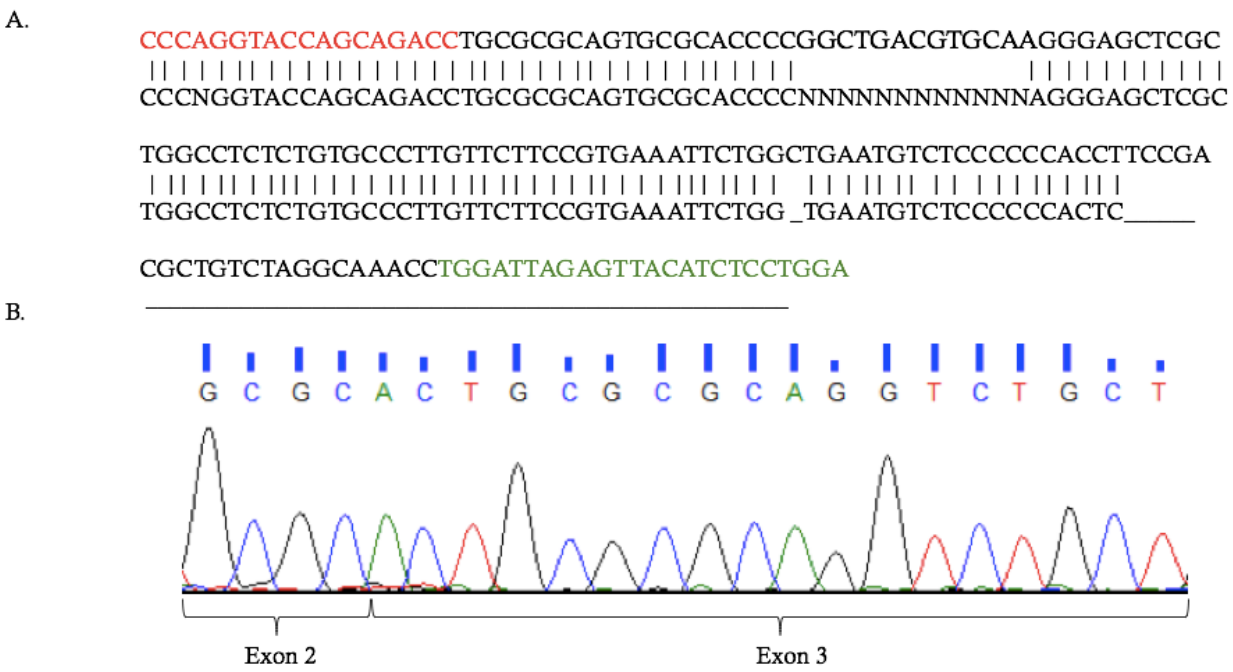

Figure 3.1: cDNA sequence analysis of *DUX4* in adult male testis

A. cDNA sequence alignment between *DUX4* mRNA and sequenced *DUX4* mRNA from human testis total RNA sample. The location of the *DUX4* forward primer is outlined in red and the *DUX4* reverse primer is outlined in blue. B. The exon 2/exon 3 junction of *DUX4* is shown in the sequence data for the sequence of interest collected from human testis total RNA sample. The RT-PCR products were analysed by electrophoresis on 2% agarose gel. The band was purified using Wizard®SV Gel and PCR Clean-Up System (Promega) and was sent to the University of Alberta Sanger sequencing facility at the Katz Center for Pharmacy and Health Research facility. Testis total RNA was purchased from Applied Biosystems (California, USA).

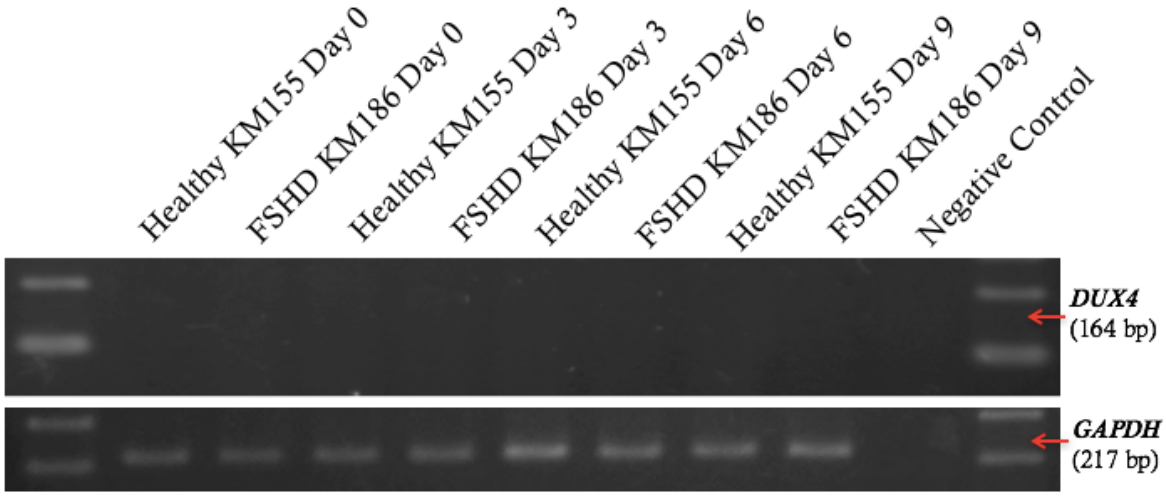

Figure 3.2: Evaluation of DUX4 expression in differentiated healthy KM155 myotubes and FHSD KM186 myotubes using SuperScript III One-Step RT-PCR System

DUX4 mRNA detection using *DUX4* PCR primers in proliferated and differentiated KM155 cells and proliferated and differentiated KM186 cells, by one-step RT-PCR. Cells were cultured using culture method one as described in Table 2.2. Two days after seeding proliferated myoblasts were collected at day 0, and at day 0 remaining myoblast cultures were differentiated into myotubes and were collected at days 3, 6 or 9. Total RNA was extracted. RT-PCR was performed using SuperScript III One-Step RT-PCR System. Experiments were repeated three times in triplicate.

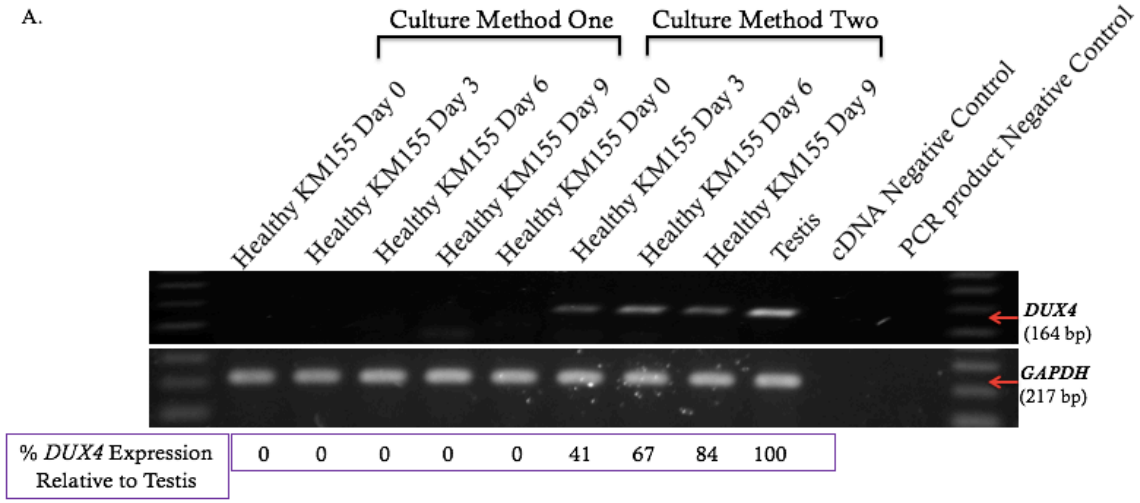

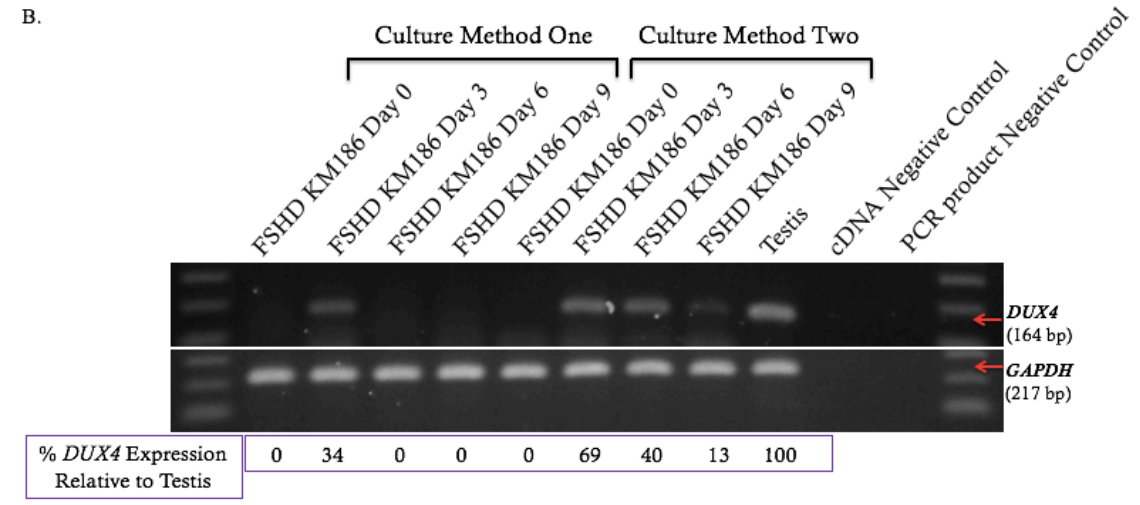

Figure 3.3: Evaluation of *DUX4* expression in healthy KM155 myotubes and FSHD KM186 myotubes using SuperScript III RT and GoTaq® G2 green master mix

A. *DUX4* mRNA detection in proliferated and differentiated healthy KM155 cells (i.e. control myoblasts derived from an unaffected individual confirmed without the FSHD genotype) cultured using culture method one (Table 2.2), and *DUX4* mRNA detection in proliferated and differentiated KM155 cells cultured using culture method two (Table 2.2), by SuperScript III RT and GoTaq®

G2 green master mix. B. *DUX4* mRNA detection in proliferated and differentiated KM186 cells cultured using culture method one (Table 2.2), and *DUX4* mRNA detection in proliferated and differentiated KM186 cells cultured using culture method two (Table 2.2), by SuperScript III RT and GoTaq® G2 green master mix. Purple outlined boxes indicate relative *DUX4* expression compared to testis, positive control sample. *DUX4* expression levels were normalized to *GAPDH* mRNA. Preliminary experiments were performed once in triplicate. RT-PCR for *GAPDH* mRNA expression was used as an internal control.

A.

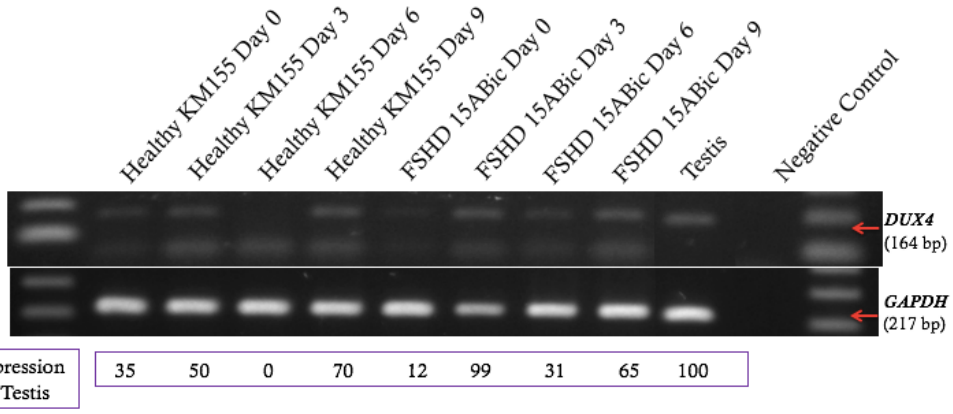

% *DUX4* Expression Relative to Testis	35	50	0	70	12	99	31	65	100

B.

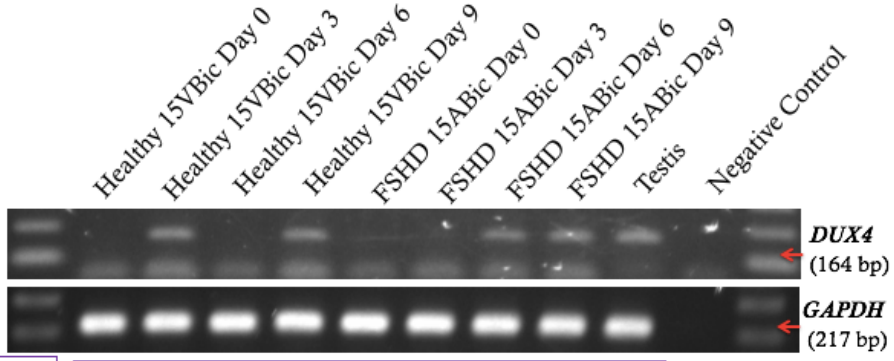

% *DUX4* Expression Relative to Testis	18	35	23	56	13	82	35	82	100

C.

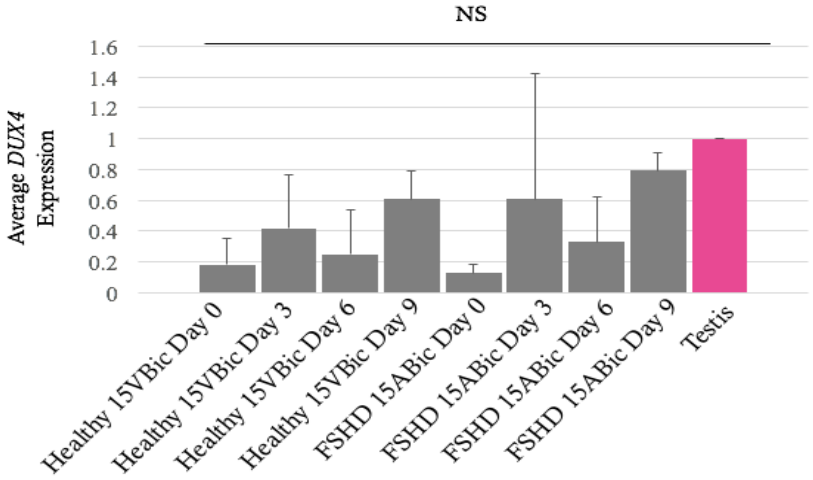

Figure 3.4: Evaluation of *DUX4* expression using culture method three

A. *DUX4* mRNA detection in proliferated and differentiated healthy KM155 cells (i.e. control myoblasts derived from an unaffected individual confirmed without the FSHD genotype) and 15ABic cells cultured using culture method three (Table 2.2), by SuperScript III RT and GoTaq® G2 green master mix. B. *DUX4* mRNA detection in proliferated and differentiated 15ABic cells and 15VBic cells cultured using culture method three (Table 2.2), by SuperScript III RT and GoTaq® G2 green master mix. C. Relative quantification of *DUX4* expression in proliferated and differentiated FSHD 15ABic cells and healthy 15VBic (i.e. control myoblasts derived from an unaffected individual confirmed without the FSHD genotype), cultured using culture method three (Table 2.2). Preliminary experiments were performed once in triplicate. Error bars represent standard deviation. NS is non-significant under one-way ANOVA. Purple outlined boxes indicate relative *DUX4* expression compared to testis, positive control sample. *DUX4* expression levels were normalized to *GAPDH* mRNA. RT-PCR for *GAPDH* mRNA expression was used as an internal control.

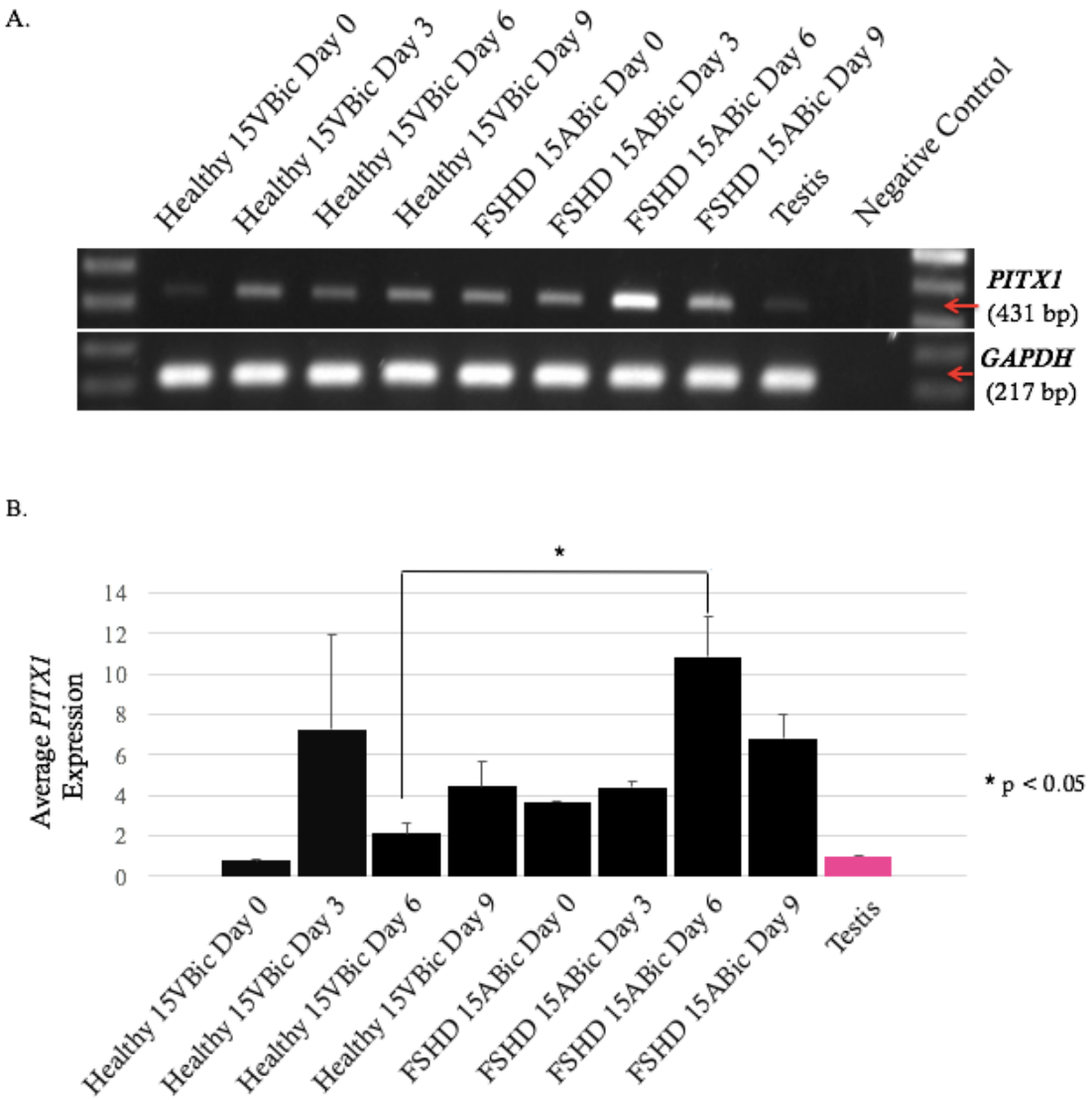

Figure 3.5: Evaluation of *PITX1* expression using culture method three

A. *PITX1* mRNA detection in proliferated and differentiated FSHD 15ABic cells and healthy 15VBic cells (i.e. control myoblasts derived from an unaffected individual confirmed without the FSHD genotype) cultured using culture method three (Table 2.2), by SuperScript III RT and GoTaq® G2 green master mix. B. Relative quantification of *PITX1* expression in proliferated and differentiated FSHD 15ABic cells and healthy 15VBic cells, cultured using culture method three. A preliminary experiment was performed once in duplicate. Error bars represent standard

deviation. *$p<0.05$ represents a significant difference between healthy day 0 (15VBic) *PITX1* expression versus FSHD day 0 (15ABic) under one-way ANOVA and Tukey HSD. *PITX1* expression levels were normalized to *GAPDH* mRNA. RT-PCR for *GAPDH* mRNA expression was used as an internal control. Human testis total RNA was used as a positive control.

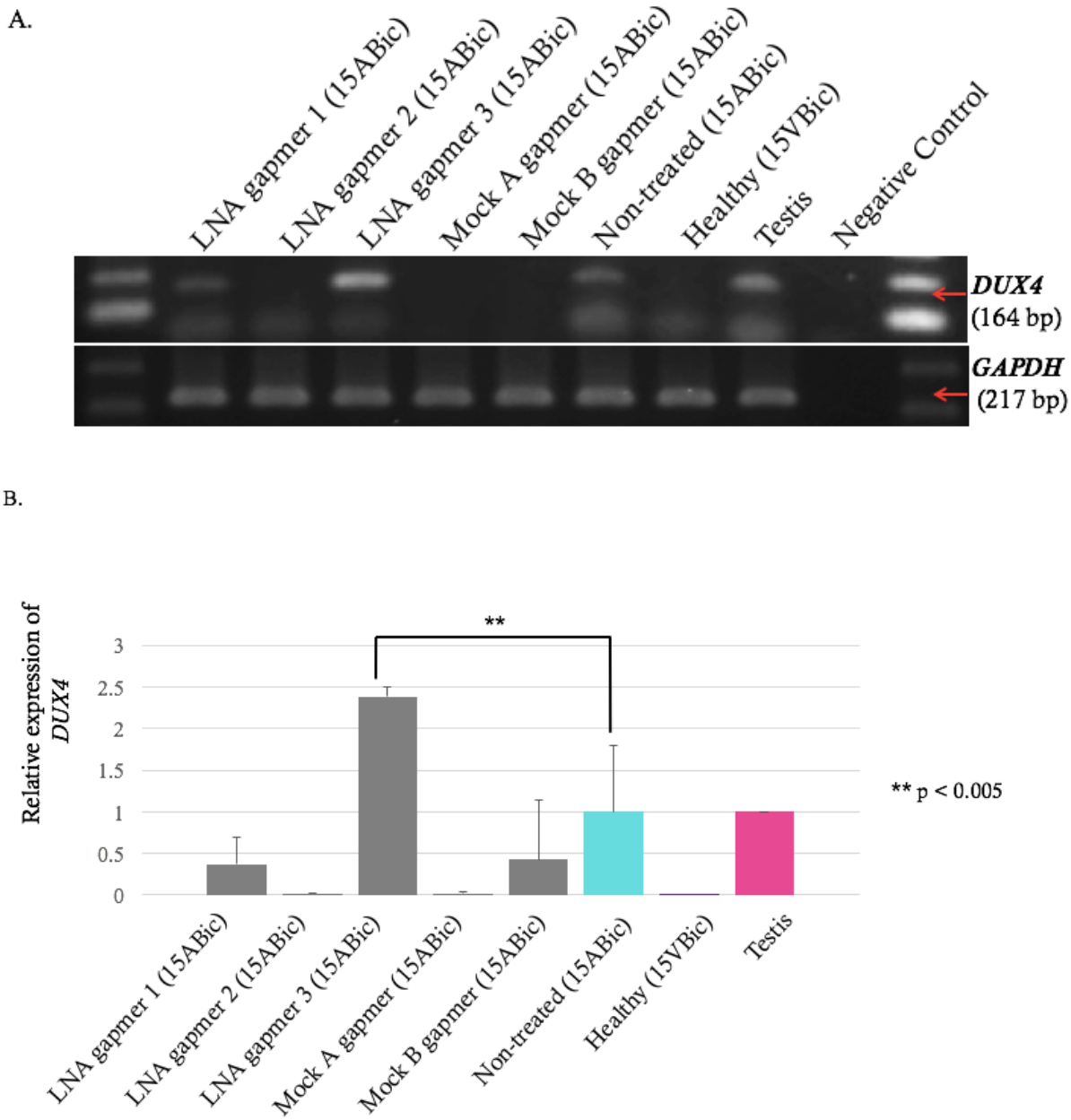

Figure 3.6: Treatment with LNA gapmer 3 at Day 0 after differentiation for 24-hours, increases *DUX4* expression in 15ABic myotubes

A. Semi-quantitative RT-PCR analysis depicting the change in *DUX4* band intensities, after transfection with LNA gapmers 1, 2 or 3 (100 nM) at Day 0 (80% confluent myoblast cultures) (Figure 2.3). B. Relative quantification of the suppression of *DUX4* following normalization to

GAPDH, compared to non-treated cells (15ABic). Preliminary experiments were performed once in triplicate. Error bars represent standard deviation. **$p<0.005$ versus non-treated (15ABic) under one-way ANOVA and Dunnett's multiple comparisons test. RT-PCR for *GAPDH* mRNA expression was used as an internal control. Human testis total RNA was used as a positive control. The healthy (15VBic) sample represents control myoblasts derived from an unaffected individual confirmed without the FSHD genotype.

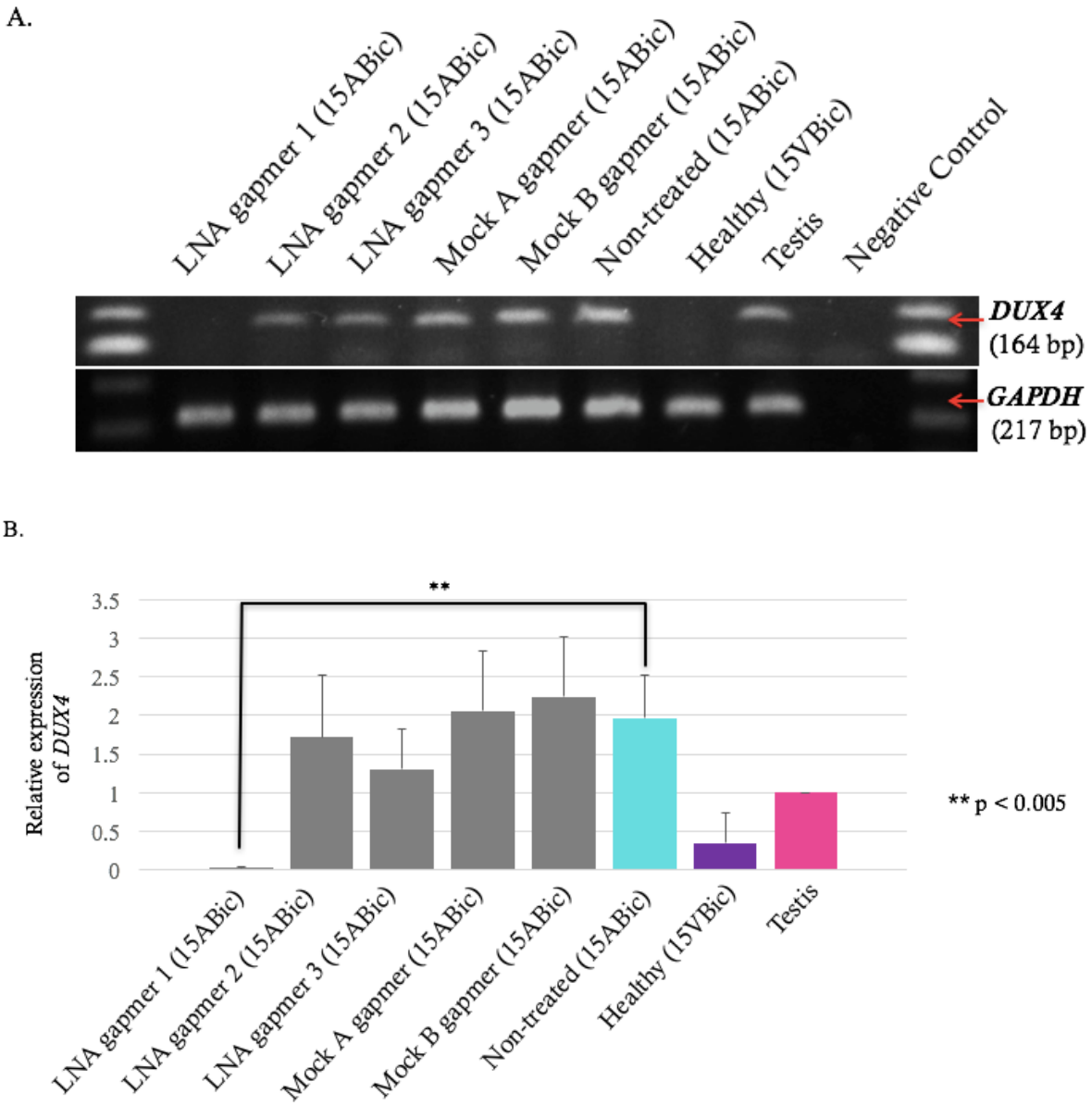

Figure 3.7: Treatment with LNA gapmer 1 at Day 4 after differentiation for 24-hours, sufficiently decreases *DUX4* expression in 15ABic myotubes

A. Semi-quantitative RT-PCR analysis depicting the change in *DUX4* band intensities, after transfection with LNA gapmers 1, 2 or 3 (100 nM) at Day 4 after differentiation with 24-hour LNA gapmer incubation (Figure 2.3). B. Relative quantification of the suppression of *DUX4* following

normalization to GAPDH, compared to non-treated cells (15ABic). Experiments were repeated two times in triplicate. Error bars represent standard error. **$p<0.005$ versus non-treated (15ABic) under one-way ANOVA and Dunnett's multiple comparisons test. RT-PCR for *GAPDH* mRNA expression was used as an internal control. Human testis total RNA was used as positive control. The healthy (15VBic) sample represents control myoblasts derived from an unaffected individual confirmed without the FSHD genotype.

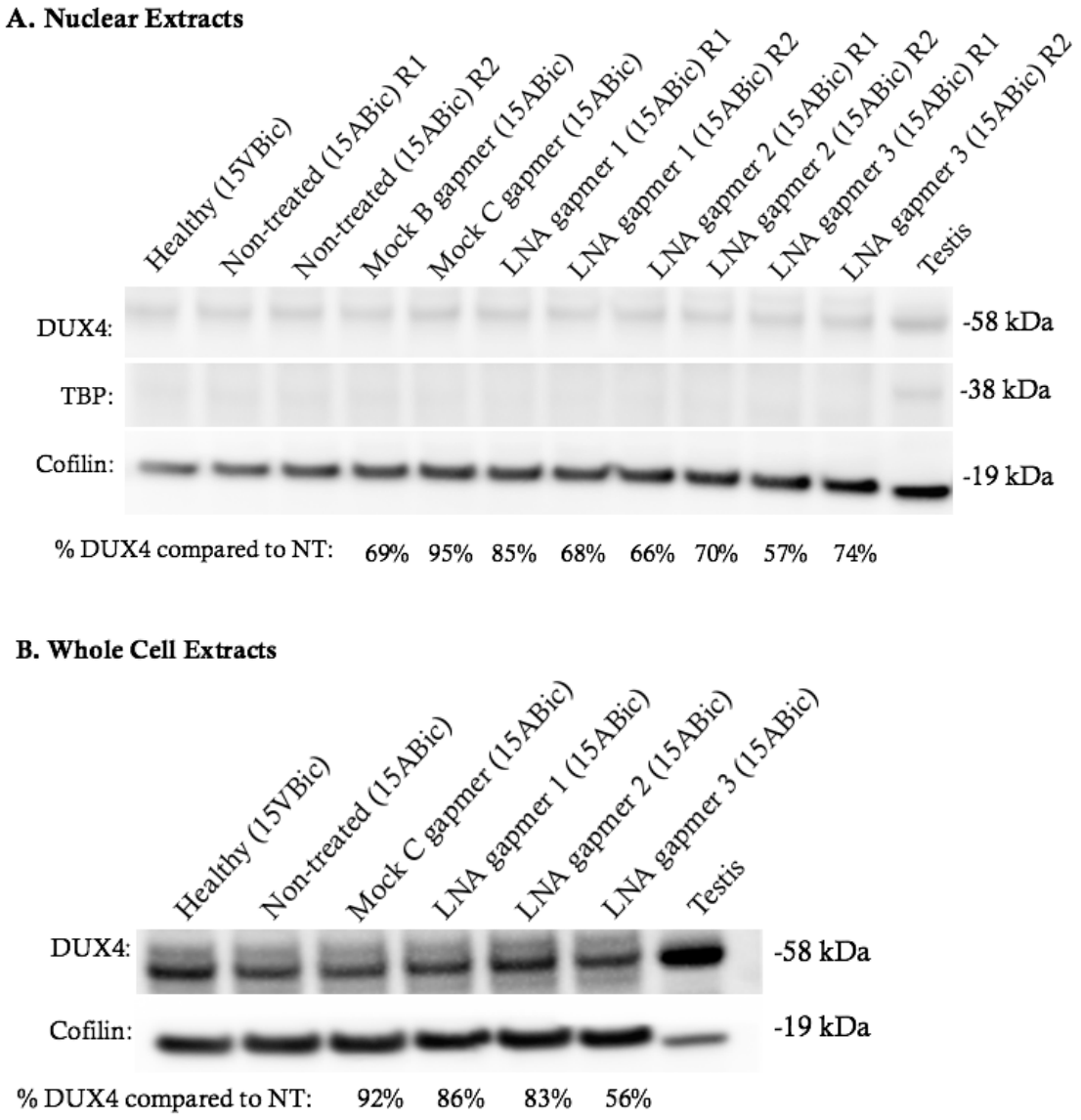

Figure 3.8: LNA gapmers 1, 2 and 3 change DUX4 protein levels in 15ABic cells

Four days after differentiating, FSHD (15ABic) cells were transfected with the indicated LNA gapmer. Data are normalized to Cofilin levels in each sample. Preliminary experiments for each extraction method were performed once. Protein was separated by electrophoresis (4-12% Bis-Tris Midi Protein Gels), transferred to a PVDF membrane and immunodetected with 9A12 anti-Dux4 primary antibody, secondary antibody HRP conjugated goat anti-mouse IgG (H+L) and the Amersham ECL Select Western blotting detection kit. Cofilin was stained with secondary antibody

HRP conjugated goat anti-mouse IgG (H+L) and was used as the loading control. The healthy (15VBic) sample represents control myoblasts derived from an unaffected individual confirmed without the FSHD genotype.

A. Nuclear extracts were prepared 24 hours after transfection. 9 μg were separated by electrophoresis. TBP nuclear loading control was used for normalization, however TBP protein levels were undetectable in 15ABic or 15VBic samples and therefore all samples were normalized to Cofilin. Testis tissue lysate (Abcam, CA) was used as a positive control.

B. Whole cell extracts were prepared 24 hours after transfection. 18 μg were separated by electrophoresis.

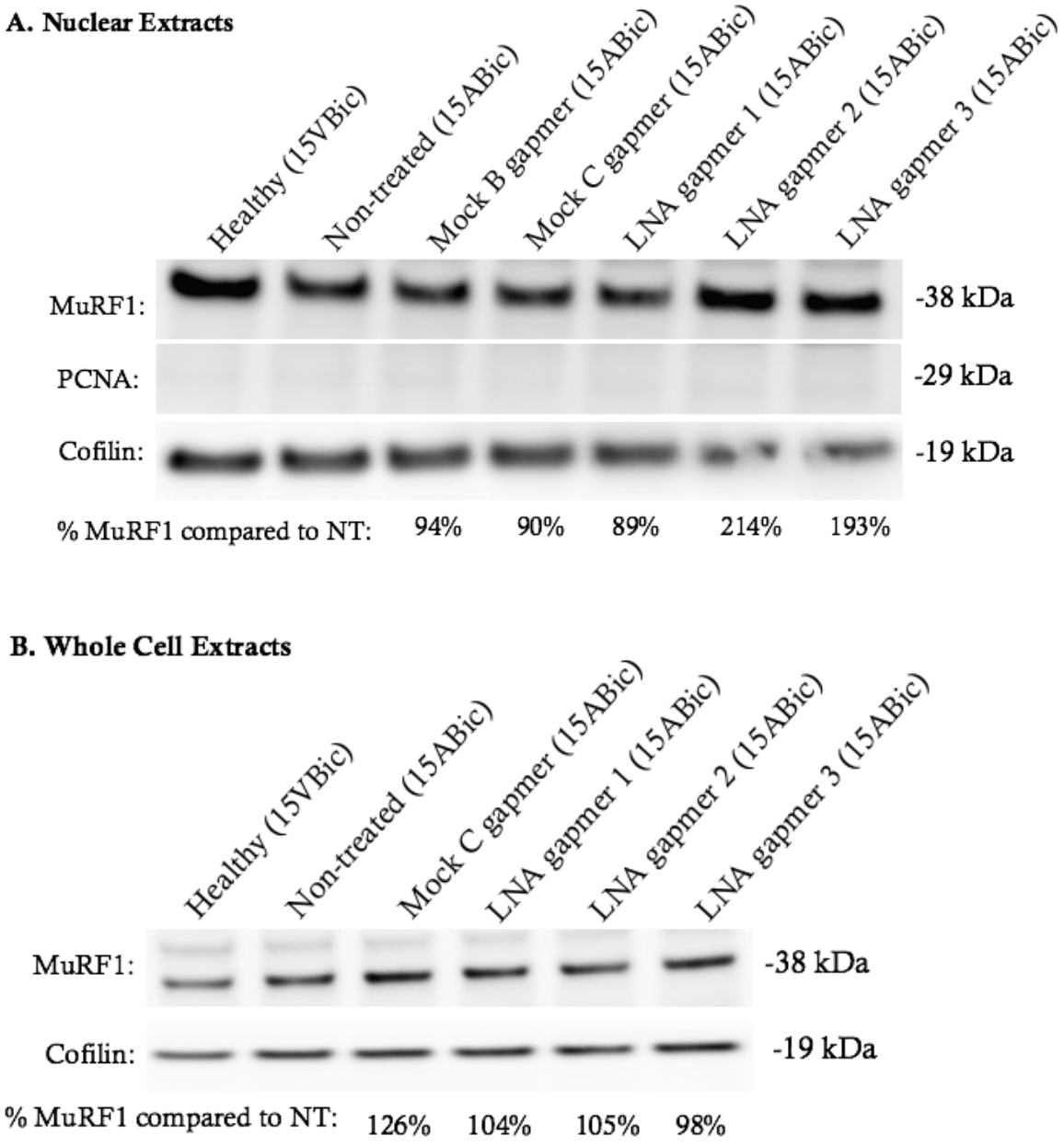

Figure 3.9: Treatment with LNA gapmers 1, 2 or 3 does not change MuRF1 protein levels in 15ABic cells

Four days after differentiating, FSHD (15ABic) cells were transfected with the indicated LNA gapmer. Data are normalized to Cofilin levels in each sample. Preliminary experiments for each extraction method were performed once. 9 µg were separated by electrophoresis (4-12% Bis-Tris Midi Protein Gels), transferred to a PVDF membrane and immunodetected with MuRF1 primary

antibody, secondary antibody HRP conjugated goat anti-rabbit IgG (H+L) and the Amersham ECL Select Western blotting detection kit. Cofilin was stained with secondary antibody HRP conjugated goat anti-mouse IgG (H+L) and was used as the loading control. The healthy (15VBic) sample represents control myoblasts derived from an unaffected individual confirmed without the FSHD genotype.

A. Nuclear extracts were prepared 24 hours after transfection. PCNA nuclear loading control was used for normalization, however PCNA protein levels were undetectable in 15ABic or 15VBic samples and therefore all samples were normalized to Cofilin.

B. Whole cell extracts were prepared 24 hours after transfection.

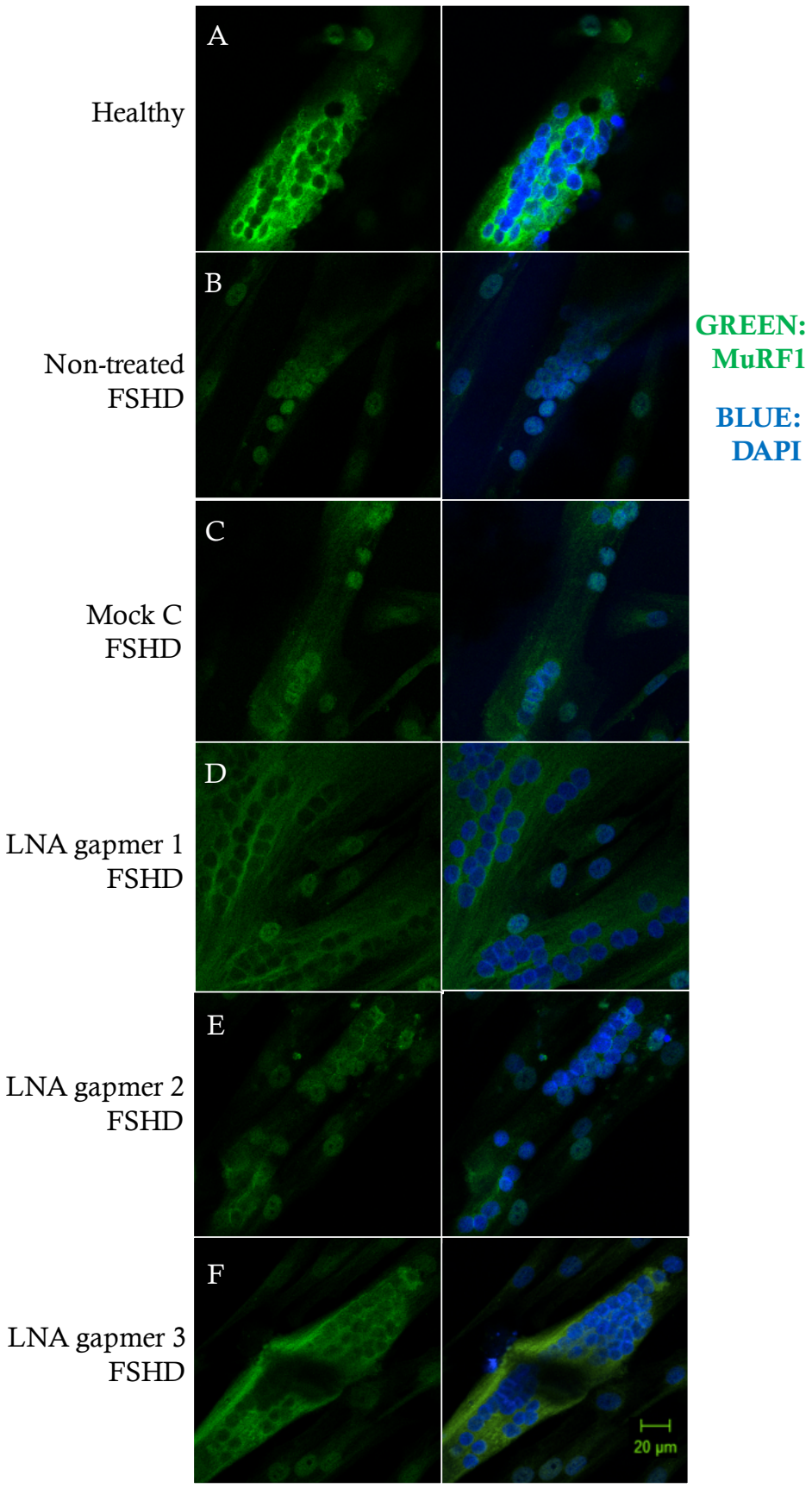
A
Healthy
B
Non-treated FSHD
C
Mock C FSHD
D
LNA gapmer 1 FSHD
E
LNA gapmer 2 FSHD
F
LNA gapmer 3 FSHD
20 µm
GREEN: MuRF1
BLUE: DAPI

Figure 3.10: LNA gapmers 1 and 3 change the localization of MuRF1

A. Control immortalized myoblasts were fixed at day 4 in differentiation, and were not t B. In NT immortalized FSHD myoblasts four days after differentiation, the spent differentiation medium was replaced with differentiation medium containing Opti-MEM and RNAiMAX. C. In immortalized FSHD myoblasts four days after differentiation, cells were transfected with Mock C LNA gapmer (100nM). D. In immortalized FSHD myoblasts four days after differentiation, cells were transfected LNA gapmer 1 (100nM). E. In immortalized FSHD myoblasts four days after differentiation, cells were transfected with LNA gapmer 2 (100nM). F. In immortalized FSHD myoblasts four days after differentiation, cells were transfected with LNA gapmer 3 (100nM).

All myoblasts were differentiated at day 0 after reaching 80% confluence. Two days after differentiation, the spent differentiation medium was replaced with new differentiation medium. Five days after differentiation all cells (A, B, C, D, E, F) were fixed with 4% PFA and incubated with MuRF1 antibody and secondary antibody Alexa Flour 594. The nuclei were labeled with DAPI. The healthy sample represents control myoblasts derived from an unaffected individual confirmed without the FSHD genotype. Scale bar: 20 μm.

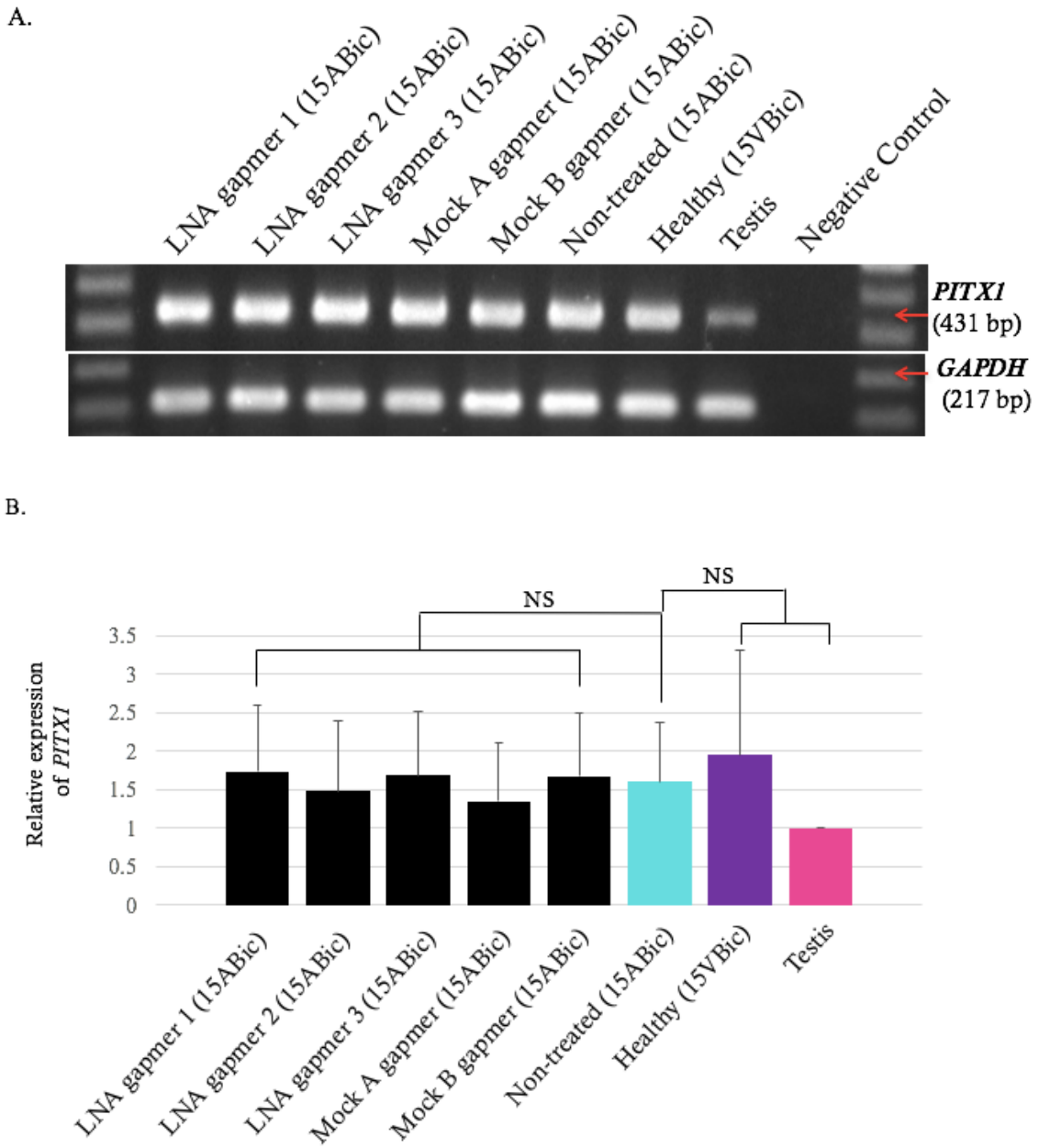

Figure 3.11: Treatment with LNA gapmers 1, 2 or 3 for 24-hours, after 4 days in differentiation, does not change expression of *PITX1* in 15ABic FSHD myotubes

A. Semi-quantitative RT-PCR analysis depicting the change in *PITX1* band intensities, after transfection with LNA gapmers 1, 2 or 3 (100 nM) at Day 4 after differentiation with 24-hour LNA gapmer incubation (Figure 2.3). B. Relative quantification of the suppression of *PITX1* following

normalization to GAPDH, compared to non-treated cells (15ABic). Experiments were repeated two times in triplicate. Error bars represent standard deviation. NS is non-significant under one-way ANOVA. RT-PCR for *GAPDH* mRNA expression was used as an internal control. Human testis total RNA was used as a positive control. The healthy (15VBic) sample represents control myoblasts derived from an unaffected individual confirmed without the FSHD genotype.

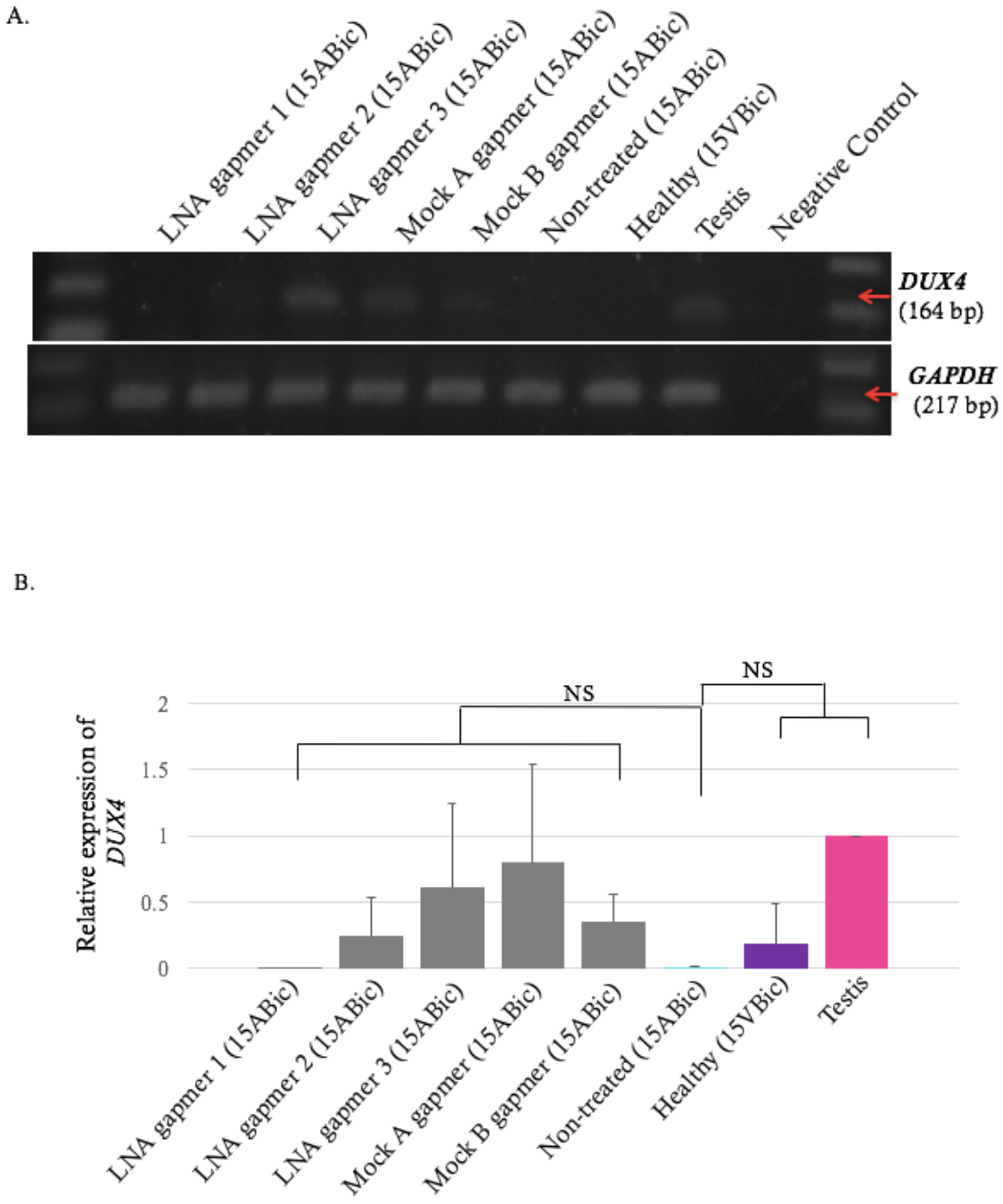

Figure 3.12: Incubation with LNA gapmers 1, 2, or 3 for 48-hours with 15ABic myotubes

A. Semi-quantitative RT-PCR analysis depicting the change in *DUX4* band intensities, after transfection with LNA gapmers 1, 2 or 3 (100 nM) at Day 4 in differentiation with 48-hour LNA

gapmer incubation (Figure 2.3). B. Relative quantification of the suppression of *DUX4* following normalization to GAPDH, compared to non-treated cells (15ABic). Preliminary experiments were performed once in triplicate. Error bars represent standard deviation. NS is non-significant under one-way ANOVA. RT-PCR for *GAPDH* mRNA expression was used as an internal control. Human testis total RNA was used as a positive control. The healthy (15VBic) sample represents control myoblasts derived from an unaffected individual confirmed without the FSHD genotype.

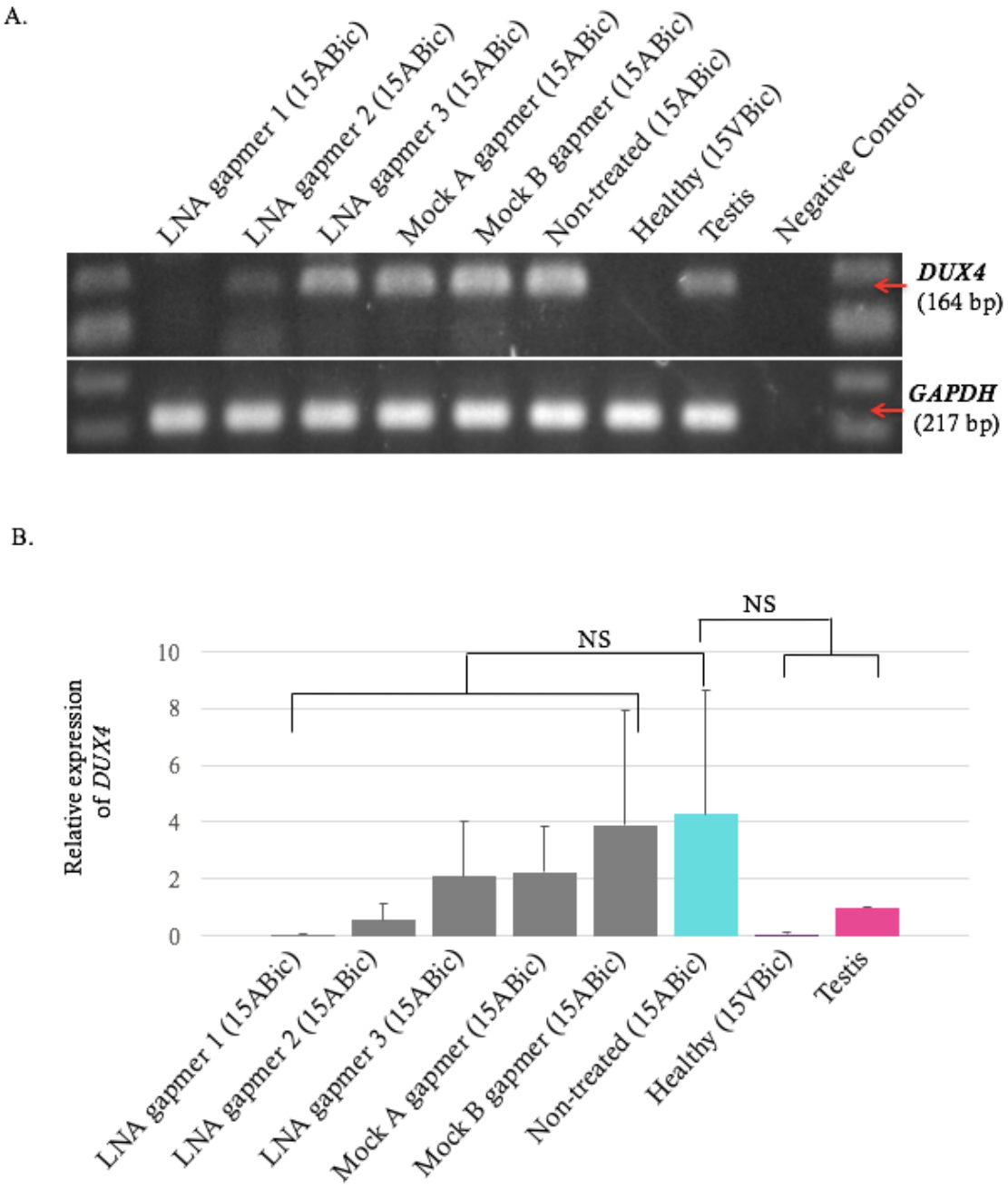

Figure 3.13: LNA gapmers 1, 2 or 3 do not significantly decrease the expression of *DUX4* in 15ABic myotubes after 24-hour transfection at Day 9 after differentiation

A. Semi-quantitative RT-PCR analysis depicting the change in *DUX4* band intensities, after transfection with LNA gapmers 1, 2 or 3 (100 nM) at Day 9 in differentiation with 24-hour LNA gapmer incubation (Figure 2.3). B. Relative quantification of the suppression of *DUX4* following

normalization to GAPDH, compared to non-treated cells (15VBic). Preliminary experiments were performed once in triplicate. Error bars represent standard deviation. NS is non-significant under one-way ANOVA. RT-PCR for *GAPDH* mRNA expression was used as an internal control. Human testis total RNA was used as a positive control. The healthy (15VBic) sample represents control myoblasts derived from an unaffected individual confirmed without the FSHD genotype.

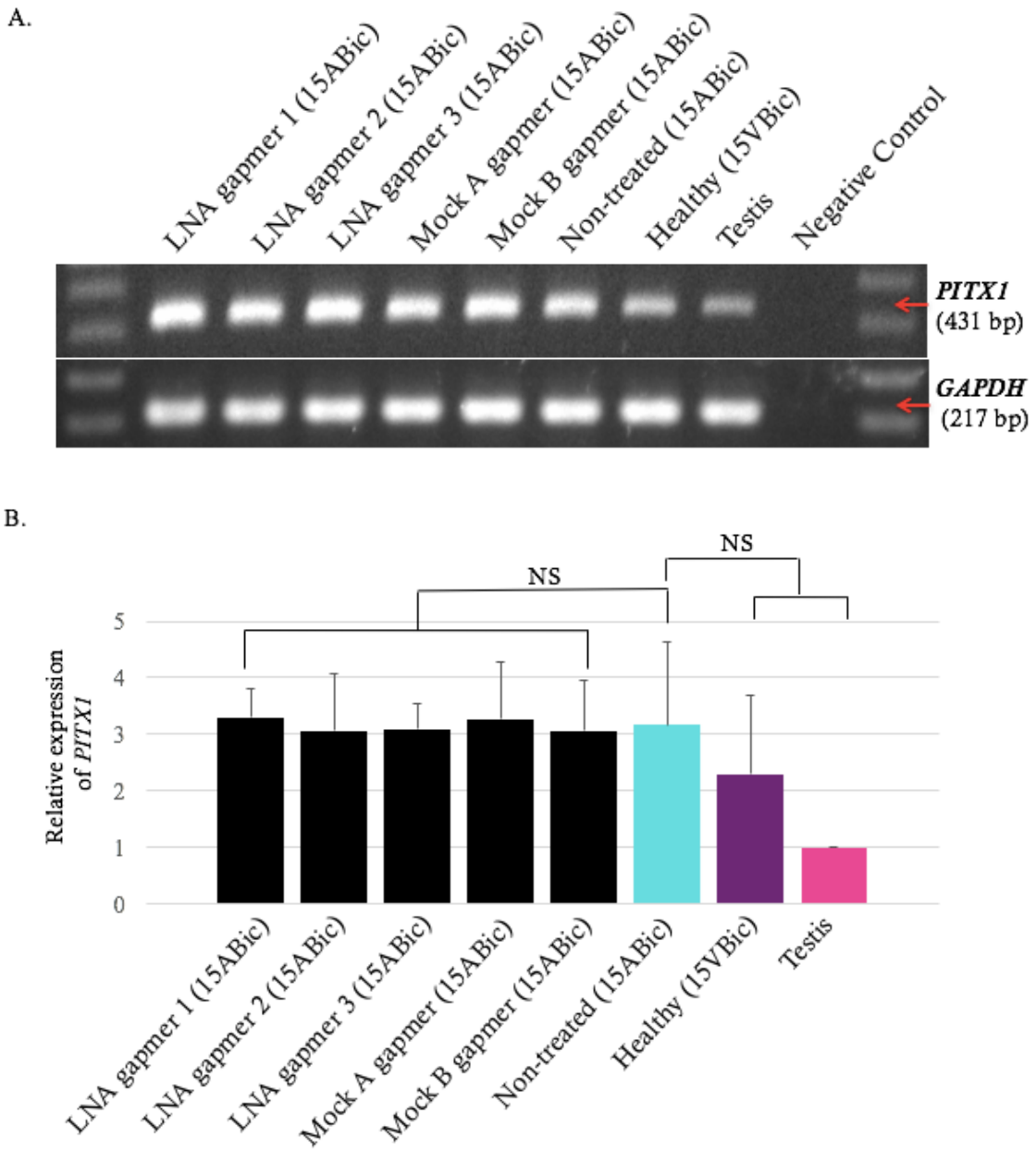

Figure 3.14: LNA gapmers 1, 2 or 3 do not efficiently decrease the expression of *PITX* in 15ABic myotubes after 24-hour transfection at Day 9 after differentiation

A. Semi-quantitative RT-PCR analysis depicting the change in *PITX1* band intensities, after transfection with LNA gapmers 1, 2 or 3 (100 nM) at Day 9 in differentiation medium with 24-hour LNA gapmer incubation (Figure 2.3). B. Relative quantification of the suppression of *PITX1*

following normalization to GAPDH, compared to non-treated cells (15ABic). Preliminary experiments were performed once in triplicate. Error bars represent standard error. NS is non-significant under one-way ANOVA. RT-PCR for *GAPDH* mRNA expression was used as an internal control. Human testis total RNA was used as a positive control. The healthy (15VBic) sample represents control myoblasts derived from an unaffected individual confirmed without the FSHD genotype.

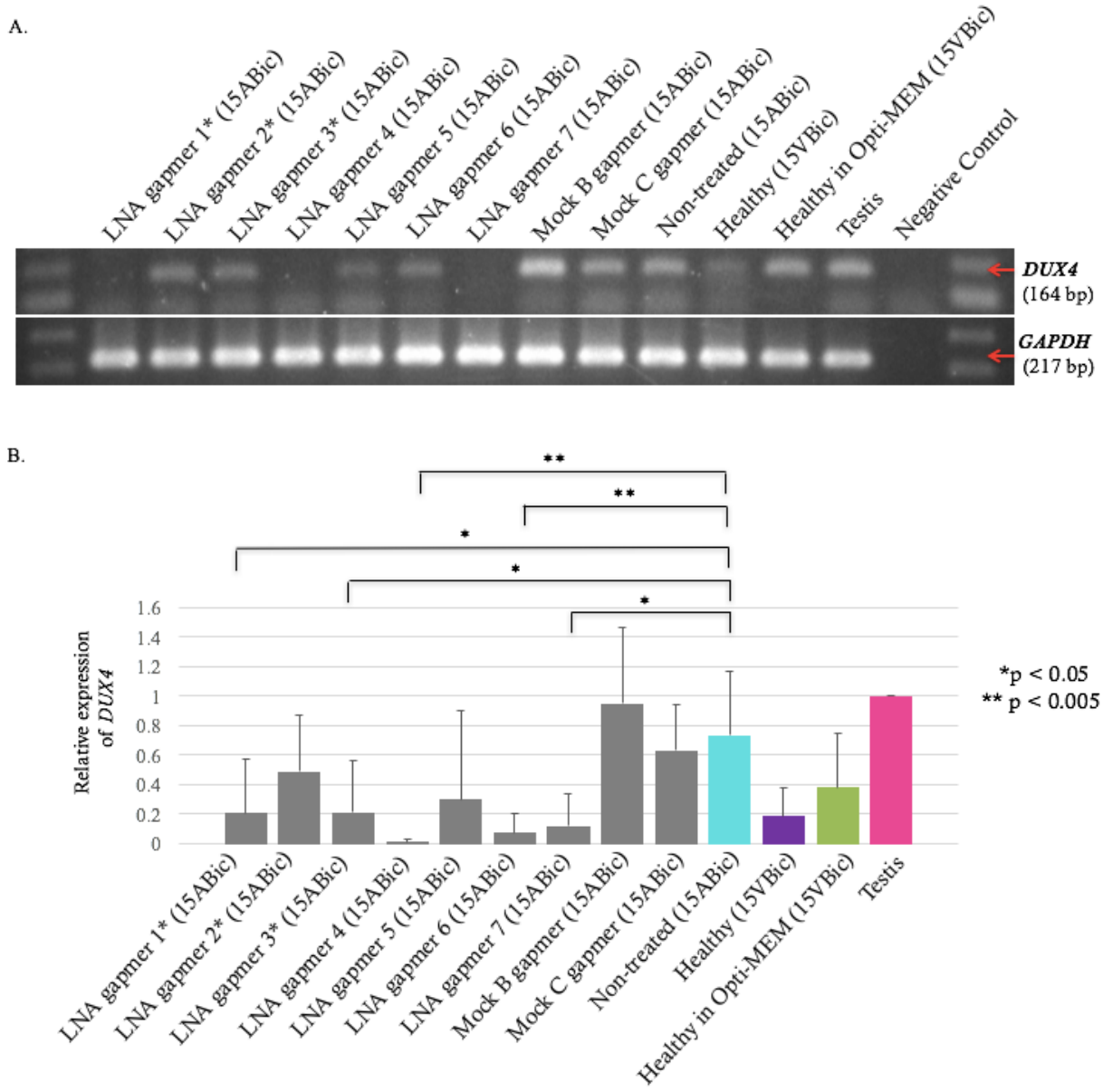

Figure 3.15 LNA gapmers 1*, 3*, 4, 6 and 7 efficiently suppress the expression of *DUX4* in 15ABic myotubes at Day 4 after differentiation with 24-hour incubation

A. Semi-quantitative RT-PCR analysis depicting the change in *DUX4* band intensities, after transfection with LNA gapmers 1*, 2*, 3*, 4, 5, 6 or 7 (100 nM) at Day 4 after differentiation with 24-hour LNA gapmer incubation (Figure 2.3). B. Relative quantification of the suppression of *DUX4* following normalization to GAPDH, compared to testis sample. Experiments were repeated

two times in triplicate. Error bars represent standard deviation. *$p<0.05$ versus non-treated (15ABic) under one-way ANOVA and Dunnett's multiple comparisons test. **$p<0.005$ versus non-treated (15ABic) under one-way ANOVA and Dunnett's multiple comparisons test. RT-PCR for *GAPDH* mRNA expression was used as an internal control. Human testis total RNA was used as a positive control. The healthy (15VBic) sample represents control myoblasts derived from an unaffected individual confirmed without the FSHD genotype.

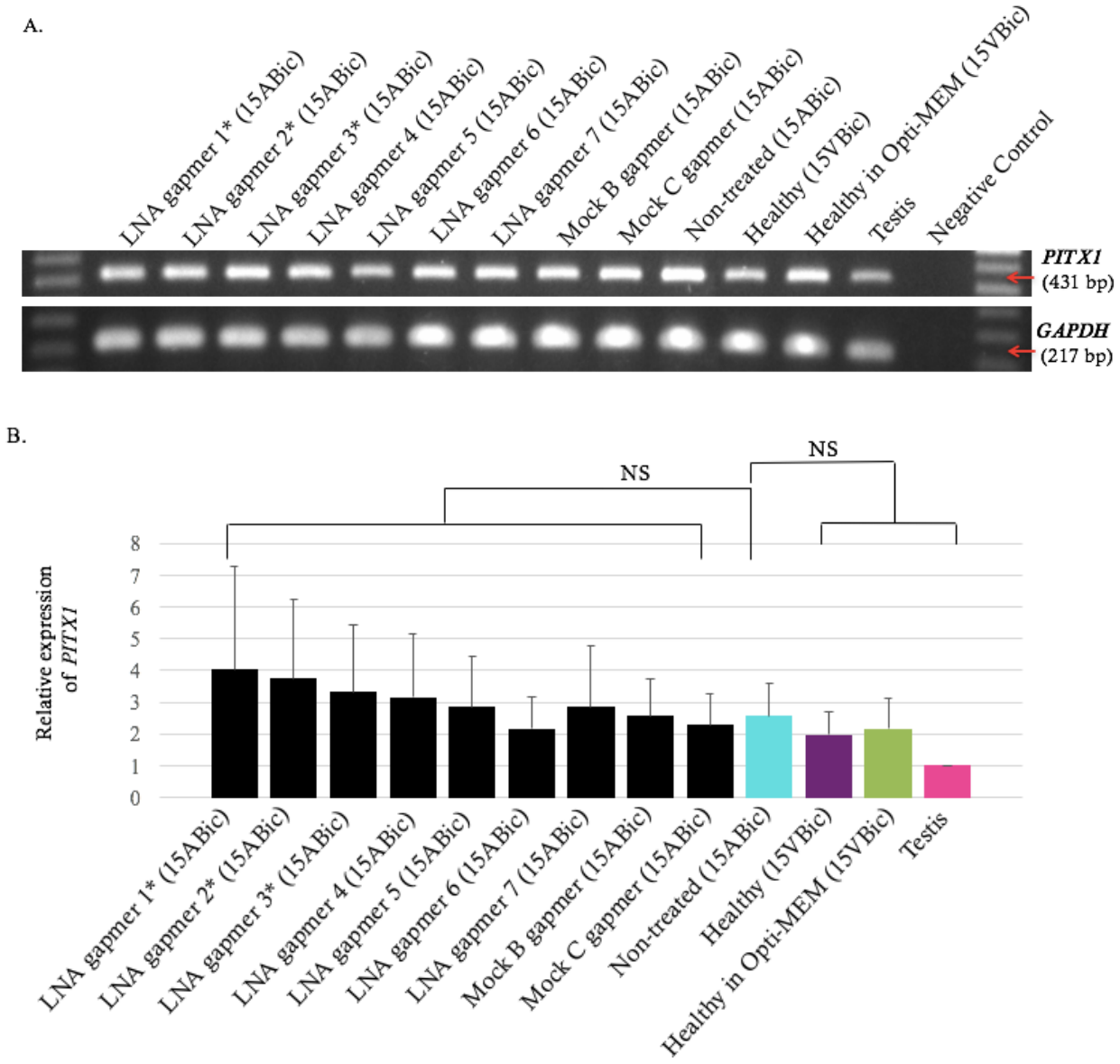

Figure 3.16 LNA gapmers 1*, 2*, 3*, 4, 5, 6 or 7 do not suppress the expression of *PITX1* in 15ABic myotubes at Day 4 after differentiation with 24-hour incubation

A. Semi-quantitative RT-PCR analysis depicting the change in *PITX1* band intensities, after transfection with LNA gapmers 1*, 2*, 3*, 4, 5, 6 or 7 (100 nM) at Day 4 after differentiation with 24-hour LNA gapmer incubation (Figure 2.3). B. Relative quantification of the suppression of *PITX1* following normalization to GAPDH, compared to testis sample. Experiments were repeated

two times in triplicate. Error bars represent standard deviation. NS is non-significant under one-way ANOVA. RT-PCR for *GAPDH* mRNA expression was used as an internal control. Human testis total RNA was used as a positive control. The healthy (15VBic) sample represents control myoblasts derived from an unaffected individual confirmed without the FSHD genotype.

Chapter 4

Discussion

4 DISCUSSION

4. 1 The SuperScript III RT and GoTaq® G2 green master mix is a sensitive detection strategy for *DUX4* transcripts

Two alternative RT-conditions were tested to determine the most sensitive detection strategy for detection of DUX4 in FSHD. Implementation of the SuperScript III one-step RT-PCR system with *Platinum Taq* DNA polymerase was sufficiently sensitive to detect *DUX4* expression in human testes total RNA. This is likely because DUX4 is expressed at relatively abundant levels in human testes (Snider *et al.*, 2010). When the SuperScript III one-step RT-PCR system was used for detection of DUX4 in KM186 FSHD cells, no detection was seen, possibly because of the extremely low mRNA levels of DUX4 in FSHD. Results showed that the SuperScript III RT and GoTaq® G2 green master mix was more sensitive than the SuperScript III one-step system for detecting DUX4 at day 3 after differentiation. SuperScript III RT was designed to provide increased thermal stability, as well as increase specificity and produce higher yields of cDNA; whereas SuperScript III one-step RT-PCR system is an optimized reaction buffer used for detection of a wide range of RNA targets, ranging from 200 bp to 4.5 kb (ThermoFisher Scientific). These results suggest that individual optimization of the first-strand cDNA synthesis and the PCR reaction procedures, using the SuperScript III RT and GoTaq® G2 green master mix, enhances the yields of cDNA and therefore the detection of DUX4. The small DUX4 amplicon size of 164 bp could make its detection harder using SuperScript III one-step RT-PCR system, unless its expression is at high levels, as seen in testis total RNA.

4. 2 Culture conditions affect *DUX4* expression

KOSR is a serum-free, artificial serum replacement, used to directly replace FBS in current protocols (Life Technologies, Frederick, MD, USA). KOSR is a defined formulation often used to culture stem cells or induced pluripotent stem cells (iPSCs). When implemented in culture medium,

KOSR has been reported to induce epigenetic modifications (Chin *et al.*, 2009), interfere with Wnt-mediated cell differentiation (Blauwkamp *et al.*, 2012) and cause increased resistance to apoptosis (Chung *et al.,* 2010). Using culture method two, the presence of 15% KOSR in the growth and differentiation medium increased the expression of *DUX4* in KM186 FSHD cells. The increase in *DUX4* expression is likely caused by the associated effects of KOSR. There are two plausible explanations for this observed increase in *DUX4* expression. First, it is possible that KOSR caused suppression of the Wnt signaling pathway, which may have activated *DUX4* expression, although the precise mechanism for Wnt-mediated suppression remains unclear (Block *et al.,* 2013). Second, it is possible that cells cultured with KOSR had greater survivability and therefore generated a higher population of DUX4-positive cells due to KOSRs protective nature against apoptosis via its main component ascorbate (Chung *et al.*, 2010).

Although *DUX4* expression increased in KM186 FSHD cells supplemented with KOSR, as suggested by Pandey *et al.,* an increase in *DUX4* expression in KM155 healthy cells was also noted. Although the precise composition of KOSR remains unknown, one study showed that KOSR contains an antioxidant known as ascorbate. Ascorbate has been shown to cause a loss of methylation in a CpG island of CD30 in embryonic stem cells (hESCs) (Chung *et al.*, 2010). Interestingly, within each D4Z4 macrosatellite repeat is feature characteristics for a CpG island (van der Marrel *et al.,* 2006); therefore, it is possible that the ascorbate component in KOSR may be triggering a loss of methylation at the D4Z4 macrosatillie repeat ultimately causing derepression of the chromatin, and expression of *DUX4*. *In vitro*, it is possible that in healthy cells, expression of *DUX4* mRNA may not require a deletion of the D4Z4 array, but instead may be influenced by culture condition manipulations resulting in expression of non-pathogenic DUX4, or *s*-DUX4 (Jones *et al.*, 2012).

Dexamethasone is a corticosteroid that has shown success when used as a supplement in culture medium. In a rat skeletal muscle cell line (L6 skeletal muscle cells), culture medium supplemented with dexamethasone enhanced cell proliferation (Giorgino and Smith, 1995) and in another study accelerated muscle differentiation in myocytes (Tehrani *et al.*, 2014). Similar, to KOSR, dexamethasone has also demonstrated suppression of Wnt signaling in epithelial and osteoblast cells, however its role in myoblasts remains unknown (Hu *et al.*, 2013 and Almeida *et al.*, 2011). Healthy KM155 cells cultured in medium containing dexamethasone (culture method three) expressed higher levels of *DUX4* than healthy KM155 cells cultured without dexamethasone (culture method one). However, KM155 cells cultured with dexamethasone (culture method three) more closely recapitulates the expected phenotype reported in patient muscle biopsies, when compared to healthy KM155 cells cultured with KOSR (culture method two). Although the expected phenotype for healthy controls is predicted to have little to no expression of DUX4, these results are similar to that found by Jones *et al.*, 2012, in which several healthy control cell lines were found to express *DUX4* when cultured in medium supplemented with dexamethasone. Further understanding of the molecular mechanisms underlying dexamethasone's effect on expression of DUX4 could help regulate DUX4 expression in FSHD immortalized cell lines.

Here it is also seen that dexamethasone is able to induce the expression of *DUX4* in both healthy 15VBic cells and in 15ABic FSHD cells, but preliminary data shows that there is an overall trend towards higher expression of *DUX4* in FSHD cells after differentiation. Different primer sets could be used to differentiate between *fl-DUX4* and *s*-DUX4 to determine whether dexamethasone is influencing pathogenic and/or non-pathogenic DUX4 isoform *in vitro*. Further exploration of the precise mechanisms involved in dexamethasone's ability to induce DUX4 expression should be conducted; however, it can be suggested that dexamethasone too is working to suppress Wnt-signaling in FSHD myoblasts causing an increase in *DUX4* expression. This data also shows that

healthy control cells and FSHD cells may be influenced by their culture environment differently from one another. Supplementation of KOSR or dexamethasone into the culture medium demonstrates that dexamethasone added to growth medium, is the most reliable culture method to use, as it produces a trend in *DUX4* expression more similar to the expected genotype of FSHD patients.

PITX1 is currently the only known direct target of DUX4. Dixit *et al*., determined the direct and specific binding of these two proteins via EMSA (Dixit *et al.*, 2007). PITX1 expression has been found to be up-regulated in FSHD compared to 11 other neuromuscular disorders and healthy individuals (Dixit *et al.*, 2007). 15ABic FSHD myotubes cultured in dexamethasone showed expression of *PITX1* in undifferentiated and differentiated myotubes but only showed a significant increase in expression at day 6 in FSHD cells compared to healthy control cells (Figure 3.5). Although a significant increase in *PITX1* expression was seen at day 6 *in vitro*, these findings deviate from the results found by Dixit *et al.*, 2007, where real-time quantitative RT-PCR in FSHD muscle biopsies showed a 24-fold increase in *PITX1* expression compared with healthy control muscle biopsies. This suggests that *PITX1* expression in cell culture may not entirely recapitulate the phenotype characterized *in vivo*. The lower expression levels of *PITX1* seen *in vitro* could suggest that *PITX1* may also be influenced by its culture conditions and that further optimization may be required in order to observe its described phenotype *in vitro*. Lastly, it is also possible that its lack of drastic up-regulation *in vitro* could be due to the fact that PITX1 may not actually be a direct target of DUX4, as suggested by recent evidence by Zhang *et al.*, 2016 and is therefore not up-regulated when DUX4 is during differentiation.

4. 3 LNA gapmers targeting *DUX4* are effective *in vitro* after differentiation

An observed increase in *DUX4* expression after differentiation suggests that efficacy of LNA gapmers before and after differentiation could be potentially variable. Time of transfection *in vitro*

using C2C12 myoblasts, or day of injection *in vivo* using *mdx*52 mice, has shown considerable variability in efficacy of PMO uptake as well as therapeutic potential (Aoki *et al.,* 2013). This study suggested that different time points for transfection with LNA gapmers should be tested in immortalized FSHD cells and were therefore explored.

For my study, initially three LNA gapmers were designed to target the *DUX4* mRNA transcript. Design of LNA gapmer sequences covering the *DUX4* transcript were limited due to the high GC content. LNA gapmers 1, 2 and 3 were designed to target locations on either exon 1 or 3 and were designed by a company called Exiqon. The gapmers were designed with LNA flanks between 2-3 nucleotides on either side of the DNA gap which is between 8 to 10 nucleotides in length. Due to company policy, however, the precise length of the LNA flanks and the DNA gap for each individual LNA gapmer sequence is reserved by the company and therefore unknown to this study. Initially, LNA gapmers 1, 2 and 3 were transfected at a concentration of 100 nM at Day 0, in which FSHD myoblasts had reached 80% confluence, but had yet to be differentiated. Preliminary results testing transfection with LNA gapmers at Day 0 showed a significant induction of *DUX4* expression, compared to non-treated FSHD, after transfection with LNA gapmer 3 (Figure 3.6). The lack of significant reduction in *DUX4* expression after transfection with LNA gapmers 1 and 2 could be due to low levels of DUX4 positive cells found in proliferating FSHD myoblasts. The extremely low levels of DUX4 expression could make targeting DUX4 by LNA gapmer and RNase H-mediated degradation difficult. Efficacy of LNA gapmer 1 and 2 transfection was also similar to what was previously found in undifferentiated C2C12 myoblasts transfected with PMO or 2'-O-methyl phosphorothioate (Aoki *et al.*, 2013), where efficient uptake during proliferation stages was poorer in comparison to uptake during stages from myogenic differentiation to myotube formation. At day 0 in undifferentiated cells it is also possible that transfection of LNA gapmers at a

concentration of 100 nM, specifically LNA gapmer 3, may be too high, resulting in cytotoxic conditions for the cells in culture.

Transfection with LNA gapmer 3 at day 0 (Figure 3.6) increases *DUX4* expression, which could suggest that at day 0, LNA gapmer 3 transfected at a concentration of 100 nM could be causing a cytotoxic effect to its surrounding environment, such as increased cell death, ultimately influencing the expression of *DUX4*. This data, however, remains preliminary, and in order to determine whether lowering the concentration of LNA gapmer 3 will reduce its effects in FSHD cells, a dose dependent analysis at day 0 in undifferentiated cells may determine its threshold of toxicity. These experiments should also be further replicated to determine LNA gapmer efficacy at this transfection point.

In contrast to LNA gapmer transfection at day 0, transfection with LNA gapmer 1 at day 4 significantly decreased *DUX4* expression in 15ABic FSHD myotubes (Figure 3.7). The transfection efficacy seen in this experiment is similar to that seen by Aoki *et al.*, in which PMO uptake efficacy increased with C2C12 myotube differentiation. Significant suppression of *DUX4* by LNA gapmer 1, which targets bases 98-112 of exon 3 compared to LNA gapmer 3, which targets position 182-197 of exon 3, suggests that LNA gapmer sequence location or LNA gapmer accessibility on the *DUX4* mRNA transcript may be crucial for efficient suppression of *DUX4*. Using an iterative HFold method, which predicts a secondary RNA structure with the minimum free energy based on the relaxed hierarchical hypothesis (Jabbari & Condon, 2014), for exon 3, LNA gapmer 1 has 12 targeted bases which are accessible, with 8 of them being G's and C's, which contain stronger bonds in comparison to bonds formed with A's and U's. LNA gapmer 3, however, has 8 targeted bases which are accessible, with only 3 of them being G's and C's (refer to Figure 4.1). The higher accessibility of LNA gapmer 1 on exon 3 of *DUX4* mRNA and its quantity of

stronger bonds (i.e. GC content), compared to LNA gapmer 3, could suggest why greater efficacy at the mRNA level is seen after transfection with LNA gapmer 1.

At day 4, transfection with LNA gapmer 1 sufficiently decreased the expression of *DUX4* via semi-quantitative RT-PCR, but contrary to Western Blotting results in both nuclear-extracted samples and whole-cell extracted samples, LNA gapmers 1, 2 and 3 changed DUX4 protein levels in comparison to the NT FSHD sample (Figure 3.8). The efficacy of all three LNA gapmers at the protein level suggests two possibilities. First, perhaps sequence design (i.e. LNA flank length, or DNA gap length) or sequence location (i.e. exon 1 or exon 3) does not affect the efficacy of LNA gapmers at the protein level. Second, it is possible that a change in relative DUX4 protein levels is noticed after transfection with LNA gapmers 1, 2 and 3, compared to semi-quantitative RT-PCR results (Figure 3.7), because of the specific DUX4 antibody used. For detection of DUX4 at the protein level, a DUX4 antibody was used, which recognizes the C-terminal region of DUX4 in exon 1, whereas in RT-PCR experiments *DUX4* RT-PCR primers targeted exons 2 and 3 of the *DUX4* mRNA. For protein analysis, the DUX4 antibody detecting the C-terminal region of DUX4 would only be able to detect fl-DUX4 in FSHD cells, whereas RT-PCR primers may potentially be amplifying both *fl-DUX4* and *s-DUX4* in FSHD cells. *s-DUX4* differs from *fl-DUX4* as it removes the carboxy-terminal end of DUX4 while maintaining the amino-terminal double-homeobox domains (i.e. exons 2 and 3). Although *s-DUX4* is more commonly detected in control myoblasts and in somatic tissues, findings by Snider *et al.*, 2010, where both the *fl-DUX4* and *s-DUX4* were amplified via RT-PCR in several different FSHD cell lines, supports the theory that RT-PCR results are amplifying both *DUX4* isoforms.

Although DUX4 protein levels were detectable using both extraction methods, nuclear loading control TBP was detected in testis tissue lysate but was not detected in treated 15ABic cells, non-treated 15ABic or 15VBic extracted using the nuclear extraction kit. Due to the fact that TBP was

unsuccessfully detected, further optimization of the nuclear extraction protocol should be performed in order to be able to claim with certainty that the nuclear extraction kit isolated nuclear located proteins. Loading control Cofilin, which can be used as either a nuclear or a cytoplasmic loading control (Munsie *et al.*, 2012), was successfully detected in both nuclear and whole cell extracted samples (Figure 3.8). Although Cofilin was detected in both nuclear and whole cell extracted samples, TBP was not, which suggests that for this experiment Cofilin was used as a cytoplasmic loading control and that the nuclear extraction kit used for the purpose of this study was unsuccessful at extracting solely nuclear proteins, due to the lack of TBP detection. Lastly, it should be noted that this data is preliminary and further replicates would have to be performed to determine the possible significance of these LNA gapmers at the protein level for DUX4.

MuRF1 is a muscle specific E3 ubiquitin ligase found to be upregulated prior to the onset of atrophy (de Palma *et al.*, 2008). In a recent study, MuRF1 was induced in FSHD myotubes compared to healthy control myotubes and was found to be co-localized with DUX4 in the nucleus of myotubes that were DUX4 positive (Vanderplanck *et al.*, 2011). To date, little is known about the cellular roles of MuRF1, specifically in the nucleus; however, it has been hypothesized by McElhinny *et al.,* 2002 that MuRF1 in the nucleus potentially controls the expression of muscle specific genes. This hypothesis suggests that MuRF1 localization in the nucleus and in the cytoplasm could play different roles.

Protein analysis showed a change in DUX4 protein levels after transfection with all three LNA gapmers; however, Western blot analysis of MuRF1 protein levels indicated that treatment with these LNA gapmers were not effective at reducing levels of this FSHD marker (Figure 3.9 A). Western blot analysis of nuclear-extracted samples showed that the relative percentage of MuRF1 proteins levels compared to NT were as follows, LNA gapmers 1 (89%), LNA gapmer 2 (214%) and LNA gapmer 3 (193%). The relatively high percentage of MuRF1 protein levels seen after

transfection with LNA gapmer 2 and LNA gapmer 3 in nuclear extracted samples was likely caused by experimental error, as the Cofilin antibody appeared to not have stained properly in the LNA gapmer 2 and LNA gapmer 3 samples (Figure 3.9 A).

Protein analysis using whole-cell extracted samples for detection of MuRF1 protein levels also did not show a considerable change, after transfection with LNA gapmers 1, 2 or 3 when compared to the NT sample. There are two possible explanations for why no change in MuRF1 protein levels was seen in whole-cell extracted samples. First, these results suggest that DUX4 may not directly activate MuRF1, but may cause its activation indirectly. Therefore, targeting DUX4 via LNA gapmers may not change MuRF1 protein levels. A second explanation could be that suppression of DUX4 via LNA gapmers could be causing a change or a decrease in the protein-protein interaction between MuRF1 and perhaps SUMO-3, a gene found to be MuRF1's RING domain that regulates its localization pattern and nuclear import (Dai and Liew, 2001 and Bodine and Baehr, 2014). Suppression of DUX4 protein levels could therefore also be affecting the localization of MuRF1 and ultimately change its role in FSHD. Due to the fact that PCNA nuclear loading control was unsuccessfully detected in MuRF1 nuclear-extracted samples (Figure 3.9 A)), there is reason to believe that the proteins isolated by use of the nuclear extraction kit are not all truly nuclear. Therefore, in both the nuclear extracted and whole cell extracted samples, MuRF1 protein levels both in the cytoplasm and in the nucleus are potentially being detected. These results further suggest that a true quantification of the change in nuclear-located MuRF1 protein may not be currently attained via Western Blotting.

Further support for this explanation is demonstrated via immunofluorescent staining of MuRF1. Transfection with LNA gapmers 1 and 3 for 24-hours after 4 days in differentiation medium changed the localization of MuRF1 in the nucleus compared to NT. However, a noticeable increase in MuRF1 expression in the cytoplasm is seen after transfection with these same LNA gapmers.

This suggests that suppression of DUX4 protein may be changing the localization pattern of MuRF1 and its ability to be imported into the nucleus. Lastly, this data also demonstrates the efficacy of LNA gapmers targeting exon 3, suggesting that these LNA gapmer sequences targeting DUX4 mRNA can prevent DUX4 protein expression and also have the potential to affect FSHD markers, such as MuRF1.

Previous reports using a 48-hour incubation with PMO or 2'OMePS chemistry using no transfection agent showed successful exon skipping efficacy of dystrophin, in *mdx*52 and in another study with 2'-O-methyl phosphorothioate oligonucleotides using Lipofectamine 2000, 48-hour incubation had the maximum transfection efficiency (Aoki *et al.*, 2013 and Vanderplanck *et al.*, 2011). These studies provided evidence to try to improve LNA gapmer efficacy at day 4 after differentiation, and incubate LNA gapmers 1, 2 and 3 for 48 hours. 48 hours after transfection with LNA gapmers, myotube cultures under the microscope appeared to have undergone cell damage. Cells appeared disrupted, with fewer cells attached to the gelatin coated well and an abundance of debris floating within the medium (data not shown). These results suggest that co-transfection with RNAiMAX or Opti-MEM for 48 hours may be too long, causing this reagent to be potentially harmful after 24 hours. This same effect has been previously demonstrated in the Yokota lab, using LNA gapmers transfected for 48-hours in Fibrodysplasia ossificans progressiva (FOP) patient cell lines (data not shown).

Although the cell cultures appeared damaged, samples were still collected 48-hours after incubation and analyzed via semi-quantitative RT-PCR. Incubation with Opti-MEM and RNAiMAX for 48-hours did not significantly change the efficacy of LNA gapmers 1, 2 or 3 compared to incubation for 24-hours (Figure 3.12). However, after 48-hour incubation, LNA gapmer 1 no longer appeared to significantly reduce *DUX4* expression levels at day 4 after differentiation. Although not statistically significant, a trend towards higher *DUX4* expression was

seen after transfection with LNA gapmer 3 further supporting the theory that 48-hour incubation may be too long, and may be potentially harmful.

This data is, however, preliminary, and further tests would have to be done in order to determine which reagent or if the combination of reagents is the cause of this noticeable trend towards increased *DUX4* expression. Additionally, more replicates of this experiment should be performed in order to determine whether 48-hours has a significant effect on the expression of *DUX4* in FSHD myotubes.

At a fourth experimental time point, *DUX4* expression was assessed after 24-hour incubation with LNA gapmers at Day 9 after differentiation (Figure 3.13). Unlike transfection at day 4 after differentiation, neither LNA gapmers 1, 2 or 3 could significantly reduce the expression of *DUX4* at day 9 after differentiation. These results suggest that LNA gapmer efficacy for LNA gapmer 1 is best at day 4 after differentiation in 15ABic FSHD myotubes.

In the present study, LNA gapmer sequences designed by Exiqon have shown differences in their ability to reduce *DUX4* expression at the mRNA level in 15ABic FSHD myotubes. These screening results indicated that LNA gapmer 1 targeting position 98-112 on exon 3 had the greatest efficacy at reducing *DUX4* expression levels, compared to LNA gapmers targeting exon 1 or position 182-197 of exon 3. Since LNA gapmer 1 showed the most promise, newly designed LNA gapmer sequences were derived from LNA gapmer 1, deviating by 1, 2 or 3 bps downstream of base pair 98, keeping a sequence length between 15 and 16 nts. All newly designed LNA gapmers contained 3 nucleotide flanks of LNA on either side of the DNA gap which contained between 8-10 nucleotides.

At day 4 after differentiation and with 24-hour incubation with the newly designed LNA gapmers, LNA gapmers 1*, 3*, 4, 6 and 7 significantly reduced the expression of *DUX4* in 15ABic FSHD myotubes (Figure 3.15). Referring to the iterative HFold method (Figure 4.1), LNA gapmers 1*

has 12 targeted bases which are accessible, with 8 of them being G's and C's, LNA gapmer 4 has 11 targeted accessible bases, with 7 being G's and C's, LNA gapmer 6 has 10 targeted accessible bases, with 6 being G's and C's and LNA gapmer has 9 targeted bases, with 7 being G's and C's (refer to Figure 4.1). Together, these LNA gapmers have high accessibility on exon 3 of *DUX4* mRNA and further suggests that LNA gapmers targeting positions 98-116 on exon 3 are successful at suppressing *DUX4* expression. Interestingly, LNA gapmer 3*, although its sequence was completely homologous and of equal length to LNA gapmer 3, was able to significantly reduce *DUX4* expression in 15ABic FSHD myotubes (Figure 3.15). This suggests that the number of LNA nts composing either LNA flank, may play a role in affecting the suppressive activity of LNA gapmers in FSHD myotubes. However, the definitive sequence of the LNA gapmers designed by Exiqon would have to be known in order to conclude this with certainty.

This research has shown that at day 4 after differentiation with 24-hour incubation with LNA gapmers 1, 1*, 3*, 4, 6 and 7 targeting *DUX4,* that these LNA gapmers were successful at suppressing the expression of *DUX4.* However, at neither day 4 or day 9 after differentiation with 24-hour incubation with the Exiqon designed or newly designed LNA gapmers targeting *DUX4,* could the expression levels of *PITX1* be significantly changed. Although DUX4 has been found to interact with a portion of the PITX1 promoter *in vitro*, recent studies have shown that in inflammatory cells *PITX1* can influence the expression of the interferon alpha (*IFN*α) gene and it can also act as a suppressor of RAS and tumorigenicity (Civas *et al.*, 2002). These findings further suggest that PITX1 can potentially be regulated by a variety of other genes associated with FSHD and that targeting DUX4 alone may not be sufficient as a therapeutic approach for FSHD.

A recent study by Zhang *et al.*, 2016 also calls into question whether *PITX1* is indeed a direct target of *DUX4*, providing support for why these preliminary results do not show a significant reduction in *PITX1* expression after transfection with LNA gapmers targeting *DUX4*. In this study it was

demonstrated by dox-dependent luciferase that the historically used DNA sequence located upstream of the mouse *Pitx1* promoter, a 30-bp oligonucleotide probe 5'-CGGATGCTGTCTTCTAATTAGTTTGGACCC-3', used to measure DUX4 activity, produced little to no induction (Dixit *et al.*, 2007 & Zhang *et al.*, 2016). Competitive experiments were also performed and when the DUX4 protein was limited, the *Pitx1* 30-bp oligo sequence could not sufficiently compete for interaction with DUX4, but was able to compete when the protein was in excess (Zhang *et al.*, 2016). This study suggests that PITX1 is not a direct target of DUX4 and therefore targeting DUX4 directly may not influence the expression of PITX1.

4.4 Future Directions

4.4.1 Perform quantitative RT-PCR

One of the major caveats of this research was the use of semi-quantitative RT-PCR for all experiments to measure the expression levels of DUX4 and PITX1 mRNA in each corresponding sample. Although semi-quantitative RT-PCR is an effective method, this method can only compare the amplified band intensities on a gel to standards of a known concentration. Alternatively, quantitative RT-PCR (qRT-PCR) could be used to quantify gene expression during the exponential growth phase of PCR. Use of qRT-PCR to analyze this data would greatly improve the robustness of this study.

4.4.2 Design new s-DUX4 and fl-DUX4 primers for both RT-PCR and qRT-PCR

In these preliminary experiments, one set of *DUX4* PCR primers was used to detect quantifiable levels of *DUX4* in both FSHD and healthy control cell lines. However, due to the design of these primers, the *DUX4* primers used were unable to differentiate between detection of *fl-DUX4* and *s-DUX4* and therefore, for future experiments, two sets of *DUX4* primers should be designed. *fl-DUX4* primers should be designed to target the carboxyterminal end (i.e. exon 1), whereas *s-DUX4* primers should be designed to target the amino-terminal double-homeobox domains (i.e. exons 2

and 3). Using two primer sets would help determine whether transfection with LNA gapmers is specifically affecting the expression of pathogenic *DUX4 in vitro.*

4.4.3 Determine whether other downstream targets and markers are affected by targeting DUX4 with LNA gapmers

Preliminary observations suggest that transfection with LNA gapmer 1 changes the localization of MuRF1 in the nucleus. A change in localization of MuRF1 suggests that suppression of *DUX4* via LNA gapmer targeting may be involved in regulating the import of MuRF1 into the nucleus. It would be interesting to examine whether the localization of any other FSHD markers, such Atrogin1, or other up-regulated genes involved in the DUX4 transcriptional cascade are also affected by transfection with LNA gapmers 1, 1*, 3, 4, 6 and 7.

Visualization of DUX4 via immunofluorescence using anti-DUX4 antibody 9A12 was unattainable (data not shown). Therefore, potential improvements to the immunocytochemistry protocol, such as increased antibody concentration, or alterations to the PFA percentage should be optimized before investigating the effects of other genes associated with FSHD after transfection with LNA gapmers.

4.4.4 Determine whether DUX4 suppression using LNA gapmers occurs in other affected muscle

For this research all experimental data was collected from FSHD cells collected from the biceps muscles; however, other muscle groups are often found to be affected in FSHD patients. Since other muscles are affected at a later stage in progression it would be interesting to see if these LNA gapmers had similar efficacies throughout different muscle types. It would also be interesting to see if a change in *DUX4* expression is seen across muscle types. Determining the potential of LNA gapmer efficacy in an array of skeletal muscles *in vitro* would further demonstrate the potential of this therapeutic approach for human applications.

4.4.5 Future approaches to examine DUX4 suppression using LNA gapmers

A second major limitation of this study was the use of immortalized FSHD myoblasts. Although immortalized cell lines are good for preliminary testing, use of immortalized cell lines can present some limitations. Cells in culture are prone to genotypic and phenotypic drifting, which can cause a cell line to lose its tissue-specific functions, causing a difference in molecular phenotype from cells *in vivo* (Pan *et al.*, 2009). To overcome these limitations, using FSHD primary cell lines to investigate the suppression of DUX4 after transfection with LNA gapmers would be a better model as they more closely mimic the physiological state of cells *in vivo*. Data collected regarding DUX4 expression levels in primary muscle cells would be more relevant to living systems and may be a better prediction of how these antisense oligonucleotides would react in human patients.

Although an animal model that efficiently mimics the FSHD phenotype is unavailable, translation of this work into one of the existing DUX4 animal models could provide insight on the biological impact of targeting DUX4, and may help to determine whether other downstream targets of DUX4 or other FSHD markers are being affected by targeting DUX4. Lastly translation of this work into an animal model may determine any detrimental effects of LNA gapmer chemistry in an FSHD model.

4.5 Conclusions

My research has identified a sensitive detection strategy and culture method for detection of *DUX4* in 15ABic FSHD immortalized cells. In addition I identified several potential LNA gapmer sequences targeting the *DUX4* mRNA, which prevent *DUX4* expression and change the localization of MuRF1 in the nucleus in FSHD. Transfection with LNA gapmers 1, 1*, 3*, 4, 6 and 7 appeared to decrease *DUX4* expression detected by RT-PCR. As well, LNA gapmers 1, 2 and 3 were able to change DUX4 protein levels in immortalized FSHD cells in preliminary Western blotting results. In addition, LNA gapmers 1 and 3 demonstrated a change in the localization of MuRF1 in the nucleus compared to the non-treated FSHD samples. The downstream target *PITX1,*

however, was not affected by transfection with any of the designed LNA gapmer sequences compared to the non-treated samples, and provides further evidence that PITX1 may not be a direct target of DUX4. All of these antisense oligonucleotides which target the 3'UTR of exon 3 of the *DUX4* transcript represent a promising approach for gene down-regulation of *DUX4*.

This study revealed the most promising target locations on *DUX4* mRNA for suppressing the expression of *DUX4* and in FSHD patient cells. This research demonstrated the importance of LNA gapmer sequence design (i.e. LNA flank length or DNA gap) and target location (i.e exon 1, exon 2 or exon 3 or location within a given exon), for suppression of *DUX4* expression. Studying the effect of transfection with LNA gapmer sequences targeting various locations on the *DUX4* mRNA transcript has implications for understanding the important role of DUX4 in this unique disease.

This research is preliminary, and should be replicated to confirm robustness and reproducibility, but has demonstrated the biological feasibility of targeting DUX4 *in vitro.* Once replicates have been demonstrated, translation of this work into a mammalian system to further understand the impact of DUX4 inhibition and its effect on other downstream targets or FSHD markers may further confirm the important role of DUX4 in FSHD. These novel LNA gapmer sequences show great promise and could contribute to the development of therapeutic approaches for FSHD.

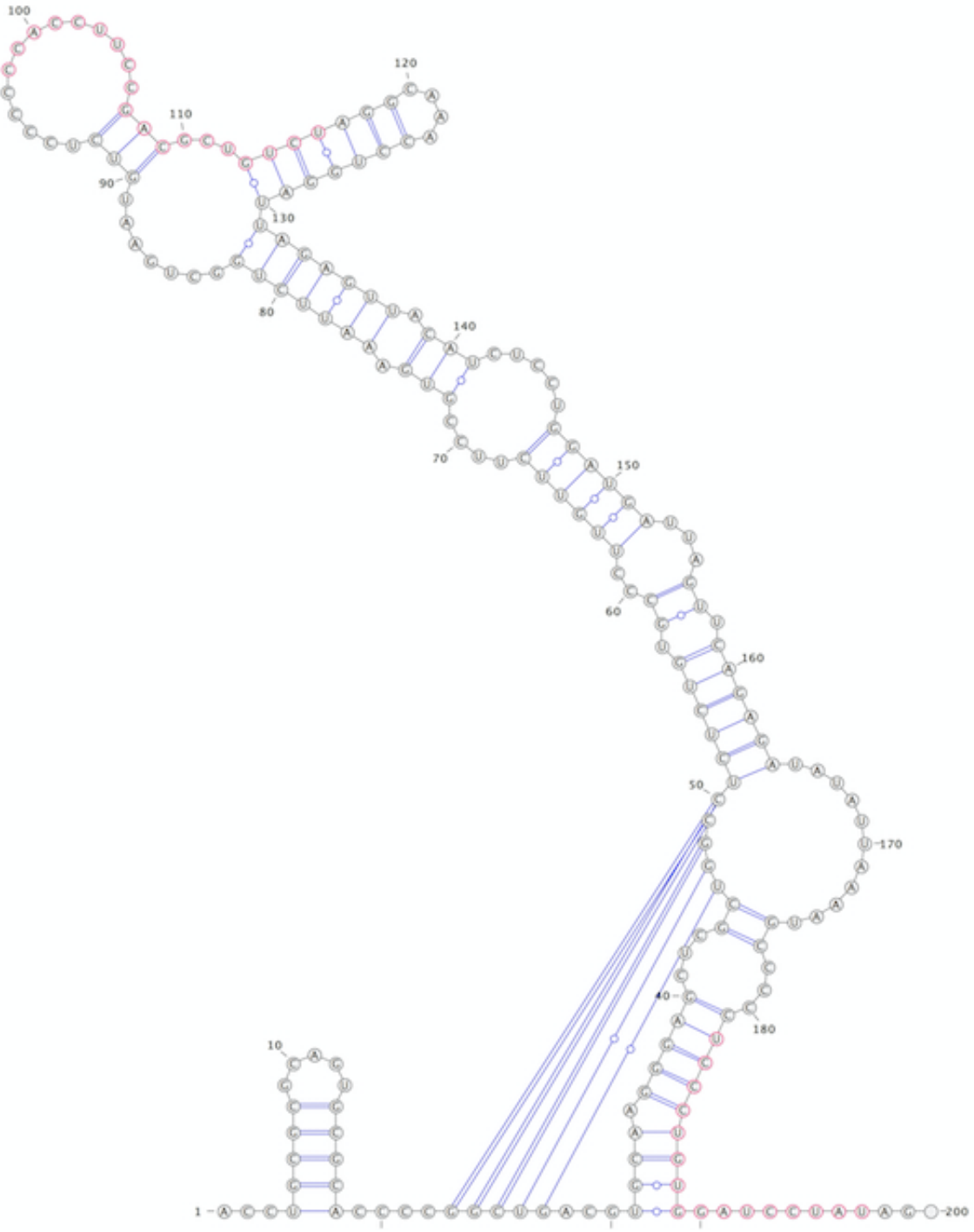
100
120
110
90
130
80
140
70
150
60
160
50
170
40
180
10
1
200

Figure 4.1: Iterative HFold for *DUX4* RNA pseudoknotted secondary structure

Predicted loops and canonical base pairs in a pseudoknotted DUX4 RNA secondary structure. LNA gapmer sequences represented by the red bases. This figure was produced using the VARNA software (Darty *et al.*, 2009).

REFERENCES

Agrawal, S., & Iyer, R. P. (1995). Modified oligonucleotides as therapeutic and diagnostic agents. *Curr Opin Biotechnol, 6*(1), 12-19.

Almeida, M., Han, L., Ambrogini, E., Weinstein, R. S., & Manolagas, S. C. (2011). Glucocorticoids and tumor necrosis factor alpha increase oxidative stress and suppress Wnt protein signaling in osteoblasts. *J Biol Chem, 286*(52), 44326-44335. doi: 10.1074/jbc.M111.283481

Aoki, Y., Nagata, T., Yokota, T., Nakamura, A., Wood, M. J. A., Partridge, T., & Takeda, S. (2013). Highly efficient in vivo delivery of PMO into regenerating myotubes and rescue in laminin-alpha 2 chain-null congenital muscular dystrophy mice. *Hum Mol Genet, 22*(24), 4914-4928. doi: 10.1093/hmg/ddt341

Barakat-Haddad, C., Shin, S., Candundo, H., Van Lieshout, P. & Martino, R. (2016). A systemic review of risk factors associated with muscular dystrophies. *NeuroToxicology,* http://dx.doi.org/10.1016/j.neuro.2016.03.007

Bharathy, N., Ling, B. & Taneja, R. (2013). Epigenetic Regulation of Skeletal Muscle Development and Differentiation. In Kundu R. K. (Ed.) *Epigenetics: Development and Disease* (pp. 139-145). New York: Springer

Bickmore, W. A., & van der Maarel, S. M. (2003). Perturbations of chromatin structure in human genetic disease: recent advances. *Hum Mol Genet, 12 Spec No 2*, R207-213. doi: 10.1093/hmg/ddg260

Bindoff, L. A., Mjellem, N., Sommerfelt, K., Krossnes, B. K., Roberts, F., . . . Haggerty, I. D. (2006). Severe faciscapulohumeral muscular dystrophy presenting with Coats' disease and mental retardation. *Neuromuscul Disord, 16*(9-10)*,* 559-563. doi: 10.1016/j.nmd.2006.06.012

Bird, T. D. (1999). Myotonic Dystrophy Type 1. [Updated 2015 Oct 22]. In: Pagon RA, Adam MP, Ardinger HH, et al., editors. GeneReviews® [Internet]. Seattle (WA): University of Washington, Seattle; 1993-2016. Available from: http://www.ncbi.nlm.nih.gov/books/NBK1165/

Blauwkamp, T. A., Nigam, S., Ardehali, R., Weissman, I. L., & Nusse, R. (2012). Endogenous Wnt signalling in human embryonic stem cells generates an equilibrium of distinct lineage-specified progenitors. *Nat Commun, 3*, 1070. doi: 10.1038/ncomms2064

Block, G. J., Narayanan, D., Amell, A. M., Petek, L. M., Davidson, K. C., Bird, T. D., . . . Miller, D. G. (2013). Wnt/beta-catenin signaling suppresses DUX4 expression and prevents apoptosis of FSHD muscle cells. *Hum Mol Genet, 22*(23), 4661-4672. doi: 10.1093/hmg/ddt314

Bodine, S. C., & Baehr, L. M. (2014). Skeletal muscle atrophy and the E3 ubiquitin ligases MuRF1 and MAFbx/atrogin-1. *Am J Physiol Endocrinol Metab, 307*(6), E469-484. doi: 10.1152/ajpendo.00204.2014

Bodine, S. C., Latres, E., Baumhueter, S., Lai, V. K., Nunez, L., Clarke, B. A., . . . Glass, D. J. (2001). Identification of ubiquitin ligases required for skeletal muscle atrophy. *Science, 294*(5547), 1704-1708. doi: 10.1126/science.1065874

Bonne, G., Leturcq, F., . . . Ben Yaou, R. (2004). Emery-Dreifuss Muscular DystrophyIn: Pagon, R.A., Bird, T.D., Dolan, C.R. (Eds.), University of Washington, Seattle (WA). . (Sep 29 [Updated 2013 Jan 17] GeneReviews™ [Internet]) http:// www.ncbi.nlm.nih.gov/books/NBK1436/.

Braasch, D. A., & Corey, D. R. (2001). Locked nucleic acid (LNA): fine-tuning the recognition of DNA and RNA. *Chem Biol, 8*(1), 1-7.

Brais, B., Rouleau, G. A., Bouchard, J. P., Fardeau, M., & Tome, F. M. (1999). Oculopharyngeal muscular dystrophy. *Seminars in Neurology*, *19*, 59–66.

Campbell, J. M., Bacon, T. A., & Wickstrom, E. (1990). Oligodeoxynucleoside phosphorothioate stability in subcellular extracts, culture media, sera and cerebrospinal fluid. *J Biochem Biophys Methods, 20*(3), 259-267.

Caruso, N., Herberth, B., Bartoli, M., Puppo, F., Dumonceaux, J., Zimmermann, A., . . . Helmbacher, F. (2013). Deregulation of the protocadherin gene FAT1 alters muscle shapes: implications for the pathogenesis of facioscapulohumeral dystrophy. *PLoS Genet, 9*(6), e1003550. doi: 10.1371/journal.pgen.1003550

Centner, T., Yano, J., Kimura, E., McElhinny, A. S., Pelin, K., Witt, C. C., . . . Labeit, S. (2001). Identification of muscle specific ring finger proteins as potential regulators of the titin kinase domain. *J Mol Biol, 306*(4), 717-726. doi: 10.1006/jmbi.2001.4448

Chin, M. H., Mason, M. J., Xie, W., Volinia, S., Singer, M., Peterson, C., . . . Lowry, W. E. (2009). Induced pluripotent stem cells and embryonic stem cells are distinguished by gene expression signatures. *Cell Stem Cell, 5*(1), 111-123. doi: 10.1016/j.stem.2009.06.008

Chung, T. L., Turner, J. P. Thaker, N. Y., Kollie, G., Cooper-White, J. H., . . . Wolvetang, E. J. (2010). Ascorbate Promotes Epigenetic Activation of CD30 in Human Embryonic Stem Cells. *Stem Cells, 28,* 1782-1793. doi: 10.1002/stem.500

Civas, A., Island, M. L., Genin, P., Morin, P., & Navarro, S. (2002). Regulation of virus-induced interferon-A genes. *Biochimie, 84*(7), 643-654.

Dai, K. S., & Liew, C. C. (2001). A novel human striated muscle RING zinc finger protein, SMRZ, interacts with SMT3b via its RING domain. *J Biol Chem, 276*(26), 23992-23999. doi: 10.1074/jbc.M011208200

Dalton, J. C., Ranum, L. P. W. & Day, J. W. (2006). Myotonic Dystrophy Type 2. [Updated 2013 Jul 3]. In: Pagon RA, Adam MP, Ardinger HH, et al., editors. GeneReviews® [Internet]. Seattle (WA): University of Washington, Seattle; 1993-2016. Available from: http://www.ncbi.nlm.nih.gov/books/NBK1466/

Dandapat, A., Bosnakovski, D., Hartweck, L. M., Arpke, R. W., Baltgalvis, K. A., Vang, D., . . . Kyba, M. (2014). Dominant lethal pathologies in male mice engineered to contain an X-linked DUX4 transgene. *Cell Rep, 8*(5), 1484-1496. doi: 10.1016/j.celrep.2014.07.056

Darty, K., Denise, A., & Ponty, Y. (2009). VRNA: interactive drawing and editing of the RNA secondary structure. *Bioinformatics, 25*(15), 1974-1975.

de Greef, J. C., Lemmers, R. J., Camano, P., Day, J. W., Sacconi, S., Dunand, M., . . . Tawil, R. (2010). Clinical features of facioscapulohumeral muscular dystrophy 2. *Neurology, 75*(17), 1548-1554. doi: 10.1212/WNL.0b013e3181f96175

de Palma, L., Marinelli, M., Pavan, M., & Orazi, A. (2008). Ubiquitin ligases MuRF1 and MAFbx in human skeletal muscle atrophy. *Joint Bone Spine, 75*(1), 53-57. doi: 10.1016/j.jbspin.2007.04.019

Deenen, J. C., Arnts, H., van der Maarel, S. M., Padberg, G. W., Verschuuren, J. J., Bakker, E., . . . van Engelen, B. G. (2014). Population-based incidence and prevalence of facioscapulohumeral dystrophy. *Neurology, 83*(12), 1056-1059. doi: 10.1212/WNL.0000000000000797

Dixit, M., Ansseau, E., Tassin, A., Winokur, S., Shi, R., Qian, H., . . . Chen, Y. W. (2007). DUX4, a candidate gene of facioscapulohumeral muscular dystrophy, encodes a transcriptional activator of PITX1. *Proc Natl Acad Sci U S A, 104*(46), 18157-18162. doi: 10.1073/pnas.0708659104

Du, L., & Gatti, R. A. (2009). Progress toward therapy with antisense-mediated splicing modulation. *Curr Opin Mol Ther, 11*(2), 116-123.

Echigoya, Y., Aoki, Y., Miskew, B., Panesar, D., Touznik, A., Nagata, T., . . . Yokota, T. (2015). Long-term efficacy of systemic multiexon skipping targeting dystrophin exons 45-55 with a cocktail of vivo-morpholinos in mdx52 mice. *Mol Ther Nucleic Acids, 4*, e225. doi: 10.1038/mtna.2014.76

Elmen, J., Zhang, H. Y., Zuber, B., Ljungberg, K., Wahren, B., Wahlestedt, C., & Liang, Z. (2004). Locked nucleic acid containing antisense oligonucleotides enhance inhibition of HIV-1 genome dimerization and inhibit virus replication. *FEBS Lett, 578*(3), 285-290. doi: 10.1016/j.febslet.2004.11.015

Emery, A.E. (1991). Population frequencies of inherited neuromuscular diseases: a world survey. *Neuromuscul. Disord*, *1*(1), 19–29.

Emery, A.E. (2000). Emery-Dreifuss muscular dystrophy - a 40 year retroscpective. *Neuromuscul. Disord.*, *10* (4-5), 228–232.

Ferreboeuf, M., Mariot, V., Bessieres, B., Vasiljevic, A., Attie-Bitach, T., Collardeau, S., . . . Dumonceaux, J. (2014). DUX4 and DUX4 downstream target genes are expressed in fetal FSHD muscles. *Hum Mol Genet, 23*(1), 171-181. doi: 10.1093/hmg/ddt409

Frieden, M., Christensen, S. M., Mikkelsen, N. D., Rosenbohm, C., Thrue, C. A., Westergaard, M., . . . Koch, T. (2003). Expanding the design horizon of antisense oligonucleotides with alpha-L-LNA. *Nucleic Acids Res, 31*(21), 6365-6372.

Gabellini, D., D'Antona, G., Moggio, M., Prelle, A., Zecca, C., Adami, R., . . . Tupler, R. (2006). Facioscapulohumeral muscular dystrophy in mice overexpressing FRG1. *Nature, 439*(7079), 973-977. doi: 10.1038/nature04422

Gabriels, J., Beckers, M. C., Ding, H., De Vriese, A., Plaisance, S., van der Maarel, S. M., . . . Belayew, A. (1999). Nucleotide sequence of the partially deleted D4Z4 locus in a patient with FSHD identifies a putative gene within each 3.3 kb element. *Gene, 236*(1), 25-32.

Geng, L. N., Yao, Z., Snider, L., Fong, A. P., Cech, J. N., Young, J. M., . . . Tapscott, S. J. (2012). DUX4 activates germline genes, retroelements, and immune mediators: implications for facioscapulohumeral dystrophy. *Dev Cell, 22*(1), 38-51. doi: 10.1016/j.devcel.2011.11.013

Giorgino, F., & Smith, R. J. (1995). Dexamethasone enhances insulin-like growth factor-I effects on skeletal muscle cell proliferation. Role of specific intracellular signaling pathways. *J Clin Invest, 96*(3), 1473-1483. doi: 10.1172/JCI118184

Harper, P. (2001). Myotonic dystrophy, 3rd edn. London: WB Saunders.

Hewitt, J. E., Lyle, R., Clark, L. N., Valleley, E. M., Wright, T. J., Wijmenga, C., . . . et al. (1994). Analysis of the tandem repeat locus D4Z4 associated with facioscapulohumeral muscular dystrophy. *Hum Mol Genet, 3*(8), 1287-1295.

Hoffman, E. P., Brown, R. H., Kunkel, L. M. (1987). Dystrophin: the protein product of the Duchenne muscular dystrophy locus. *Cell, 51*(6), 919–928.

Hu, X., Gao, J. H., Liao, Y. J., Tang, S. J., & Lu, F. (2013). Dexamethasone alters epithelium proliferation and survival and suppresses Wnt/beta-catenin signaling in developing cleft palate. *Food Chem Toxicol, 56*, 67-74. doi: 10.1016/j.fct.2013.02.003

Jabbari, H., & Codon A. (2014). A fast and robust iterative algorithm for prediction of RNA pseudoknotted secondary structures. *BMC Bioinformatics, 15*(147). doi: 10.1186/1471-2015-15-147

Jalali Tehrani, H., Parivar, K., Ai, J., Kajbafzadeh, A., Rahbarghazi, R., Hashemi, M., & Sadeghizadeh, M. (2014). Effect of dexamethasone, insulin and EGF on the myogenic potential on human endometrial stem cell. *Iran J Pharm Res, 13*(2), 659-664.

Jones, T. I., Chen, J. C., Rahimov, F., Homma, S., Arashiro, P., Beermann, M. L., . . . Jones, P. L. (2012). Facioscapulohumeral muscular dystrophy family studies of DUX4 expression: evidence for disease modifiers and a quantitative model of pathogenesis. *Hum Mol Genet, 21*(20), 4419-4430. doi: 10.1093/hmg/dds284

Jones, T. I., Yan, C., Sapp, P. C., McKenna-Yasek, D., Kang, P. B., Quinn, C., . . . Jones, P. L. (2014). Identifying diagnostic DNA methylation profiles for facioscapulohumeral muscular dystrophy in blood and saliva using bisulfite sequencing. *Clin Epigenetics, 6*(1), 23. doi: 10.1186/1868-7083-6-23

Kauppinen, S., Vester, B., & Wengel, J. (2005). Locked nucleic acid (LNA): High affinity targeting of RNA for diagnostics and therapeutics. *Drug Discov Today Technol, 2*(3), 287-290. doi: 10.1016/j.ddtec.2005.08.012

Koenig, M., Hoffman, E. P., . . . Bertelson, C. J. (1987) Complete cloning of the Duchenne muscular dystrophy (DMD) cDNA and preliminary genomic organization of the DMD gene in normal and affected individuals. *Cell*, *50*(3), 509-17.

Koivisto, H., Hyvarinen, M., Stromberg, A. M., Inzunza, J., Matilainen, E., Mikkola, M., . . . Teerijoki, H. (2004). Cultures of human embryonic stem cells: serum replacement medium or serum-containing media and the effect of basic fibroblast growth factor. *Reprod Biomed Online, 9*(3), 330-337.

Krom, Y. D., Thijssen, P. E., Young, J. M., den Hamer, B., Balog, J., Yao, Z., . . . van der Maarel, S. M. (2013). Intrinsic epigenetic regulation of the D4Z4 macrosatellite repeat in a transgenic mouse model for FSHD. *PLoS Genet, 9*(4), e1003415. doi: 10.1371/journal.pgen.1003415

Kurreck, J., Wyszko, E., Gillen, C., & Erdmann, V. A. (2002). Design of antisense oligonucleotides stabilized by locked nucleic acids. *Nucleic Acids Res, 30*(9), 1911-1918.

Laishes, B. A., & Williams, G. M. (1976). Conditions affecting primary cell cultures of functional adult rat hepatocytes. II. Dexamethasone enhanced longevity and maintenance of morphology. *In Vitro, 12*(12), 821-832.

Lamonerie, T., Tremblay, J. J., Lanctot, C., Therrien, M., Gauthier, Y., & Drouin, J. (1996). Ptx1, a bicoid-related homeo box transcription factor involved in transcription of the pro-opiomelanocortin gene. *Genes Dev, 10*(10), 1284-1295.

Lanctot, C., Lamolet, B., & Drouin, J. (1997). The bicoid-related homeoprotein Ptx1 defines the most anterior domain of the embryo and differentiates posterior from anterior lateral mesoderm. *Development, 124*(14), 2807-2817.

Lanctot, C., Moreau, A., Chamberland, M., Tremblay, M. L., & Drouin, J. (1999). Hindlimb patterning and mandible development require the Ptx1 gene. (vol 126, pg 1805, 1999). *Development, 126*(15), U5-U5.

Landouzy, L., & Dejerine, J. (1884). De la myopathie atrophique progressive (myopathie héréditaire, débutant dans l'enfance par la face, sans altération du système nerveux). *Comptes rendus de l'Académie des sciences* **98**: 53–55.

Landouzy, L., & Dejerine, J. Contribution à l'étude de la myopathie atrophique progressive (myopathie atrophique progressive, à type scapulo-huméral). *Comptes rendus de la Société de biologie* **38**: 478–481.

Lee, J. E., Bennett, C. F., & Cooper, T. A. (2012). RNase H-mediated degradation of toxic RNA in myotonic dystrophy type 1. *Proc Natl Acad Sci U S A, 109*(11), 4221-4226. doi: 10.1073/pnas.1117019109

Lee, J. J., & Yokota, T. (2013). Antisense therapy in neurology. *J Pers Med, 3*(3), 144-176. doi: 10.3390/jpm3030144

Leidenroth, A., & Hewitt, J. E. (2010). A family history of DUX4: phylogenetic analysis of DUXA, B, C and Duxbl reveals the ancestral DUX gene. *BMC Evol Biol, 10*, 364. doi: 10.1186/1471-2148-10-364

Lek, A., Rahimov, F., Jones, P. L., & Kunkel, L. M. (2015). Emerging preclinical animal models for FSHD. *Trends Mol Med, 21*(5), 295-306. doi: 10.1016/j.molmed.2015.02.011

Lemmers, R. J., Tawil, R., Petek, L. M., Balog, J., Block, G. J., Santen, G. W., . . . van der Maarel, S. M. (2012). Digenic inheritance of an SMCHD1 mutation and an FSHD-permissive D4Z4 allele causes facioscapulohumeral muscular dystrophy type 2. *Nat Genet, 44*(12), 1370-1374. doi: 10.1038/ng.2454

Lemmers, R. J., van der Vliet, P. J., Klooster, R., Sacconi, S., Camano, P., Dauwerse, J. G., . . . van der Maarel, S. M. (2010). A unifying genetic model for facioscapulohumeral muscular dystrophy. *Science, 329*(5999), 1650-1653. doi: 10.1126/science.1189044

Lemmers, R. J., Van Overveld, P. G., Sandkuijl, L. A., Vrieling, H., Padberg, G. W., Frants, R. R., & van der Maarel, S. M.(2004). Mechanism and timing of mitotic rearrangements in the subtelomeric D4Z4 repeat involved in facioscapulohumeral muscular dystrophy. *Am J Hum Genet*, *75*, 44–53.

Lunt, P. W. (1998). 44th ENMC International Workshop: Facioscapulohumeral Muscular Dystrophy: Molecular Studies 19-21 July 1996, Naarden, The Netherlands. *Neuromuscul Disord, 8*(2), 126-130.

Koshkin, A. A., Singh, S. K., Nielsen, P., Rajwanshi, V., Kumar, R., Meldgaard, M., Olsen, C. E., & Wengel, J. (1998). LNA (Locked Nucleic Acids): Synthesis of the adenine, cytosine, guanine, 5-methylcytosine, thymine and uracil bicyclonucleoside monomers, oligomerisation, and unprecedented nucleic acid recognition. *Tetrahedron,* 54(14), 3607-3630. doi:10.1016/S0040-4020(98)00094-5

Mamchaoui, K., Trollet, C., Bigot, A., Negroni, E., Chaouch, S., Wolff, A., . . . Mouly, V. (2011). Immortalized pathological human myoblasts: towards a universal tool for the study of neuromuscular disorders. *Skelet Muscle, 1*, 34. doi: 10.1186/2044-5040-1-34

Marcil, A., Dumontier, E., Chamberland, M., Camper, S. A., & Drouin, J. (2003). Pitx1 and Pitx2 are required for development of hindlimb buds. *Development, 130*(1), 45-55. doi: 10.1242/dev.00192

Marsollier, A. C., Ciszewski, L., Mariot, V., Popplewell, L., Voit, T., Dickson, G., & Dumonceaux, J. (2016). Antisense targeting of 3' end elements involved in DUX4 mRNA processing is an efficient therapeutic strategy for facioscapulohumeral dystrophy: a new gene-silencing approach. *Hum Mol Genet, 25*(8), 1468-1478. doi: 10.1093/hmg/ddw015

Marusin, A.V., Kurtanov, H.A., Maksimova, N.R., Swarovsakaja, M. G., & Stepanov, V. A. (2016). Haplotype analaysis of oculopharyngeal muscular dystrophy (OPMD) locus in Yakutia. *Russ J Genet, 52* (3): 331-338. doi:10.1134/S1022795416030091

McElhinny, A. S., Kakinuma, K., Sorimachi, H., Labeit, S., & Gregorio, C. C. (2002). Muscle-specific RING finger-1 interacts with titin to regulate sarcomeric M-line and thick filament structure and may have nuclear functions via its interaction with glucocorticoid modulatory element binding protein-1. *J Cell Biol, 157*(1), 125-136. doi: 10.1083/jcb.200108089

Milner-Brown, H. S., & Miller, R. G. (1988). Muscle strengthening through high-resistance weight training in patients with neuromuscular disorders. *Arch Phys Med Rehabil, 69*(1), 14-19.

Mitsuhashi, H., Mitsuhashi, S., Lynn-Jones, T., Kawahara, G., & Kunkel, L. M. (2013). Expression of DUX4 in zebrafish development recapitulates facioscapulohumeral muscular dystrophy. *Hum Mol Genet, 22*(3), 568-577. doi: 10.1093/hmg/dds467

Mostacciuolo, M. L., Pastorello, E., Vazza, G., Miorin, M., Angelini, C., Tomelleri, G., . . . Trevisan, C. P. (2009). Facioscapulohumeral muscular dystrophy: epidemiological and molecular study in a north-east Italian population sample. *Clin Genet, 75*(6), 550-555. doi: 10.1111/j.1399-0004.2009.01158.x

Munsie, L. N., Desmond, C. R. & Truant, R. (2012). Cofilin nuclear-cytoplasmic shuttling affects cofilin-actin rod formation during stress. *Cell Science, 125,* 3977-3988. doi: 10.1242/jcs.097667

Muntoni, F., & Wood, M. J. (2011). Targeting RNA to treat neuromuscular disease. *Nat Rev Drug Discov, 10*(8), 621-637. doi: 10.1038/nrd3459

Nielsen, K. E., Rasmussen, J., Kumar, R., Wengel, J., Jacobsen, J. P., & Petersen, M. (2004). NMR studies of fully modified locked nucleic acid (LNA) hybrids: solution structure of an LNA:RNA hybrid and characterization of an LNA:DNA hybrid. *Bioconjug Chem, 15*(3), 449-457. doi: 10.1021/bc034145h

Padberg, G. W. (1982). Facioscapulohumeral Disease [these], Leiden, the Netherlands.

Padberg, G. W., Frants, R. R., Brouwer, O. F., Wijmenga, C., Bakker, E., & Sandkuijl, L. A. (1995). Facioscapulohumeral muscular dystrophy in the Dutch population. *Muscle Nerve, 2,* S81-S84.

Pan, C., Kumar, C., Bohl, S., Klingmueller, U., & Mann, M. (2009). Comparative proteomic phenotyping of cell lines and primary cells to assess preservation of cell type-specific functions. *Mol Cell Proteomics, 8*(3), 443-450. doi: 10.1074/mcp.M800258-MCP200

Pandey, S. N., Cabotage, J., Shi, R., Dixit, M., Sutherland, M., Liu, J., . . . Chen, Y. W. (2012). Conditional over-expression of PITX1 causes skeletal muscle dystrophy in mice. *Biol Open, 1*(7), 629-639.

Pandey, S. N., Lee, Y. C., Yokota, T., & Chen, Y. W. (2014). Morpholino treatment improves muscle function and pathology of Pitx1 transgenic mice. *Mol Ther,* 22(2), 390-396.

Pandey, S. N., Khawaja, H., & Chen, Y. W. (2015). Culture Conditions Affect Expression of DUX4 in FSHD Myoblasts. *Molecules, 20*(5), 8304-8315. doi: 10.3390/molecules20058304

Pegoraro, E., Hoffman, E.P. (2000). Limb-girdle muscular dystrophy overview. [updated 2012 Aug 30]. In: Pagon R,A.,, Bird, T.D., Dolan, C.R., et al. (eds.). GeneReviews™ [Internet]. Seattle (WA): University of Washington, Seattle; 1993. Available from: http://www.ncbi.nlm.nih.gov/books/NBK1408/.

Ramellia, G.P., Joncourt, F., Luetschg, J., Weis, J., Tolnay, M. & Burgunder, J.M. (2006). Becker muscular dystrophy with marked divergence between clinical and molecular genetic findings: case series. *Swiss Med*, *136*, 189–193.

Sbiti, A., El Kerch, F. & Sefiani, A. (2002). Analysis of Dystrophin gene deletions by multiplex PCR in Moroccan patients. *Biomed. Biotechnol, 2* (3), 158–160.

Skottman, H., Stromberg, A. M., Matilainen, E., Inzunza, J., Hovatta, O., & Lahesmaa, R. (2006). Unique gene expression signature by human embryonic stem cells cultured under serum-free conditions correlates with their enhanced and prolonged growth in an undifferentiated stage. *Stem Cells, 24*(1), 151-167. doi: 10.1634/stemcells.2004-0189

Snider, L., Asawachaicharn, A., Tyler, A. E., Geng, L. N., Petek, L. M., Maves, L., . . . Tapscott, S. J. (2009). RNA transcripts, miRNA-sized fragments and proteins produced from D4Z4 units: new candidates for the pathophysiology of facioscapulohumeral dystrophy. *Hum Mol Genet, 18*(13), 2414-2430. doi: 10.1093/hmg/ddp180

Snider, L., Geng, L. N., Lemmers, R. J., Kyba, M., Ware, C. B., Nelson, A. M., . . . Miller, D. G. (2010). Facioscapulohumeral dystrophy: incomplete suppression of a retrotransposed gene. *PLoS Genet, 6*(10), e1001181. doi: 10.1371/journal.pgen.1001181

Stadler, G., Rahimov, F., King, O. D., Chen, J. C., Robin, J. D., Wagner, K. R., . . . Wright, W. E. (2013). Telomere position effect regulates DUX4 in human facioscapulohumeral muscular dystrophy. *Nat Struct Mol Biol, 20*(6), 671-678. doi: 10.1038/nsmb.2571

Summerton, J., & Weller, D. (1997). Morpholino antisense oligomers: design, preparation, and properties. *Antisense Nucleic Acid Drug Dev, 7*(3), 187-195. doi: 10.1089/oli.1.1997.7.187

Tassin, A., Laoudj-Chenivesse, D., Vanderplanck, C., Barro, M., Charron, S., Ansseau, E., . . . Belayew, A. (2013). DUX4 expression in FSHD muscle cells: how could such a rare protein cause a myopathy? *J Cell Mol Med, 17*(1), 76-89. doi: 10.1111/j.1582-4934.2012.01647.x

Tawil, R., Forrester, J., Griggs, R. C., Mendell, J., Kissel, J., McDermott, M., . . .Figlewicz, D. (1996). Evidence for anticipation and association of deletion size with severity in facioscapulohumeral muscular dystrophy. The FSH-DY Group. *Ann Neurol, 39*, 744-748.

Tawil, R., Kissel, J. T., Heatwole, C., Pandya, S., Gronseth, G., Benatar, M., . . . Electrodiagnostic, M. (2015). Evidence-based guideline summary: Evaluation, diagnosis, and management of facioscapulohumeral muscular dystrophy: Report of the Guideline Development, Dissemination, and Implementation Subcommittee of the American Academy of Neurology and the Practice Issues Review Panel of the American Association of Neuromuscular & Electrodiagnostic Medicine. *Neurology, 85*(4), 357-364. doi: 10.1212/WNL.0000000000001783

Tehrani, H. J., Parivar, K., Ai, J., Kajbafzadeh, A., Rahbarghazi, R., Hashemi, M., & Sadeghizadeh, M. (2014). Effect of Dexamethasone, Insulin and EGF on the Myogenic Potential on Human Endometrial Stem Cell. *Iranian Journal of Pharmaceutical Research, 13*(2), 659-664.

Torchilin, V. P. (2006). Recent approaches to intracellular delivery of drugs and DNA and organelle targeting. *Annu Rev Biomed Eng, 8*, 343-375. doi: 10.1146/annurev.bioeng.8.061505.095735

Touznik, A., Lee, J. J., & Yokota, T. (2014). New developments in exon skipping and splice modulation therapies for neuromuscular diseases. *Expert Opin Biol Ther, 14*(6), 809-819. doi: 10.1517/14712598.2014.896335

Upadhyaya, M., Maynard, J., Rogers, M. T., Lunt, P. W., Jardine, P., Ravine, D., & Harper, P. S. (1997). Improved molecular diagnosis of facioscapulohumeral muscular dystrophy (FSHD): validation of the differential double digestion for FSHD. *J Med Genet, 34*(6), 476-479.

Urtasun, M., Saenz, A., Roudaut, C., Poza, J.J., Urtizberea, J.A., Cobo, A.M., Richard, I., . . . López de Munain, A. (1998). Limb-girdle muscular dystrophy in guipuzcoa. *Brain*, *121*, 1735–1747.

van der Kooi, A.J., Barth, P.G., Busch, H.F., de Haan, R., Ginjaar, H.B., van Essen, A.J., . . . de Visser, M. (1996). The clinical spectrum of limb girdle muscular dystrophy. A survey in the Netherlands. *Brain, 119*, 1471–1480.

van der Maarel, S. M., Deidda, G., Lemmers, R. J., van Overveld, P. G., van der Wielen, M., Hewitt, J. E., . . . Frants, R. R. (2000). De novo facioscapulohumeral muscular dystrophy: frequent somatic mosaicism, sex-dependent phenotype, and the role of mitotic transchromosomal repeat interaction between chromosomes 4 and 10. *Am J Hum Genet, 66*(1), 26-35. doi: 10.1086/302730

van Geel, M., Dickson, M. C., Beck, A. F., Bolland, D. J., Frants, R. R., van der Maarel, S. M., . . . Hewitt, J. E. (2002). Genomic analysis of human chromosome 10q and 4q telomeres suggests a common origin. *Genomics, 79*(2), 210-217. doi: 10.1006/geno.2002.6690

van Overveld, P. G., Enthoven, L., Ricci, E., Rossi, M., Felicetti, L., Jeanpierre, M., . . . van der Maarel, S. M. (2005). Variable hypomethylation of D4Z4 in facioscapulohumeral muscular dystrophy. *Ann Neurol, 58*(4), 569-576. doi: 10.1002/ana.20625

van Overveld, P. G., Lemmers, R. J., Sandkuijl, L. A., Enthoven, L., Winokur, S. T., Bakels, F., . . . van der Maarel, S. M. (2003). Hypomethylation of D4Z4 in 4q-linked and non-4q-linked facioscapulohumeral muscular dystrophy. *Nat Genet, 35*(4), 315-317. doi: 10.1038/ng1262

Vanderplanck, C., Ansseau, E., Charron, S., Stricwant, N., Tassin, A., Laoudj-Chenivesse, D., . . . Belayew, A. (2011). The FSHD atrophic myotube phenotype is caused by DUX4 expression. *PLoS One, 6*(10), e26820. doi: 10.1371/journal.pone.0026820

Vie, M. P., Evrard, C., Osty, J., Breton-Gilet, A., Blanchet, P., Pomerance, M., . . . Blondeau, J. P. (1997). Purification, molecular cloning, and functional expression of the human nicodinamide-adenine dinucleotide phosphate-regulated thyroid hormone-binding protein. *Mol Endocrinol, 11*(11), 1728-1736. doi: 10.1210/mend.11.11.9915

Voit, T. (2001). Congenital muscular dystrophies. In Karpati, G., Hilton-Jones, D., Griggs, R. C. (Ed.). *Disorders of Voluntary Muscle. 7th ed.* (pp.503-524). Cambridge, UK: Press Syndicate of the University of Cambridge.

Wallace, L. M., Garwick, S. E., Mei, W., Belayew, A., Coppee, F., Ladner, K. J., . . . Harper, S. Q. (2011). DUX4, a candidate gene for facioscapulohumeral muscular dystrophy, causes p53-dependent myopathy in vivo. *Ann Neurol, 69*(3), 540-552. doi: 10.1002/ana.22275

Wang CH, Bönnemann CG, Rutkowski A, Sejersen T, Bellini J, Battista V, Florence JM., . . . Zeller R. (2010). International Standard of Care Committee for Congenital Muscular Dystrophy. Consensus statement on standard of care for congenital muscular dystrophies. *J Child Neurol, 25*, 1559–1581.

Wang, M. X., Wu, B., Tucker, J. D., Lu, P. J., Cloer, C., & Lu, Q. L. (2014). Evaluation of Tris[2-(Acryloyloxy) Ethyl]Isocyanurate Cross-Linked Polyethylenimine as Antisense Morpholino Oligomer Delivery Vehicle in Cell Culture and Dystrophic mdx Mice. *Hum Gene Ther, 25*(5), 419-427. doi: 10.1089/hum.2013.156

Wijmenga, C., Frants, R. R., Brouwer, O. F., Moerer, P., Weber, J. L., & Padberg, G. W. (1990). Location of facioscapulohumeral muscular dystrophy gene on chromosome 4. *Lancet, 336*(8716), 651-653.

Wijmenga, C., Hewitt, J. E., Sandkuijl, L. A., Clark, L. N., Wright, T. J., Dauwerse, H. G., . . . et al. (1992). Chromosome 4q DNA rearrangements associated with facioscapulohumeral muscular dystrophy. *Nat Genet, 2*(1), 26-30. doi: 10.1038/ng0992-26

Wijmenga, C., Padberg, G. W., Moerer, P., Wiegant, J., Liem, L., Brouwer, O. F., . . . et al. (1991). Mapping of facioscapulohumeral muscular dystrophy gene to chromosome 4q35-qter by multipoint linkage analysis and in situ hybridization. *Genomics, 9*(4), 570-575.

Wohlgemuth, M., van der Kooi, E. L., van Kesteren, R. G., van der Maarel, S. M., & Padberg, G. W. (2004). Ventilatory support in facioscapulohumeral muscular dystrophy. *Neurology, 63*(1), 176-178.

Yamada, T., Pfaff, S. L., Edlund, T. & Jessell, T. M. (1993). Control of cell pattern in the neural tube: motor neuron induction by diffusible factors from notochord and floor plate. *Cell*, *73*(4), 673 -686. doi: 10.1016/0092-8674(93)90248-O

Yokota, T., Hoffman, E., & Takeda, S. (2011). Antisense oligo-mediated multiple exon skipping in a dog model of duchenne muscular dystrophy. *Methods Mol Biol, 709*, 299-312. doi: 10.1007/978-1-61737-982-6_20

Zamecnik, P. C., & Stephenson, M. L. (1978). Inhibition of Rous sarcoma virus replication and cell transformation by a specific oligodeoxynucleotide. *Proc Natl Acad Sci U S A, 75*(1), 280-284.

Zatz, M., Marie, S. K., Passos-Bueno, M. R., Vanizof, M., Campiotto, S., . . . Frants, R. (1995). High proportion of new mutations and possible anticipation in Brazilian facioscapulohumeral muscular dystrophy families. *Am J Hum Genet, 56,* 99-105.

Zhang, Y., King, O. D., Rahimov, F., Jones, T. I., Ward, C. W., Kerr, J. P., . . . Wagner, K. R. (2014). Human skeletal muscle xenograft as a new preclinical model for muscle disorders. *Hum Mol Genet, 23*(12), 3180-3188. doi: 10.1093/hmg/ddu028

Zhang, Y., Lee, J. K., Toso, E. A., Lee, J. S., Choi, S. H., Slattery, M., Aihara, H., & Kyba, M. (2016). DNA-binding sequence specificity of DUX4. *Skeletal Muscle, 6*(8). doi: 10.1186/s13395-016-0080-z